

UC Santa Barbara

UC Santa Barbara Electronic Theses and Dissertations

Title

Balancing Complexity and Conceptualization in Hydrological Modeling: Insights into Process Representation, Spatial Variability, and the Urban-Natural Hydrological Interface

Permalink

<https://escholarship.org/uc/item/5nc2r0xk>

Author

Kim, Dong-Hyun (Donny)

Publication Date

2024

Peer reviewed|Thesis/dissertation

SAN DIEGO STATE UNIVERSITY AND
UNIVERSITY OF CALIFORNIA SANTA BARBARA

Balancing Complexity and Conceptualization in Hydrological Modeling: Insights into
Process Representation, Spatial Variability, and the Urban-Natural Hydrological Interface

A Dissertation submitted in partial satisfaction of the
requirements for the degree Doctor of Philosophy
in Geography

by

Dong-Hyun Kim

Committee in charge:

Professor Hilary McMillan, Chair

Professor Trent Biggs

Professor Hugo Loáiciga

Professor Christina (Naomi) Tague

September 2024

The dissertation of Dong-Hyun Kim is approved.

Trent Biggs

Hugo Loáiciga

Christina (Naomi) Tague

Hilary McMillan, Committee Chair

September 2024

Balancing Complexity and Conceptualization in Hydrological Modeling: Insights into
Process Representation, Spatial Variability, and the Urban-Natural Hydrological Interface

Copyright © 2024

by

Dong-Hyun Kim

ACKNOWLEDGEMENTS

I would like to acknowledge and pay my sincere gratitude for all the support I have received throughout my PhD journey, both within and outside the program:

I am truly grateful to my advisor Dr. Hilary McMillan for her support and guidance. I was given many amazing research opportunities, and it means a lot to be her first doctoral student. I also want to express my gratitude to my committee members; Dr. Trent Biggs not only influenced my view on hydrological modeling, but his passion for hydrology also inspired me. I was able to learn about engineering and management aspects in hydrology from Dr. Hugo Loaiciga, widening my view of the practical applications of hydrology. I learned a lot on how hydrological and environmental modeling should be from Dr. Naomi (Christina) Tague, which has greatly benefited my research.

I also wish to acknowledge the Geography Department(s) of San Diego State University and University of California Santa Barbara for financial and academic support, without which none of this could have begun. I should also mention my important collaborators: Dr. Mike Johnson, Amina Naliaka, Dr. Fred Ogden, Dr. Kris Taniguchi-Quan, and Zhipeng Zhu.

Finally, I wish to give my special thanks to my parents and family for all the love and support, including my soon-to-be-wife fiancé Christina Zhu, whom I met only because of this program. I am truly grateful for continuous support and understanding. I also want to thank all my friends and lab mates, who made this journey more enjoyable.

Doing my PhD in SDSU-UCSB Geography Joint Doctoral Program was one of the best decisions I've ever made, and I will strive to build my future upon this experience.

VITA OF DONG-HYUN KIM
September 2024

EDUCATION

Bachelor of Science in Geography, Konkuk University, Seoul, Korea, February 2015
Master of Science in Geography, Konkuk University, Seoul, Korea, February 2017
Doctor of Philosophy in Geography, San Diego State University / University of California,
Santa Barbara, September 2024

PROFESSIONAL EMPLOYMENT

2014-2017: Research Assistant, Department of Geography, Konkuk University
2018-2021: Graduate Assistant, Department of Geography, San Diego State University
Summer 2019: Summer Student Research Fellow, National Water Center
Summer 2021/2022: Research Assistant, Southern California Coastal Water Research Project
2021-2023: Teaching Associate, Department of Geography, San Diego State University

PUBLICATIONS

“Variations in the Hydro-Geomorphological Environment in the Baekgok Wetland due to Reservoir Water-level Fluctuation,” *Journal of the Korean Geomorphological Association*, (2017), vol.24 iss.1, 39-50.

“Experimental Coupling of TOPMODEL with the National Water Model: Effects of Coupling Interface Complexity on Model Performance,” *Journal of the American Water Resources Association* (2022), vol.58.iss.1, 50-74.

“Untangling the impacts of land cover representation and resampling in distributed hydrological model predictions,” *Environmental Modelling & Software* (2023).

FIELDS OF STUDY

Major Field: Water Resources Management and Hydrologic Modeling

Studies in Hydrologic Research with Professors Hilary McMillan

ABSTRACT

Balancing Complexity and Conceptualization in Hydrological Modeling: Insights into Process Representation, Spatial Variability, and the Urban-Natural Hydrological Interface

by

Dong-Hyun Kim

This dissertation explores the delicate balance between complexity and conceptual clarity in hydrological modeling, with an emphasis on principles that support flexible modular frameworks; these frameworks not only allow for a range of process formulations, but also facilitate the integration of diverse models across different watersheds and the use of spatial data most relevant to watershed characteristics and model structure. Recognizing the challenges of capturing the complex interactions between climate and land-surface hydrology—especially in environments altered by urbanization and other anthropogenic factors—the study investigates how different model configurations impact predictive accuracy and process representation across varied watershed environments. This journey is guided by two core assumptions; First, the research posits that integrating distributed Land Surface Models (LSMs) with simpler hydrologic models can enhance explanatory power. Second, the usefulness of the spatial model inputs (static watershed characteristics), such as land cover and topography, has varying effects depending on modeling decisions related to spatial

representations (e.g., resampling algorithm, resolution). These insights aim to advance both academic understanding and practical strategies in hydrology.

The first study (Chapter 2) addresses the integration of TOPMODEL, a conceptual hydrologic model, with Noah-MP, the land surface model of the National Water Model (NWM), through a one-way coupling approach. This chapter demonstrates that simplifying the complex subsurface representation of NWM can enhance streamflow predictions, especially in headwater catchments. By testing six different coupling scenarios, the study reveals that preserving the internal states of both models yields the best results, outperforming either model used independently. However, the research also highlights that the design of the coupling interface can introduce structural uncertainty, significantly impacting model performance and parameter sensitivity. These findings emphasize the need for a cautious approach in model coupling to maintain consistency and accuracy.

The second study (Chapter 3) focuses on the influence of land cover representation and resampling methods within the WRF-Hydro/NWM framework. Through a controlled sensitivity analysis, the research uncovers that the areal proportion of land cover classes significantly affects vertical hydrologic fluxes and streamflow characteristics at the catchment scale. In contrast, the spatial arrangement of land cover has a minimal impact on vertical hydrological fluxes, though it can slightly alter streamflow through routing processes. These results challenge the necessity of detailed representation spatial pattern and allocation of land cover in large-scale hydrologic modeling, suggesting that a flexible, modular approach to spatial configuration may be more effective. The chapter advocates for land surface modeling strategies that balance the need for detailed process representation with the simplicity required for broader applicability.

The third study (Chapter 4) investigates the effects of urbanization on hydrologic processes within a landscape-oriented model, focusing on the incorporation of spatially variable effective impervious area (EIA). The EIA is estimated using the latest techniques involving series of statistical regressions and publicly available soil and landcover dataset. By modeling two watersheds with contrasting climates and urbanization patterns, the research demonstrates that integrating urban impact significantly enhances model performance, far surpassing the original model configuration. Notably, a simpler EIA-only adjustment outperformed a more complex configuration that also included additional subsurface urban impacts. Furthermore, the study finds that models with coarser spatial resolutions often outperform those with finer resolutions, despite the loss of detailed spatial information. This outcome challenges the assumption that detailed spatial representation is necessary for accurate urban hydrologic modeling. Instead, it suggests that capturing the most relevant spatial aspect for hydrological flux calculation is more crucial. The chapter underscores the importance of balancing model complexity with practical applicability, particularly in urban hydrology, where both oversimplification and overcomplication present significant challenges.

Overall, this dissertation stressed the challenges of developing scalable hydrologic modeling approaches that are both effective and adaptable. The findings confirm that increased complexity and spatial detail do not necessarily improve model performance. Instead, a balanced approach that considers both complexity and conceptual clarity proves to be more effective. The principles reaffirmed and new insights gained in this study can be applied to modular modeling approaches, contributing to the development of more scalable frameworks that enhance model suitability testing and explanation of hydrologic processes

across diverse watershed environments. The dissertation advocates for more robust, adaptable, and transparent modeling practices, which are essential for expanding the hydrologic knowledge base, addressing future environmental changes, and enhancing water resource management amidst evolving hydrologic demands.

TABLE OF CONTENTS

Chapter 1.	Introduction.....	1
1.1.	Introduction to Hydrologic Modeling and Modular Approaches ..	1
1.2.	Purpose of the Study	4
1.3.	Dissertation Structure and Overview	5
1.4.	References.....	7
Chapter 2.	Experimental Coupling of TOPMODEL with the National Water Model: Effects of coupling interface complexity on model performance.	13
	Abstract.....	13
2.1.	Introduction.....	14
2.2.	Review	18
2.2.1.	Purpose of Coupling Hydrological Models	18
2.2.2.	Coupling in hydrological modeling and relationship with a software design perspective.....	19
2.2.3.	Model Description: NWM and Its Coupling Scheme.....	22
2.2.4.	Model Description: TOPMODEL and its Coupling with LSMs	24
2.3.	Methods	26
2.3.1.	Workflow Overview	26
2.3.2.	NWM LSM (Noah-MP) Set-up and Arranging Coupling Fluxes	28
2.3.3.	TOPMODEL Set-up	31
2.3.4.	Performance Evaluation, and Uncertainty/Sensitivity Analysis	34
2.3.5.	Model Coupling Options	37

2.4.	Study Area	41
2.5.	Results.....	44
2.5.1.	Model Performance Evaluation	44
2.5.2.	Behavioral Changes in Coupled TOPMODEL.....	50
2.6.	Discussion.....	54
2.6.1.	Improvement in Streamflow Predictive Performance	54
2.6.2.	Coupling Interface Strongly Affects Hydrologic Model Behavior	55
2.6.3.	Implications in coupling method	57
2.6.4.	Limitations.....	58
2.6.5.	Broader applications	59
2.7.	Conclusions.....	60
2.8.	References.....	61
Chapter 3.	Untangling the impacts of land cover representation and resampling in distributed hydrological model predictions.	69
	Abstract.....	69
3.1.	Introduction.....	69
3.2.	Study Area	72
3.2.1.	Selection Criteria	72
3.2.2.	Study Watersheds	73
3.3.	Methods	74
3.3.1.	Overview of Study Design.....	74
3.3.2.	Land Cover Resampling (Upscaling) Schemes	76
3.3.3.	WRF-Hydro Implementation.....	79

3.3.4.	Catchment-scale Water Balance Analysis	80
3.3.5.	Analyzing Simulated Streamflow Characteristics Using Hydrologic Signatures	80
3.4.	Results.....	83
3.4.1.	Land Cover Statistics and Spatial Correlation.....	84
3.4.2.	Water Balance Analysis.....	86
3.4.3.	Hydrologic Signature Analysis.....	90
3.5.	Discussion.....	96
3.5.1.	Basin-scale Water Balance: Land Cover Influence on Vertical Processes.....	97
3.5.2.	Land Cover Influence on Simulated Streamflow Characteristics	97
3.5.3.	Recommendations on Land Cover Input Practices for WRF-Hydro	99
3.5.4.	Implications for Land Cover Resampling in LSM-based Distributed Hydrologic Modeling.....	100
3.6.	Conclusions.....	101
3.7.	References.....	103
3.8.	Appendix.....	108
Chapter 4.	Landscape-based Conceptual Modeling Framework to Delineate Urban Impact on Runoff Processes and Hydrological Pathways using Effective Impervious Area	109
	Abstract.....	109
4.1.	Introduction.....	110
4.1.1.	Urbanization impact on watershed hydrological processes..	110
4.1.2.	Landscape-based FLEX-Topo model	112

4.1.3.	Scope of the Study	114
4.2.	Study Area	115
4.3.	Methods	118
4.3.1.	The FLEX-Topo model configurations and preparations.....	119
4.3.2.	Conceptualizing the urban impact	122
4.3.3.	Calculation of Effective Impervious Area (EIA).....	131
4.3.4.	Model Experiment Design: Urban Adjustment Level and Spatial Resolution	135
4.4.	Results.....	140
4.4.1.	Pre-Analysis of Water Balance in study watersheds	140
4.4.2.	EIA estimation and its spatial relationship with classified HRU	142
4.4.3.	Comparative Analysis: General Insight.....	146
4.4.4.	Parameter Sensitivity	148
4.4.5.	Extended Comparative Analysis.....	152
4.5.	Discussion.....	156
4.5.1.	EIA, Urban Adjustment, and Model Performance/Behavior	156
4.5.2.	Spatial resolution and Model Performance/Behavior.....	159
4.5.3.	Limitations	160
4.6.	Conclusions.....	162
4.7.	References.....	163
Chapter 5.	Conclusion	169

LIST OF FIGURES

- Figure 2-1.** Workflow overview for one-way coupling of TOPMODEL and NWM’s LSM (Noah-MP). Coupling fluxes are arranged from NWM outputs and used as input for six options according to varying coupling interfaces.....28
- Figure 2-2.** Concept of TOPMODEL and its schematic diagram in r.TOPMODEL package. Modified from Jeziorska and Niedzielski (2018).32
- Figure 2-3.** Study area: 17 km² Elder Creek-South Fork Eel River watershed in California in black outline.....43
- Figure 2-4.** Comparison of hydrographs (the wet season of the water year 2017, Oct 2016 to Mar 2017), flow duration curve (FDC; whole simulation period, Oct 2015 to Sep 2019) from observation, National Water Model (NWM), and coupled models (with uncertainty bounds). Outputs from stand-alone TOPMODEL not included. A: Hydrograph of Option 1 and 2, B: FDC of Option 1 and 2, C: Hydrograph of Option 3 and 4, D: FDC of Option 3 and 4, E: Hydrograph of Option 5 and 6, F: FDC of Option 5 and 6.46
- Figure 2-5.** Total Sobol’ indices of each TOPMODEL parameters in six coupled models. Parameter sensitivities are affected by varying coupling interface and modification of TOPMODEL structure.....52
- Figure 2-6.** Flow components of TOPMODEL in six coupled models and TOPMODEL-control. The total observed runoff at the outlet of the catchment (Q_{obs}) through the simulation period (Oct 2015 to Sep 2019) is set to 1.00 as a standard. The Sum of each flow component is equal to simulated runoff (Q_{sim}).54

Figure 3-1. Location of six study basins. The names are assigned by the county containing the catchment outlet gage.74

Figure 3-2. Model experiment overview. (a) LULC subset/resampling and statistical analysis. Discussed in section 3.3.2. (b) Detailed WRF-Hydro set up under National Water Model configuration. Discussed in section 3.3. (c) Catchment scale water balance analysis. Discussed in section 3.3.4. (d) Analyzing simulated streamflow characteristics using hydrologic signatures. Discussed in section 3.3.5.76

Figure 3-3. Comparison of NWM, AP, HUC12L, and SHUF against NLCD 2016 at “Berkeley” basin (Opequon Creek watershed in West Virginia). SHUF-NWM is not presented as it shares arbitrary spatial pattern similar to SHUF-AP.84

Figure 3-4. Flow Duration Curve (FDC) from each scheme and USGS observation in six study basins. The X-axis is exceedance probability in percent (%), and Y-axis is catchment discharge in cubic meters per second. USGS observation provides the context regarding the magnitude of impact of LULC on simulated water availability....91

Figure 3-5. Summary of percent difference in hydrologic signatures comparing NWM-AP, HUC12L-AP, and SHUF-AP (and SHUF-NWM). The highlights on X-axis labels correspond to how the hydrologic signatures were reviewed together in section 4.3. Y-axis represents the proportional change in %. (a) Comparison of NWM and AP (b) Comparison of HUC12L and AP (c) Comparison of SHUF-AP and AP (d) Comparison of SHUF-NWM and NWM.94

Figure 4-1. Location of the watersheds and their landscape statistics (average slope in %, median HAND value, watershed area, and imperviousness). The legend of the maps indicates the elevation in meters..... 117

Figure 4-2. Streamflow seasonality quantified with Pardé coefficient for monthly average discharge. X-axis as a month where 1=January.....118

Figure 4-3. FLEX-Topo model structure schematics including EIA and meteorological input modifications made in the study. Modified from Euser et al. (2015).....121

Figure 4-4. Relationship between Qu_{pref} , $Su/Sumax$, and β127

Figure 4-5. Comparison for fractional EIA calculated from the original Ebrahimian et al. (2018) and the modified version for the study watersheds.....134

Figure 4-6. Example of resampling a finer model grid into coarser model grid137

Figure 4-7. TIA, Ksat, and EIA in SD and Fulton watershed.....143

Figure 4-8. Lowland, Hillslope, and Upland HRU distribution and its overlay with EIA in 90m resolution. EIA is displayed with dynamical range adjustment for easy indication.145

Figure 4-9. Comparison of NSE performance in Sim and FA under identical parameter set inputs.....148

Figure 4-10. Relationship between parameter value and NSE performance in 1km models. Scatter points are stacked together in certain parameter groups for legibility. Kf_{Fast} (Kf for overland flows), Kf_{Slow} (Kf for subsurface flows), and $Sumax_{Hi}$ (Hillslope and Upland).149

Figure 4-11. Parameter importance estimated by Random Forest algorithm (top 10% performing models)151

Figure 4-12. Average performance metric scores and hydrologic signature values from top 1% performing Sim and FA models153

Figure 4-13. Runoff contribution from HRUs. GW: deep groundwater runoff, U-SSF & U-HOF: Upland preferential subsurface flow and Hortonian overland flow, L-SOF: Lowland Saturation excess overland flow, H-SSF: Hillslope preferential subsurface flow, Imp: Direct runoff from EIA.154

Figure 4-14. Decomposed Hydrograph from best performing 1% Sim and FA model ensemble in Fulton.....155

LIST OF TABLES

Table 2-1. Simplified Definition for Myers Coupling Levels (Alghamdi, 2008; Fenton and Melton, 1990)21

Table 2-2. Range of reasonable TOPMODEL parameter ranges (Cho *et al.*, 2019; Nan *et al.*, 2011; Sigdel *et al.*, 2011).....33

Table 2-3. Summary of affected TOPMODEL structure and coupling flux usage for each NWM-TOPMODEL one-way coupling options.38

Table 2-4. Statistical scores of NWM and NWM-TOPMODEL coupling options with the best parameter-set and GLUE bound related statistics (Simulation period Oct 01, 2015~Sep 30, 2019).....44

Table 3-1. Catchment information73

Table 3-2. Selected hydrologic signatures for each signature set.83

Table 3-3. (A) Ratio of cells overlap with identical values and (B) spatial correlation (raster modified T-test; Clifford *et al.*, 1989; Dutilleul *et al.*, 1993) between different land cover schemes.....86

Table 3-4. Water balance components in NWM, AP, and HUC12L (left), and proportional differences against AP in % (right). ET: Evapotranspiration, SFC: surface runoff, GW: subsurface runoff.88

Table 3-5. Comparison of water balance components between original and shuffled schemes. Percent-point difference in percent-point (left), and proportional difference in % (right). ET: Evapotranspiration, SFC: surface runoff, GW: subsurface runoff (“underground runoff”).89

Table 3-6. Qualitative summary and interpretation of relationship between LULC spatial representation aspects (areal Proportion and spatial pattern), model vertical water fluxes (catchment water balance), watershed response characteristics observed from streamflow hydrologic signatures (*Sigsfc – vt*: hydrologic signatures linked to near-surface vertical flux exchange, and *Siglat*: hydrologic signatures linked to lateral processes). X indicates the primary influencing factor, and (x) indicates potential influence may be present but its impact was insignificant (median change less than 5%) or highly variable.

.....96

Table 4-1. Basic information on the SD and Fulton Watershed 116

Table 4-2. Summary of urban adjustment by HRU-type 123

Table 4-3. Relational parameter constraints for major parameter groups, and their sampling range for the study watersheds 136

Table 4-4. Comparison plan for model configurations with different urban adjustment levels and affected model components in each of them. For comprehensive details, refer back to Table 4-2..... 138

Table 4-5. Average of annual water year water balance during the study period (WY 2014 - 2018)..... 141

Table 4-6. Comparison of EIA estimation from empirical formulas’ mean (compiled by Sultana et al., 2020), original and modified method of Ebrahimian et al. (2018). 144

Table 4-7. HRU distribution in SD and Fulton study watersheds, and each proportion of TIA situated in each HRU to total watershed TIA 144

Table 4-8. Comparison of model performance metric and hydrologic signature average in top 10% performing (NSE) parameter sets for original FLEX-Topo, Sim, and FA model.

.....147

Chapter 1. Introduction

This dissertation explores the balanced integration of watershed data, hydrologic process knowledge, and diverse models within a particular modular framework that enables users to apply multiple different models across different watersheds. Through experiments with various model configurations across different watershed environments, the research assesses their impact on predictive accuracy and process representation. The aim is to enhance water resources management by addressing often overlooked questions in hydrologic modeling. This study provides practical insights for improving watershed management practices, contributing both to academic knowledge and practical modeling strategies. The findings are expected to contribute both to academic knowledge and practical modeling strategies, advancing the field of hydrology and its application in real-world scenarios.

1.1. Introduction to Hydrologic Modeling and Modular Approaches

Hydrologic modeling is fundamental to understanding the dynamic interactions between climate and land-surface hydrology (Singh and Woolhiser, 2002). Over the years, a range of hydrologic model representations have been developed, evolving from simple empirical formulas to sophisticated and physically-based simulations that attempt to capture the complex behaviors of water movement within various landscapes. Despite their importance and advancement, the inherent heterogeneity and uncertainty of hydrological processes remain a challenge for hydrological modeling, as balancing realism with model structure complexity remains crucial for achieving "the right answer for the right reason" (Kirchner, 2006). This is particularly important because the understanding of reality is shaped by the frameworks of scientific models and their explanatory power (Hawking, 2010).

The quest for realism has led to two distinct predominant model formulation and design philosophies in hydrology: bottom-up methods and top-down methods. Bottom-up methods build spatially explicit, detailed, and physics-based model formulation and structures, often referred to as physically based models (Ebel and Loague, 2006; Wagener et al., 2007). These models offer detailed process insights but can become overly complex and difficult to understand (Beven, 1993; Wagener et al., 2003, 2007; Wagener and Gupta, 2005). In contrast, top-down design, which opt for simplicity and parsimony, capture dominant watershed behaviors by testing multiple working hypotheses (Klemeš, 1986) often referred as conceptual models. Advocated by researchers like Klemeš (1986), these models provide generalized yet effective solutions that manage the heterogeneity and complexities of hydrological processes (Savenije, 2010). The optimal modeling strategy may involve blending these approaches, balancing complexity with simplification to handle diverse water management demands and accurately represent large-scale interactions (Archfield et al., 2015). These strategies should complement each other based on modeling goals rather than being mutually exclusive (Hrachowitz and Clark, 2017).

Such philosophical considerations become even more challenging when accounting for the complex interplay between natural and artificial components resulting from human impact and environmental changes. Many studies that focused on how different model philosophies (e.g., top-down vs bottom-up) affect model outcomes are primarily conducted in pristine watersheds, often neglecting the complexities introduced by human activities. The integration of these real-world factors into hydrologic models adds another layer of complexity. As urbanization continues—with over 68% of the global population expected to reside in urban areas by 2050 (United Nations, 2018)—and urban land use expands rapidly (Seto et al., 2010),

assessing both intended and unintended impacts becomes crucial for effective water management amid climate change (Haddeland et al., 2014). While modeling techniques have evolved from a single focus on peak flows to encompassing holistic watershed behaviors, they often suffer from inconsistencies in data availability and heterogeneity in local hydrologic processes (Fletcher et al., 2013; Salvadore et al., 2015).

In response to these challenges, the hydrology community has been moving towards more modularized hydrologic modeling approaches. These modular systems, such as NOAA's next-generation National Water Model (Johnson et al., 2019) or DELFT-FEWS (Werner et al., 2013) exemplify the shift toward frameworks that integrate various models and formulations, each chosen for its ability to address specific aspects of the hydrological cycle. This flexibility allows models to be tailored to specific environmental settings, enhancing their relevance in applications ranging from urban to natural landscapes.

Modular modeling supports the idea of model-dependent realism (Hawking, 2010), where the reality captured by a model depends on its design and the specific phenomena it aims to represent. This approach acknowledges that no single model can capture every aspects of complex hydrological processes across different watersheds, particularly in rapidly changing or highly impacted environments (Fletcher et al., 2013; Salvadore et al., 2015). By incorporating various model structures—top-down (physically based), bottom-up (conceptual), urban, and pristine—under a modular system, the hydrology community can better address the diverse challenges posed by different landscapes. This advocacy for adaptable modular modeling is expected to aid water resource management decisions across various environments undergoing rapid changes.

This introduction to hydrologic modeling and the necessity for modular approaches sets the stage for a detailed exploration of how these systems can be effectively implemented to address the challenges posed by diverse and changing hydrologic environments. The subsequent sections will delve deeper into the specific aspects of modular modeling explored in this study. They will introduce the purpose of the study and provide an overview of each chapter, detailing their specific goals, methodologies, and anticipated impacts of the research.

1.2. Purpose of the Study

The overarching objective of this dissertation is to navigate the balance between complexity and conceptual clarity in hydrological modeling to support modular approaches. This research explores the integration of watershed data, hydrologic process knowledge, and diverse model structures. By experimenting with various model configurations, this study examines the relationships between unique hydrological processes controlled by landscape, their conceptualization and formulation in model structures, the spatial representation of heterogeneity, and prediction accuracy.

Two central driving assumptions guided the direction of this research. The first assumption is that in a modular modeling setup, combining two different models with contrasting design philosophy can still improve explanatory power as a whole. For example, handling more uncertain hydrological processes with a simpler conceptual model while calculating surficial processes based on a spatially distributed and physically based Land Surface Model. This is because distributed meteorological inputs are often crucial for accurate sub-daily streamflow predictions, even with semi-lumped hydrologic models (Atkinson et al., 2003).

The second assumption is that watershed static inputs, like topography, soil types, and land cover, have varying usefulness depending on the region and how models conceptualize and aggregate water fluxes. In highly uncertain processes, conceptualizing the context of how macroscale hydrological processes could occur based on given landscape data may be more important than explicit and full spatial variability. This idea is supported by findings that lumped conceptual models can better conceptualize and represent macroscale hydrological systems in some regions, while other regions need more spatial detail (Hrachowitz and Clark, 2017).

By testing these assumptions, this dissertation aims to provide insights into the practical applications and benefits of modular hydrologic models. The findings will help determine how different modeling approaches can be integrated to improve the accuracy and explanatory power of hydrological predictions across various landscapes. Ultimately, this research seeks to contribute valuable insights for enhancing water resource management in both urban and natural settings. The next section will outline the structure of this dissertation, detailing the specific goals, methodologies, and expected impacts of each chapter.

1.3. *Dissertation Structure and Overview*

This dissertation is divided into three main chapters that each address research questions that are related to the overarching purpose of the study and two hypotheses discussed in the previous section.

Chapter 2, titled “Experimental Coupling of TOPMODEL with the National Water Model: Effects of Coupling Interface Complexity on Model Performance,” and published in the Journal of the American Water Resources Association (Kim et al., 2021), focuses on testing the validity of combining models with distinct spatial and process representations. It

also aimed to understand the importance of coupling methods within modular frameworks. This study couples a distributed LSM-module of the National Water Model (NWM) with a simpler, process-based runoff model to show the performance improvements and analyze how varying details in coupling methods can strongly affect predictive accuracy and model parameter sensitivity.

Chapter 3, titled “Untangling the Impacts of Land Cover Representation and Resampling in Distributed Hydrological Model Predictions,” published in *Environmental Modelling & Software* (Kim et al., 2024), studies how the spatial aspects of land cover inputs in a Land Surface Model (LSM) affect vertical and lateral hydrologic processes and simulated runoff. By comparing several commonly-used and synthetic land cover resampling methods, this study identifies how different spatial aspects (areal proportions of land cover classes and spatial patterns in land cover) impact catchment water balance calculations and runoff predictions.

Chapter 4, titled “Landscape-based Conceptual Modeling Framework to Delineate Urban Impact on Runoff Processes and Hydrological Pathways Using Effective Impervious Area,” investigates how landscape-based information can be embedded into a top-down landscape-oriented hydrologic model to represent complex alterations in hydrological pathways in urbanized watersheds. The study introduces a novel workflow that uses only the publicly available landscape data without considering detailed and often out-of-reach information (e.g., stormwater management plans, green infrastructure) to implement simplified urban hydrology concepts, guiding the modification of the Flex-Topo model to represent hydrologic process alterations for urban applications. The study assesses model behavior using a suite of

performance metrics to evaluate which types of model adjustments are effective in simulating urban flow dynamics and how they are affected by the model's spatial resolution.

The final chapter summarizes the overall conclusions of the research, discusses its implications for hydrologic research and water resources management, and outlines limitations and future research questions.

1.4. References

- Addor, N., G. Nearing, C. Prieto, A.J. Newman, N. Le Vine, and M.P. Clark, 2018. A Ranking of Hydrological Signatures Based on Their Predictability in Space. *Water Resources Research* 54:8792–8812.
- Archfield, S.A., M. Clark, B. Arheimer, L.E. Hay, H. McMillan, J.E. Kiang, J. Seibert, K. Hakala, A. Bock, T. Wagener, W.H. Farmer, V. Andréassian, S. Attinger, A. Viglione, R. Knight, S. Markstrom, and T. Over, 2015. Accelerating Advances in Continental Domain Hydrologic Modeling. *Water Resources Research* 51:10078–10091.
- Atkinson, S.E., M. Sivapalan, N.R. Viney, and R.A. Woods, 2003. Predicting Space-Time Variability of Hourly Streamflow and the Role of Climate Seasonality: Mahurangi Catchment, New Zealand. *Hydrological Processes* 17:2171–2193.
- Beven, K., 1993. Prophecy, Reality and Uncertainty in Distributed Hydrological Modelling. *Advances in Water Resources* 16:41–51.
- Beven, K.J., 2000. Uniqueness of Place and Process Representations in Hydrological Modelling. *Hydrology and Earth System Sciences* 4:203–213.
- Beven, K.J. and M.J. Kirkby, 1979. A Physically Based, Variable Contributing Area Model of Basin Hydrology. *Hydrological Sciences Bulletin* 24:43–69.
- Blöschl, G., M.F.P. Bierkens, A. Chambel, C. Cudennec, G. Destouni, A. Fiori, J.W. Kirchner, J.J. McDonnell, H.H.G. Savenije, M. Sivapalan, C. Stumpff, E. Toth, E. Volpi, G. Carr, C. Lupton, J. Salinas, B. Széles, A. Viglione, H. Aksoy, S.T. Allen, A. Amin, V. Andréassian, B. Arheimer, S.K. Aryal, V. Baker, E. Bardsley, M.H. Barendrecht, A. Bartosova, O. Batelaan, W.R. Berghuijs, K. Beven, T. Blume, T. Bogaard, P. Borges de Amorim, M.E. Böttcher, G. Boulet, K. Breinl, M. Brilly, L. Brocca, W. Buytaert, A. Castellarin, A. Castelletti, X. Chen, Y. Chen, Y. Chen, P. Chiffard, P. Claps, M.P. Clark, A.L. Collins, B. Croke, A. Dathe, P.C. David, F.P.J. de Barros, G. de Rooij, G. Di Baldassarre, J.M. Driscoll, D. Duethmann, R. Dwivedi, E. Eris, W.H. Farmer, J. Feiccabrino, G. Ferguson, E. Ferrari, S. Ferraris, B. Fersch, D. Finger, L. Foglia, K. Fowler, B. Gartsman, S. Gascoin, E. Gaume, A. Gelfan, J. Geris, S. Gharari, T. Gleeson, M. Glendell, A. Gonzalez Bevacqua, M.P. González-Dugo, S. Grimaldi, A.B. Gupta, B. Guse, D. Han, D. Hannah, A. Harpold, S. Haun, K. Heal, K. Helfricht, M. Herrnegger, M. Hipsey, H. Hlaváčiková, C. Hohmann, L. Holko, C. Hopkinson, M. Hrachowitz, T.H. Illangasekare, A. Inam, C. Innocente, E. Istanbuluoglu, B. Jarihani, Z. Kalantari, A. Kalvans, S. Khanal, S. Khatami, J.

- Kiesel, M. Kirkby, W. Knoben, K. Kochanek, S. Kohnová, A. Kolechkina, S. Krause, D. Kremer, H. Kreibich, H. Kunstmann, H. Lange, M.L.R. Liberato, E. Lindquist, T. Link, J. Liu, D.P. Loucks, C. Luce, G. Mahé, O. Makarieva, J. Malard, S. Mashtayeva, S. Maskey, J. Mas-Pla, M. Mavrova-Guirguinova, M. Mazzoleni, S. Mernild, B.D. Misstear, A. Montanari, H. Müller-Thomy, A. Nabizadeh, F. Nardi, C. Neale, N. Nesterova, B. Nurtaev, V.O. Odongo, S. Panda, S. Pande, Z. Pang, G. Papacharalampous, C. Perrin, L. Pfister, R. Pimentel, M.J. Polo, D. Post, C. Prieto Sierra, M.H. Ramos, M. Renner, J.E. Reynolds, E. Ridolfi, R. Rigon, M. Riva, D.E. Robertson, R. Rosso, T. Roy, J.H.M. Sá, G. Salvadori, M. Sandells, B. Schaeffli, A. Schumann, A. Scolobig, J. Seibert, E. Servat, M. Shafiei, A. Sharma, M. Sidibe, R.C. Sidle, T. Skaugen, H. Smith, S.M. Spiessl, L. Stein, I. Steinsland, U. Strasser, B. Su, J. Szolgay, D. Tarboton, F. Tauro, G. Thirel, F. Tian, R. Tong, K. Tussupova, H. Tyralis, R. Uijlenhoet, R. van Beek, R.J. van der Ent, M. van der Ploeg, A.F. Van Loon, I. van Meerveld, R. van Nooijen, P.R. van Oel, J.P. Vidal, J. von Freyberg, S. Vorogushyn, P. Wachniew, A.J. Wade, P. Ward, I.K. Westerberg, C. White, E.F. Wood, R. Woods, Z. Xu, K.K. Yilmaz, and Y. Zhang, 2019. Twenty-Three Unsolved Problems in Hydrology (UPH)—a Community Perspective. *Hydrological Sciences Journal* 64:1141–1158.
- Cristiano, E., M.C. Ten Veldhuis, and N. Van De Giesen, 2017. Spatial and Temporal Variability of Rainfall and Their Effects on Hydrological Response in Urban Areas - A Review. *Hydrology and Earth System Sciences* 21:3859–3878.
- Ebel, B.A. and K. Loague, 2006. Physics-Based Hydrologic-Response Simulation: Seeing through the Fog of Equifinality. *Hydrological Processes* 20:2887–2900.
- Ebrahimian, A., J.S. Gulliver, and B.N. Wilson, 2018. Estimating Effective Impervious Area in Urban Watersheds Using Land Cover, Soil Character and Asymptotic Curve Number. *Hydrological Sciences Journal* 63:513–526.
- Ebrahimian, A., B.N. Wilson, and J.S. Gulliver, 2016. Improved Methods to Estimate the Effective Impervious Area in Urban Catchments Using Rainfall-Runoff Data. *Journal of Hydrology* 536:109–118.
- Endreny, T.A., 2005. Land Use and Land Cover Effects on Runoff Processes: Urban and Suburban Development. *Encyclopedia of Hydrological Sciences*. John Wiley & Sons, Ltd, Chichester, UK, p. . doi:10.1002/0470848944.hsa122.
- Epps, T.H. and J.M. Hathaway, 2019. Using Spatially-Identified Effective Impervious Area to Target Green Infrastructure Retrofits: A Modeling Study in Knoxville, TN. *Journal of Hydrology* 575:442–453.
- Euser, T., H.C. Winsemius, M. Hrachowitz, F. Fenicia, S. Uhlenbrook, and H.H.G. Savenije, 2013. A Framework to Assess the Realism of Model Structures Using Hydrological Signatures. *Hydrology and Earth System Sciences* 17:1893–1912.
- Fletcher, T.D., H. Andrieu, and P. Hamel, 2013. Understanding, Management and Modelling of Urban Hydrology and Its Consequences for Receiving Waters: A State of the Art. *Advances in Water Resources* 51:261–279.
- Gao, H., M. Hrachowitz, N. Sriwongsitanon, F. Fenicia, S. Gharari, and H.H.G. Savenije, 2016. Accounting for the Influence of Vegetation and Landscape Improves Model Transferability in a Tropical Savannah Region. *Water Resources Research* 52:7999–8022.

- Gharari, S., M.P. Clark, N. Mizukami, W.J.M. Knoben, J.S. Wong, and A. Pietroniro, 2020. Flexible Vector-Based Spatial Configurations in Land Models. *Hydrology and Earth System Sciences* 24:5953–5971.
- Gharari, S., M.P. Clark, N. Mizukami, J.S. Wong, A. Pietroniro, and H.S. Wheatler, 2019. Improving the Representation of Subsurface Water Movement in Land Models. *Journal of Hydrometeorology* 20:2401–2418.
- Gharari, S., M. Hrachowitz, F. Fenicia, H. Gao, and H.H.G. Savenije, 2014. Using Expert Knowledge to Increase Realism in Environmental System Models Can Dramatically Reduce the Need for Calibration. *Hydrology and Earth System Sciences* 18:4839–4859.
- Gharari, S., M. Hrachowitz, F. Fenicia, and H.H.G. Savenije, 2011. Hydrological Landscape Classification: Investigating the Performance of HAND Based Landscape Classifications in a Central European Meso-Scale Catchment. *HYDROLOGY AND EARTH SYSTEM SCIENCES* 15:3275–3291.
- Gharari, S., M. Shafiei, M. Hrachowitz, R. Kumar, F. Fenicia, H. V. Gupta, and H.H.G. Savenije, 2014. A Constraint-Based Search Algorithm for Parameter Identification of Environmental Models. *Hydrology and Earth System Sciences* 18:4861–4870.
- Haddeland, I., J. Heinke, H. Biemans, S. Eisner, M. Flörke, N. Hanasaki, M. Konzmann, F. Ludwig, Y. Masaki, J. Schewe, T. Stacke, Z.D. Tessler, Y. Wada, and D. Wisser, 2014. Global Water Resources Affected by Human Interventions and Climate Change. *Proceedings of the National Academy of Sciences of the United States of America* 111:3251–3256.
- Hawking, S., 2010. *The Grand Design*. Random House Digital, Inc.
- Hrachowitz, M. and M.P. Clark, 2017. HESS Opinions: The Complementary Merits of Competing Modelling Philosophies in Hydrology. *Hydrology and Earth System Sciences* 21:3953–3973.
- Jencso, K.G. and B.L. McGlynn, 2011. Hierarchical Controls on Runoff Generation: Topographically Driven Hydrologic Connectivity, Geology, and Vegetation. *Water Resources Research* 47:1–16.
- Jencso, K.G., B.L. McGlynn, M.N. Gooseff, S.M. Wondzell, K.E. Bencala, and L.A. Marshall, 2009. Hydrologic Connectivity between Landscapes and Streams: Transferring Reach- and Plot-Scale Understanding to the Catchment Scale. *Water Resources Research* 45:1–16.
- Johnson, J.M. and K.C. Clarke, 2021. An Area Preserving Method for Improved Categorical Raster Resampling. *Cartography and Geographic Information Science* 48:292–304.
- Johnson, D.W., N.J. Frazier, F.L. Ogden, S. Cui, D.L. Blodgett, J.D. Hughes, I. Norton, P. A., R. Cabell, D.W. Johnson, N.J. Frazier, F.L. Ogden, S. Cui, D.L. Blodgett, J.D. Hughes, I. Norton, P. A., and R. Cabell, 2019. Next Generation National Water Model Architecture: Organizing Principles to Support Evolving Capabilities. *AGUFM* 2019:H43I-2145.
- Kim, D.-H., Naliaka, A., Zhu, Z., Ogden, F. L., & McMillan, H. K. (2021). Experimental Coupling of TOPMODEL with the National Water Model: Effects of Coupling Interface Complexity on Model Performance. *Journal of the American Water Resources Association*. <https://doi.org/10.1111/1752-1688.12953>

- Kim, D.-H., Johnson, J. M., Clarke, K. C., & McMillan, H. K. (2024). Untangling the impacts of land cover representation and resampling in distributed hydrological model predictions. *Environmental Modelling & Software*, 172, 105893. <https://doi.org/10.1016/j.envsoft.2023.105893>
- Kirchner, J.W., 2006. Getting the Right Answers for the Right Reasons: Linking Measurements, Analyses, and Models to Advance the Science of Hydrology. *Water Resources Research* 42. doi:10.1029/2005WR004362.
- Klemeš, V., 1986. Dilettantism in Hydrology: Transition or Destiny? *Water Resources Research*. doi:10.1029/WR022i09Sp0177S.
- Knoben, W.J.M., J.E. Freer, M.C. Peel, K.J.A. Fowler, and R.A. Woods, 2020. A Brief Analysis of Conceptual Model Structure Uncertainty Using 36 Models and 559 Catchments. *Water Resources Research* 56. doi:10.1029/2019wr025975.
- Mai, J., J.R. Craig, B.A. Tolson, and R. Arsenault, 2022. The Sensitivity of Simulated Streamflow to Individual Hydrologic Processes across North America. *Nature Communications* 2022 13:1 13:1–11.
- Markstrom, S.L., L.E. Hay, and M.P. Clark, 2016. Towards Simplification of Hydrologic Modeling: Identification of Dominant Processes. *Hydrology and Earth System Sciences* 20:4655–4671.
- McDonnell, J.J., M. Sivapalan, K. Vaché, S. Dunn, G. Grant, R. Haggerty, C. Hinz, R. Hooper, J. Kirchner, M.L. Roderick, J. Selker, and M. Weiler, 2007. Moving beyond Heterogeneity and Process Complexity: A New Vision for Watershed Hydrology. *Water Resources Research* 43. doi:10.1029/2006WR005467.
- McMillan, H., 2020. Linking Hydrologic Signatures to Hydrologic Processes: A Review. *Hydrological Processes* 34:1393–1409.
- Nobre, A.D., L.A. Cuartas, M. Hodnett, C.D. Renno, G. Rodrigues, A. Silveira, M. Waterloo, and S. Saleska, 2011. Height Above the Nearest Drainage - a Hydrologically Relevant New Terrain Model. *JOURNAL OF HYDROLOGY* 404:13–29.
- Ogden, F.L., N. Raj Pradhan, C.W. Downer, and J.A. Zahner, 2011. Relative Importance of Impervious Area, Drainage Density, Width Function, and Subsurface Storm Drainage on Flood Runoff from an Urbanized Catchment. *Water Resources Research*. doi:10.1029/2011WR010550.
- Prieto, C., N. Le Vine, D. Kavetski, F. Fenicia, A. Scheidegger, and C. Vitolo, 2022. An Exploration of Bayesian Identification of Dominant Hydrological Mechanisms in Ungauged Catchments. *Water Resources Research*:e2021WR030705.
- Rahman, M. and R. Rosolem, 2017. Towards a Simple Representation of Chalk Hydrology in Land Surface Modelling. *Hydrology and Earth System Sciences* 21:459–471.
- Renno, C.D., A.D. Nobre, L.A. Cuartas, J.V. Soares, M.G. Hodnett, J. Tomasella, and M.J. Waterloo, 2008. HAND, a New Terrain Descriptor Using SRTM-DEM: Mapping Terra-Firme Rainforest Environments in Amazonia. *REMOTE SENSING OF ENVIRONMENT* 112:3469–3481.
- Rosero, E., L.E. Gulden, Z.L. Yang, L.G. de Goncalves, G.Y. Niu, and Y.H. Kaheil, 2011. Ensemble Evaluation of Hydrologically Enhanced Noah-LSM: Partitioning of the Water Balance in High-Resolution Simulations over the Little Washita River Experimental Watershed. *Journal of Hydrometeorology* 12:45–64.

- Saadi, M., L. Oudin, and P. Ribstein, 2020. Beyond Imperviousness: The Role of Antecedent Wetness in Runoff Generation in Urbanized Catchments. *Water Resources Research*. doi:10.1029/2020WR028060.
- Salvadore, E., J. Bronders, and O. Batelaan, 2015. Hydrological Modelling of Urbanized Catchments: A Review and Future Directions. *Journal of Hydrology* 529:62–81.
- Savenije, H.H.G., 2010. HESS Opinions “Topography Driven Conceptual Modelling (FLEX-Topo).” *Hydrology and Earth System Sciences* 14:2681–2692.
- Schaake, J.C., V.I. Koren, Q.Y. Duan, K. Mitchell, and F. Chen, 1996. Simple Water Balance Model for Estimating Runoff at Different Spatial and Temporal Scales. *Journal of Geophysical Research Atmospheres* 101:7461–7475.
- Seto, K.C., R. Sánchez-Rodríguez, and M. Fragkias, 2010. The New Geography of Contemporary Urbanization and the Environment. *Annual Review of Environment and Resources* 35:167–194.
- Shuster, W.D., J. Bonta, H. Thurston, E. Warnemuende, and D.R. Smith, 2005. Impacts of Impervious Surface on Watershed Hydrology: A Review. *Urban Water Journal* 2:263–275.
- Sikorska, A.E., D. Viviroli, and J. Seibert, 2015. Flood-Type Classification in Mountainous Catchments Using Crisp and Fuzzy Decision Trees. *Water Resources Research* 51:7959–7976.
- Singh, V.P. and D.A. Woolhiser, 2002. Mathematical Modeling of Watershed Hydrology. *Journal of Hydrologic Engineering* 7:270–292.
- Smith, J.A., M.L. Baeck, J.E. Morrison, P. Sturdevant-Rees, D.F. Turner-Gillespie, and P.D. Bates, 2002. The Regional Hydrology of Extreme Floods in an Urbanizing Drainage Basin. *Journal of Hydrometeorology* 3:267–282.
- Stieglitz, M., D. Rind, J. Famiglietti, and C. Rosenzweig, 1997. An Efficient Approach to Modeling the Topographic Control of Surface Hydrology for Regional and Global Climate Modeling. *Journal of Climate* 10:118–137.
- Tehrany, M.S., B. Pradhan, and M.N. Jebur, 2013. Spatial Prediction of Flood Susceptible Areas Using Rule Based Decision Tree (DT) and a Novel Ensemble Bivariate and Multivariate Statistical Models in GIS. *Journal of Hydrology* 504:69–79.
- Umair, M., D. Kim, and M. Choi, 2019. Impacts of Land Use/Land Cover on Runoff and Energy Budgets in an East Asia Ecosystem from Remotely Sensed Data in a Community Land Model. *Science of The Total Environment* 684:641–656.
- United Nations, 2018. World Urbanization Prospects: The 2018 Revision. doi:10.18356/b9e995fe-en.
- Van De Ven, F.H.M., 1990. Water Balances of Urban Areas. *Hydrological Processes and Water Management in Urban Areas. Lectures and Papers, UNESCO/IHP Symposium, Duisburg, Lelystad, Amsterdam, and Rotterdam, 1988:21–32.*
- Vrebos, D., T. Vansteenkiste, J. Staes, P. Willems, and P. Meire, 2014. Water Displacement by Sewer Infrastructure in the Grote Nete Catchment, Belgium, and Its Hydrological Regime Effects. *Hydrology and Earth System Sciences* 18:1119–1136.
- Wagener, T. and H. V. Gupta, 2005. Model Identification for Hydrological Forecasting under Uncertainty. *Stochastic Environmental Research and Risk Assessment* 19:378–387.

- Wagener, T., N. McIntyre, M.J. Lees, H.S. Wheater, and H. V. Gupta, 2003. Towards Reduced Uncertainty in Conceptual Rainfall-Runoff Modelling: Dynamic Identifiability Analysis. *Hydrological Processes* 17:455–476.
- Wagener, T., M. Sivapalan, P. Troch, and R. Woods, 2007. Catchment Classification and Hydrologic Similarity. *Geography Compass* 1:1–31.
- Werner, M., J. Schellekens, P. Gijssbers, M. van Dijk, O. van den Akker, and K. Heynert, 2013. The Delft-FEWS Flow Forecasting System. *Environmental Modelling and Software* 40:65–77.
- White, M.D. and K.A. Greer, 2006. The Effects of Watershed Urbanization on the Stream Hydrology and Riparian Vegetation of Los Peñasquitos Creek, California. *Landscape and Urban Planning* 74:125–138.
- Zhang, Z., L.E. Bortolotti, Z. Li, L.M. Armstrong, T.W. Bell, and Y. Li, 2021. Heterogeneous Changes to Wetlands in the Canadian Prairies Under Future Climate. *Water Resources Research* 57:e2020WR028727.
- Zhao, W. and A. Li, 2015. A Review on Land Surface Processes Modelling over Complex Terrain. *Advances in Meteorology* 2015. doi:10.1155/2015/607181.

Chapter 2. Experimental Coupling of TOPMODEL with the National Water Model: Effects of coupling interface complexity on model performance.

Abstract

The study had two objectives; (1) Substitute National Water Model's (NWM) runoff calculation with a conceptual hydrologic model (TOPMODEL) to simplify the model structure and resolve potential drawbacks of applying NWM in headwater catchments. (2) investigate how varying the coupling interface (location of coupling, type of fluxes used, modification of sub-models) affects model behavior of when one-way coupling the NWM's Land Surface Model (LSM; Noah-MP), which focuses on calculation of land-vegetation-atmospheric water/energy flux exchange, with TOPMODEL using 6 different scenarios. The one-way coupled model outperformed NWM and non-coupled TOPMODEL. The coupling option limiting reliance on LSM's surface and subsurface water fluxes by constraining them within the TOPMODEL structure was the most successful. Performance declined when coupling configurations relied more on LSM calculated fluxes to override TOPMODEL internal processes. Varying the coupling interface brought unexpected changes in TOPMODEL's parameter sensitivity and water budget even while the statistical score remained similar. The coupling interface represents a source of structural uncertainty that could be identified through conventional evaluation of performance, uncertainty, and sensitivity due to the simple structure of our one-way coupling design. The study shows the benefits of combining the strengths of land surface and conceptual hydrological models, while recognizing that structural uncertainty from coupling design needs to be acknowledged.

2.1. Introduction

The National Water Model (NWM) is an operational system that provides hourly streamflow predictions for over 12.8 million km of streams and rivers in the Continental United States, and recently extended to Hawaii, Puerto Rico, and portions of Alaska. This system pursues the highest accuracy possible and requires the best available forcing data for reliable operation. It provides complementary hydrologic guidance for National Weather Service (NWS) river forecast locations and covers under-served locations (Office of Water Prediction, The National Water Model. Accessed March 17, 2020, <https://water.noaa.gov/about/nwm>). The current version of NWM is based on the Weather Research and Forecasting Hydrologic model (WRF-Hydro) v5.1.2 developed and supported by the National Center for Atmospheric Research (NCAR), which couples land surface model (LSM; Noah-MP) and routing modules and offers several physics options based on grid-cell spatial representation.

Even though NWM has been successful through several years of operation, it is found that forecast skill is limited by model architecture that applies a uniform model structure and spatial scale over the whole domain (Johnson et al., 2019). The majority of U.S. river network and watershed areas in the US can be classified as headwaters and 34% of stream length has a moderate-high (2 - 4%) gradient (McManamay and Derolph, 2019). Topographical influence on hydrological processes can be significant in smaller catchments (Stieglitz et al., 1997; Zhao and Li, 2015), but the spatial resolution of NWM's terrain routing grid (250m) is coarse enough to miss some topographic details. Further, the interface between shallow soil water, conceptual nonlinear groundwater reservoir, and underground discharge is controlled by simplified representations and calibrated parameters (Gochis et al., 2018, 2015), not by

detailed consideration of factors such as watershed landforms. Although Noah-MP can apply simplified runoff generation routines based on topography index at LSM grid scale (Niu et al., 2005, 2007), this option is not used in the current NWM configuration.

NWM has high computational demand due to LSM-based model structure, and it hinders solutions such as applying a finer resolution grid or applying watershed-by-watershed calibration for better parameterization. Finer resolution increases the number of cells to calculate by the square and requires a smaller flow routing time-step to maintain a stable calculation with the Courant number under 1.0 (Gochis et al., 2018). Calibration of individual watersheds requires supercomputer support even at US Geological Survey Hydrologic Unit Code 10 watershed scale (160 to 1010 km² or 62 to 390 mi²) (Gochis et al., 2015; Seaber et al., 1987; Xue et al., 2018).

Application of land surface models offers the benefit of providing a process-rich simulation of terrestrial hydrology (Archfield et al., 2015; Clark, Fan, et al., 2015; Fan et al., 2019). However, recent studies pointed out several shortcomings related to applying LSM based streamflow prediction. LSMs do not typically consider macropore water movement or preferential flow scheme in subsurface representation, and rely solely on Richards equation within 1-D soil column. This can result in poor streamflow prediction with flashy runoff superimposed on slow recessions, but can be improved by including such processes into LSMs (Gharari et al., 2019; Rahman and Rosolem, 2017). At watershed scale, experiments with spatially flexible vector-based LSM configurations have shown that varying spatial discretization of land cover, soil types, and topography did not significantly affect streamflow prediction performance (Gharari et al., 2020).

Mendoza et al. (2015) claimed that poor performance of hydrologic modeling using complex physics-based models originates from the inflexible structure and unnecessarily strict constraints, and integration of strengths of both physics-based and conceptual modeling philosophy is needed. From such, the study suggests that the current subsurface representation of LSMs lacks an ability to upscale runoff processes from soil-column, to hillslope, and to watershed. Applying hillslope-scale terrain structure to LSMs or Earth System Models (ESM) has the potential to fundamentally change the way of organizing water, energy, and biogeochemical storage and fluxes (Fan et al., 2019), however, such redesign is still in early stage. Therefore, a solution to provide stable streamflow prediction with the current soil column grid based LSM structure is still lacking.

The next-generation NWM architecture tries to provide solutions to such demand. It aims to build the framework that enables heterogeneous, regionalized physics for continental to a local extent, integrating conceptual to physical models with a consistent model coupling method to overcome such limitations (Johnson et al., 2019). This future design concept of NWM provided a basis for this study to derive two objectives as follows:

1. To test implementation of alternate subsurface representation in NWM in headwater catchment using an existing simple hydrologic model. The study aimed to explore potential benefits in hydrologic fidelity when coupling NWM's LSM (Noah-MP) with a conceptual hydrologic model instead of WRF-Hydro runoff routing modules.

2. To identify the effects of the coupling method or interface using a simplistic modular approach in consideration of the next-generation NWM blueprint. The term "coupling interface" is defined as a composite of coupling elements such as the location where coupling

engages, level of dependency between models, type of fluxes (hydrologic variable) transferred, and level of modification of the sub-models' internal processes.

The controlled model experiment was planned to fulfill both objectives. Multiple coupled model scenarios were tested to investigate how various coupling interfaces affect the behavior of hydrologic models by tracking changes in predictive performance, uncertainty, and parameter sensitivity. TOPography-based hydrological MODEL (TOPMODEL; Beven and Kirkby, 1979) was selected to be coupled with Noah-MP according to following general criteria; 1) the model should use high-resolution topographical data not only to calculate surface routing but to represent hydrologic characteristics of the area, 2) the model should simulate soil moisture, groundwater, and their interaction 3) the model should have low computational demand to enable experiments with parameter optimization.

The literature is replete with examples where TOPMODEL successfully simulates runoff, and it is often used as a benchmark model for studies that expand or propose new formulations of the relationship between the water table and runoff processes (Clark, Fan, et al., 2015; Van Den Hurk et al., 2011). TOPMODEL proposes a combined groundwater pathway that respects topography and simulates the decrease of hydraulic conductivity with depth as commonly observed in field studies. Watershed hydrology studies often seek to understand and model the emergent behavior at a watershed scale, because some hydrologic responses become comprehensible when simplified at this scale. From this perspective, TOPMODEL, which operates at the watershed scale, may also provide an advantage over grid-based NWM in applying domain knowledge about watersheds. The study compared NWM v1.2.2 and original TOPMODEL as benchmarks, with a total of six LSM-TOPMODEL one-way coupled scenarios to test the effects of alternative coupling interfaces to meet both of study objectives.

2.2. Review

2.2.1. Purpose of Coupling Hydrological Models

Hydrological models have been widely coupled with GIS or land surface models for flood prediction or environmental modeling (Shen and Phanikumar, 2010; Vincendon et al., 2010; Walko et al., 2000). Since numerous applications exist, detailed objectives vary by case; however, they share a similar intention of coupling existing concepts or models to expand modeling capability, to better represent real-world phenomena, and to improve model prediction.

The coupling of different models is intrinsic to hydrologic modeling frameworks with a modular design. The need for a modular modeling approach to allow multiple physics options has been suggested by the research community in hydrological modeling. For instance, Butts et al. (2004) suggested that exploration of various combinations and ensembles of model structures can improve the capability of hydrological modeling. The Structure for Unifying Multiple Modeling Alternatives (SUMMA) model is one example of the modular approach (Clark, Nijssen, et al., 2015). Similarly, the core of the NWM, Noah-MP and WRF-Hydro, use a modular approach, by enabling the users to choose different formulations to calculate infiltration, subsurface flow, channel flow, and more (Gochis et al., 2015; Xue et al., 2018).

The development of hydrologic models requires hydrologists to create their own ‘perceptual model’, a simplified analysis that identifies the dominant processes in the watershed, before encoding these ideas into a computer model (Beven, 2012). Such perceptual models depend on the watershed and climate of interest, and have been criticized as being centered on temperate regions, while being less suitable for arid or tropical regions (Linton, 2008). Considering this link between hydro-climatic setting and model structure, the

expectation that a single model formulation to perform reliably in all possible situations seems unlikely. However, it may not be easy for researchers to switch between modeling software or platform according to region-specific needs because the model operation and data requirements can vary greatly. The modular approach enables researchers to more easily choose a model formulation that is expected to suit the situation, instead of forcing a pre-selected model to fit a new region by using excessive parameter calibration or adopting a whole new modeling framework.

2.2.2. Coupling in hydrological modeling and relationship with a software design perspective

Coupling of hydrological models and larger-scale models can be categorized into three types (Mölders, 2001); 1) parameterizing atmospheric models with hydrologic descriptions, 2) coupling hydrologic models by data exchange, 3) integrating hydrologic model structure with land surface models (hydrometeorological models). In the study we investigate the second and third types. Within these types, the coupling of hydrologic models can be one-way or two-way. One-way coupling transfers the data (flux) from one model to another model in sequential order and can be also called “external coupling” (Morita and Yen, 2000). Two-way coupling allows two-way transfer of data between models, usually forming an implicitly coupled set of equations involving hydrological variables for each timestep. Coupling of hydrological models is done by software implementation, therefore, brief knowledge of coupling from a software design perspective is beneficial.

Coupling denotes the connection and relationships between different modules or functions. On the other hand, cohesion represents the internal relationship and functional strength within each module or function. “Coupling” and “cohesion” are two key elements of

structured modular design that determine the ease of software maintenance or modification (Yourdon and Constantine, 1979). Low level or loose coupling indicates lower interdependency between modules. Higher cohesion keeps modules contained to themselves and their objectives. The general rule of thumb is to keep coupling low and keep cohesion high. Establishing low coupling and high cohesion provide two benefits; changing one component without affecting others, and easier to understand each component without having to investigate others (Yourdon and Constantine, 1979). One-way coupling of hydrological models is typically considered as loose coupling, and two-way coupling is typically considered as tight coupling.

After Myers (1975) defined six levels of coupling, and metrics and coupling levels were ordered by Page-Jones (1988) according to their effects on understandability, maintainability, modifiability, and reusability (Offutt et al., 1993). Some variability may exist in detailed definitions or classifications between different studies (Alghamdi, 2008; Fenton and Melton, 1990); however, we summarized five basic types of coupling with a simplified plain-language explanation (Table 2-1).

Each type of coupling (one-way and two-way) in hydrological modeling has tradeoffs. Numerous studies concluded that tight two-way coupling generally delivers an improvement in model prediction compared to one-way coupling, at the expense of higher computation load for processing feedback loops. For instance, full two-way coupling outperforms one-way coupling in WRF/WRF-Hydro system in streamflow estimation and precipitation simulation, however, the mechanism behind the improvement in the model simulations was not systematically studied together (Givati et al., 2016; Senatore et al., 2015).

Table 2-1. Simplified Definition for Myers Coupling Levels (Alghamdi, 2008; Fenton and Melton, 1990)

Coupling Level	Coupling Type	Simplified Definition
0	Uncoupled	No communication
1	Data Coupling	Modules communicate by passing data structure as a parameter and the whole component of it is used in the receiving module (no control element included)
2	Stamp Coupling	Modules share common data structure, but only some part or field being used (passing record type variable)
3	Control Coupling	One module passes a control parameter to the next module (decide function or flow of execution)
4	Common Coupling	Multiple modules refer to the same global data (can access and change the value)
5	Content Coupling	Modules can directly access or change other module's internal components (data or procedural state)

Meanwhile, uncertainty in coupled hydrologic models is not always well understood nor defined, and it is especially challenging in two-way coupling mostly due to high computation cost and complex interplay between components (Moges et al., 2020). Moges et al. (2020) developed an uncertainty propagation framework that provides relatively comprehensive uncertainty information on coupled models; interaction between input variables, uncertainty from sub-models, and how it propagates through the coupled model. Even though the framework is extensive, structural uncertainty from the sub-model or coupling interface was not included. Alternatively, each sub-model can remain cohesive and independent in one-way coupling. This allows a straightforward application of traditional uncertainty/sensitivity analysis based on a random sampling method. However, such technical advantage comes with

the expense of not including feedback processes that exist in real-world phenomenon into the model representation.

Coupling of hydrological models and coupling in software design is not directly comparable, but it provides some useful insights. The goal and practical implementation of hydrological modeling is unlikely to allow the lowest level of coupling or the highest cohesion. However, software coupling knowledge on the effects of higher level (two-way) coupling alerts us to potential pitfalls in hydrological application. For instance, a higher level of software coupling can reduce the understandability of internal processes and interplay between components, and such can impede the modifiability of the whole system (Offutt et al., 1993; Page-Jones, 1988). When considering the future of modular modeling approaches in hydrology, the coupling design should therefore pay particular attention to our ability to understand coupled model behavior and modify the component models in a flexible way, rather than only focusing on computational expense and prediction performance.

2.2.3. Model Description: NWM and Its Coupling Scheme

The WRF-Hydro model, which presently serves as the core of the NWM, not only can be coupled with the atmospheric model's (WRF) forecast, but is itself a coupled model, consisting of multiple modules and their couplings. Each module is designed with its own task: land surface model, subsurface flow routing, overland flow routing, channel routing, conceptual groundwater, and optional water management modules. WRF-Hydro offers multiple physics options or formulations to be used in the model simulation, and it enables more flexible applications compared to fully integrated models that can only operate in a single configuration. However, the current version of NWM represents a single configuration of the WRF-Hydro and the operational model is not necessarily easily extensible.

Simulation in the NWM consists of a complex workflow that can be summarized as follows. Noah-MP (Multi Parameterization), which is one of the WRF-Hydro's LSM options and the norm for the NWM, simulates land surface processes on a 1km x 1km grid. Routing modules (surface, subsurface, and channel) run simultaneously based on geographical domain, but on a different spatial scale and time step. For instance, the NWM uses a 250m x 250m routing grid and a 15 second time step (Gochis et al., 2018). Rainfall, snow-melt, and throughfall are partitioned into soil moisture and direct runoff in the NWM using the empirical function of runoff/infiltration parameter (REFKDT; Schaake et al., 1996), which is similar to probability distributed approach by Moore (1985). Both methods are essentially nonlinear regressions, not dissimilar from the widely used Curve Number (CN) approach (Cronshey et al., 1985). Sub-surface and overland flow routing modules import different target variables (fluxes) from the LSM to calculate runoff. Routing modules redistribute the water laterally, and feedback into the LSM, updating soil moisture status. Groundwater is represented as a lumped conceptual nonlinear conceptual reservoir model for each catchment and receives spatially aggregated drainage from the soil profile (Gochis et al., 2015; Senatore et al., 2015). The channel flow routing module imports multiple state variables from other runoff related modules, then solves the channel flow using Muskingum-Cunge hydrologic routing (Arnault et al., 2016).

NWM's complex design can impede its modifiability. Even though we believe NWM is designed to be "data coupled" at the code to function level, its overall behavior can be comparable to a mixture of "Data coupling", "Stamp Coupling", or even "Control Coupling" (Table 1). Simulation involves numerical solutions for which execution or timestep can vary based on other modules' output. The structure of the data that includes hydrological fluxes

can vary between each module's internal processes due to the different temporal and spatial scales of different modules. This ultimately requires a sort of data parsing for data sharing. All these needs increase the level of coupling and one module's dependency on the previous process step. Underlying constraints originating from the model's purpose to pursue hydrological integrity can build up and make the model less flexible than intended. In such a complex system, a small change in one component's usage or option can affect the whole following process steps with a "ripple effect" (Bilal and Black, 2006). Due to this nature of complexity, newly coupling an existing hydrologic model's component and structure into NWM (WRF-Hydro) system can be difficult.

2.2.4. Model Description: TOPMODEL and its Coupling with LSMs

TOPMODEL, initially published by Beven and Kirkby (1979), is considered as a set of conceptual tools utilized to model hydrological processes, specifically surface and subsurface contributing area dynamics, in a relatively simple way (Beven, 1997; Beven and Kirkby, 1979). It is based on a theory of hydrological similarity of points in a catchment, determined by deriving a Topographic Wetness Index (TWI) from a Digital Elevation Model (DEM) (Beven and Kirkby, 1977). The TWI represents a hydrological similarity of an area and categorizing these continuous values into simplified classes in TOPMODEL reduces data and the number of model parameters required in simulations (Kirkby, 1975; Kirkby and Weyman, 1974). The simplified structure of TOPMODEL gives it a combination of computational and parametric efficiency with clear foundations in physics (Beven et al., 1995; Beven, 1984).

TOPMODEL's ability to aptly represent the impacts of terrain on hydrological processes (soil and groundwater movement) using digital terrain model data has led to its popularity in application of its concept to many LSMs. Noah-MP (LSM) offers runoff/groundwater scheme

options based on a simplified version of TOPMODEL concepts to substitute the original gravitational free drainage option; “simple groundwater model” (SIMGM; Niu et al., 2007) and “simple TOPMODEL-based runoff parameterization” (SIMTOP, Niu et al., 2005) both parameterize surface and subsurface runoff as functions of water table depth (Gan et al., 2019). These simplifications include the use of an assumed topographic index distribution based on the global average value. This means that local topography is not necessarily used to derive the topographic index. While this may be appropriate for atmosphere modeling, it is an omission from the standpoint of local hydrologic prediction.

TOPMODEL has also been coupled with the other land surface models such as the Simplified Simple Biosphere Model (SSiB) (Deng and Sun, 2012), the soil–vegetation–atmosphere transfer (SVAT) and the Interactions between Soil, Biosphere, and Atmosphere model (ISBA) (Bouilloud et al., 2010; Decharme and Douville, 2006; Habets and Saulnier, 2001; Vincendon et al., 2010). HydroBlocks (Chaney et al., 2016) takes a slightly different approach by coupling Noah-MP with a fully operational Dynamic TOPMODEL, which is a hydrologic response unit (HRU) based semi-distributed hydrologic model that solves the kinematic wave routing algorithm instead of using a quasi-steady-state water table configuration. The result from previous implementations is promising; whether dedicated flow routing is involved or not, the studies have shown similar conclusions that the coupling of TOPMODEL with LSM improved discharge prediction.

Coupling design is an important aspect alongside any prediction improvement because it has a close relationship with hydrological process representation. Common strategies in previous studies can be summarized into two types. One is to integrate TOPMODEL concepts to laterally redistribute soil water in a watershed scale and feed it back LSM grid cell (two-

way coupling). Another is to provide water-table depth from LSM to TOPMODEL to calculate flow, then update LSM with the changed water-table depth in TOPMODEL (also two-way coupling). Deng and Sun (2012) imply that two-way feedback interaction between LSM and TOPMODEL results in complete hydrologic interdependency and cannot expect to entirely inherit the process representations of the base models. Even though coupling designs from previous studies resulted in successful streamflow prediction, there remains significant scope to improve our understanding of the effect of coupling interfaces on the coupled model's behavior and representation of hydrological processes.

2.3. Methods

2.3.1. Workflow Overview

In this research, we aimed to establish a low level of coupling to perform a controlled model experiment. Therefore, we did not do two-way couple or integrate models into NWM, and instead, a stand-alone model was one-way coupled by transferring hydrologic flux data. One-way coupling is more common between models that covers distinct aspect of hydrological processes. For instance, Nguyen et al., (2016) reviewed numerous hydrology-hydraulic coupled models during a development of the HiResFlood-UCI model, most of which used a one-way approach. One-way coupling is less common in cases where models have overlapping process representations (e.g., coupling a hydrologic model with LSM or hydrometeorological model), and a majority were found in model performance comparison studies that such as Givati et al. (2016), Hay et al.(2006), and Lahmers et al.(2020). The one-way coupling method fits the aim of our research by providing ease of understanding the processes, modifiability, and faster model execution. It enabled us to focus on hydrological

perspectives of coupling and efficiently test how the details in the coupling interface, such as the level of dependency, location of coupling, type of transferred flux, or modification of process steps, impact the behavior of a conceptual hydrologic model coupled with NWM's LSM (Noah-MP).

In summary, we formatted the hydrologic variables from Noah-MP output and internal state data and passed it to TOPMODEL as coupling fluxes in varying ways. Then, we analyzed the coupled model's streamflow prediction performance, uncertainty, and parameter sensitivity. Regionally calibrated NWM v1.2.2 configuration was used as a control that provides a performance baseline to compare with TOPMODEL coupling cases.

This research established six versions of Noah-MP + TOPMODEL coupling options, where TOPMODEL substitutes varying parts of NWM's runoff calculation and flow-routing capability. The type of hydrological state or flux values transferred from Noah-MP to TOPMODEL defined the level of dependency between models. TOPMODEL as a standalone hydrologic model takes hourly rainfall and potential evapotranspiration rate as meteorological inputs for the simulation. In each coupling option, TOPMODEL's internal process steps were modified to accommodate the dependency accordingly. Hydrological fluxes transferred from Noah-MP to TOPMODEL varied from fluxes equivalent to meteorological input to fluxes that are comparable to the internal state variables of TOPMODEL. The workflow overview and coupling options are summarized in Figure 2-1.

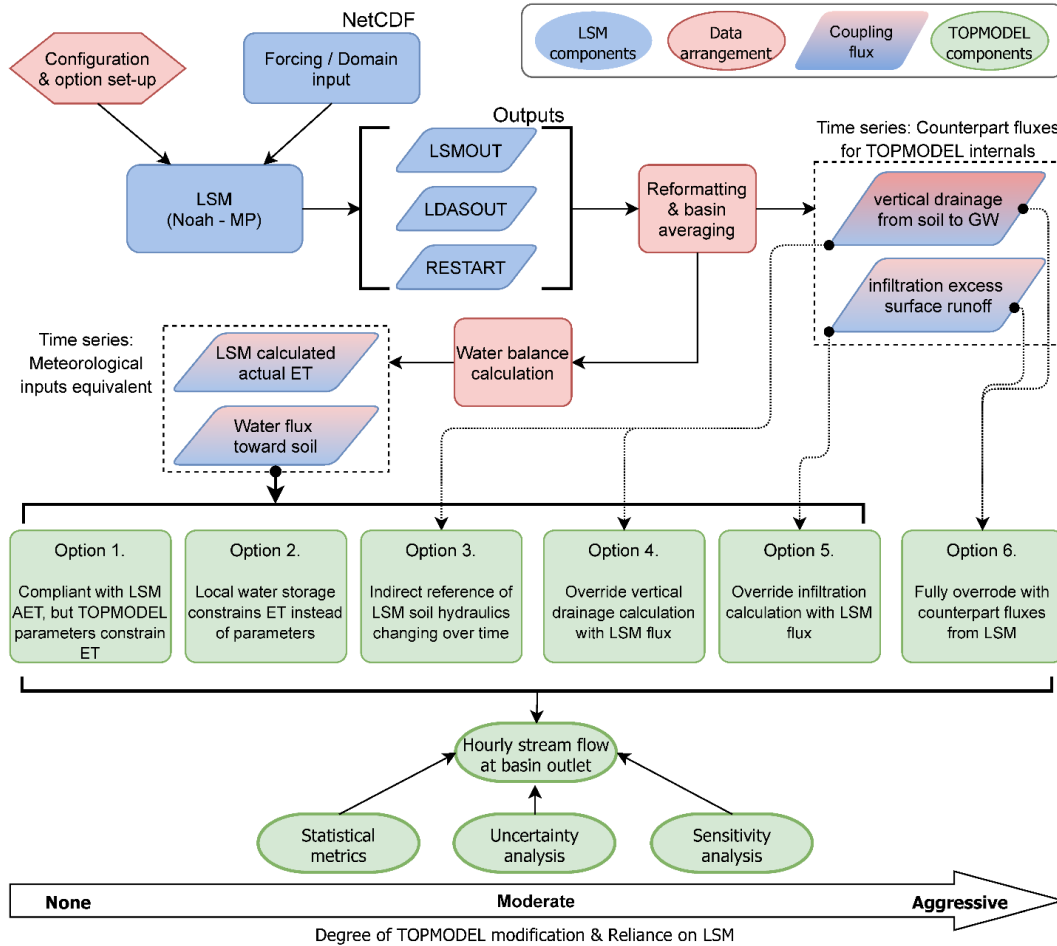


Figure 2-1. Workflow overview for one-way coupling of TOPMODEL and NWM’s LSM (Noah-MP). Coupling fluxes are arranged from NWM outputs and used as input for six options according to varying coupling interfaces.

2.3.2. NWM LSM (Noah-MP) Set-up and Arranging Coupling Fluxes

National Water Model v 1.2.2 was used as a base model. The domain data for the study area were subsetted using CUAHSI Domain subsetter (Castronova and Tijerina, 2019), and used North American Land Data Assimilation System-2 (NLDAS) as a forcing data for the simulation (National Aeronautics and Space Administration, Earthdata repository. Accessed June 2019 - July 2020, <https://earthdata.nasa.gov>. Unless otherwise noted all forcing data in this paper are from this source).

To generate transferable coupling data for TOPMODEL coupling options from Noah-MP outputs, soil and groundwater-related parameter and model run options were adjusted in the NWM configuration. Surface and subsurface flow routing were turned off to prevent Noah-MP's soil moisture contents being disturbed by feedback from unused downstream routing modules that are replaced by TOPMODEL components. The RESTART output file, which is originally intended for providing “hot start” or initial conditions for the model run, was set to write every timestep. This was because some essential output variables to calculate hydrologic balance were only included in RESTART files, not in standard NWM output files. This measure was quite sufficient for the goals of the study; however, any operational one-way coupling implementation would require a more efficient data management between Noah-MP and TOPMODEL.

The SLOPE or slope index parameter in Noah-MP modifies the hydraulic gradient at the bottom of the soil profile to regulate drainage to the groundwater reservoir as a coefficient. It is one of the key model parameters and can range from 0 to 1. In this study, the slope index parameter of Noah-MP was modified (set to 1) to allow free gravitational drainage from the lower soil boundary to the groundwater reservoir. This is necessary because any oversaturation of the soil column can affect our target subsurface flux "underground runoff" variable from Noah-MP.

Noah-MP outputs are in Network Common Data Format (NetCDF); the “rwrhydro” package was used to disaggregate and reformat NetCDF files for ingest into TOPMODEL (NCAR Research Application Laboratory, 2015). Target output variables were collated from multiple output files, such as LDASOUT (Land surface model output), LSMOUT (Land surface diagnostic output), and RESTART (Land surface model internal state output) file.

Several variables in RESTART file are expressed as an accumulated value, and hourly change in values must be back-calculated. All units were converted into meters per hour (m/h). Using a water balance equation, hourly water flux from Noah-MP outputs in the study's configuration can be expressed as follows,

$$(P - \Delta Can - \Delta Snw) - ET_a = Q_{sfc} + Q_{ugd} + \Delta S \quad (\text{Eq. 2-1})$$

where P is precipitation, ΔCan is a change in canopy water storage, ΔSnw is a change in snow water storage, ET_a is actual evapotranspiration calculated from Noah-MP. On the right-hand side, Q_{sfc} is surface runoff, which is expressed as infiltration excess in WRF-Hydro, but it derives from REFKDT (Schaake et al., 1996) parameter that partitions direct runoff from rainfall based on empiricism. Q_{ugd} is underground runoff, which is a vertical drainage from the lower boundary of bottom the soil layer, and WRF-Hydro uses this value to calculate the recharge rate of non-linear conceptual groundwater reservoir. ΔS is a change in total volumetric soil moisture content, while water cannot move upward from the groundwater reservoir to soil layers. Variables on the left-hand side, the water flux toward the soil-system ($P - \Delta Can - \Delta Snw$) and actual evapotranspiration rate (ET_a), are not identical but comparable to TOPMODEL's meteorological input (rainfall and potential evapotranspiration rate). These coupling fluxes will be called “(meteorological) input-equivalent fluxes” in the following sections.

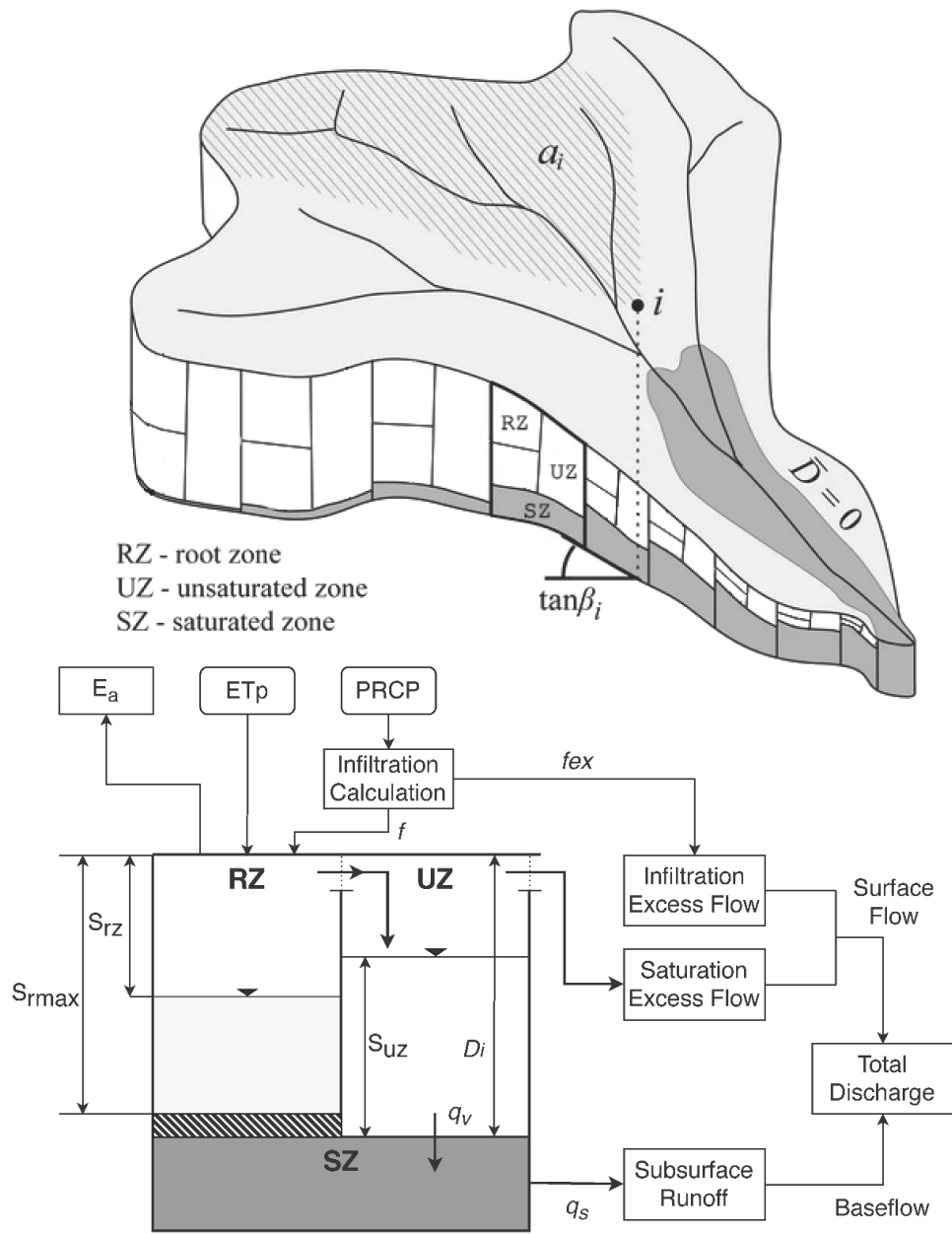
TOPMODEL calculates runoff and dynamic soil/groundwater contents at watershed scale, however, due to the nature of the one-way coupling method, Noah-MP also independently calculates variables such as Q_{sfc} , Q_{ugd} and ΔS . In our coupling options, if/how these runoff related variables (Q_{sfc} and Q_{ugd}) from Noah-MP on the right-hand side are transferred to TOPMODEL defines the dependency. When transferred, these variables can override

TOPMODEL's input parameter, internal state, or calculation processes, and we refer to them as "counterpart" coupling fluxes. Details on usage of these different types of coupling flux and coupling interface are discussed in the section "Model coupling options".

2.3.3. TOPMODEL Set-up

TOPMODEL is described as a conceptual approach by the original paper (Cho, 2000; Conrad 2003. Accessed March 2020, <http://www.saga-gis.org>), however, multiple efforts have developed it into an accessible hydrological modeling tool. We used an R-implemented version of TOPMODEL (Buytaert, 2011), coupling it as a stand-alone model via hydrologic flux transfer. TOPMODEL requires pre-computation of the topographic index, which was processed from a 10-meter resolution digital elevation model (DEM) using the TauDEM package (Tarboton, 2015). TOPMODEL concepts and r.TOPMODEL's schematic diagram are shown in Figure 2-2.

One advantage of coupling watershed-scale TOPMODEL to the NWM is the reduced effort needed for optimizing parameters due to the simple structure of TOPMODEL. It is possible to reduce the number of parameters used in TOPMODEL, depending on how LSM data are used for coupling. Parameter ranges were chosen to keep the parameter optimization process as efficient as possible (Table 2-2). Reasonable bounds were selected based on recommendations from previous studies (Cho et al., 2019; Nan et al., 2011; Sigdel et al., 2011). Random sampling methods were applied to perform model runs and parameter sensitivity analysis based on parameter bounds. However, we made an exception for surface hydraulic conductivity (k_0), setting the upper bound to a very high value (10 meters/hour) to allow the model to simulate the case that infiltration excess does not occur at all, and sampled on a logarithmic scale to prevent it from being biased to high values.



A_i: area associated with topographic index class, **RZ**: Rootzone, **UZ**: Unsaturated zone, **SZ**: Saturated zone, **ET_p**: Potential evapotranspiration as meteorological input, **E_a**: Actual evaporation, **PRCP**: Precipitation as meteorological input, **f**: Infiltration, **f_{ex}**: infiltration excess flow, **S_{rz}**: Rootzone deficit, **S_{rmax}**: Maximum rootzone storage parameter, **S_{uz}**: Unsaturated zone storage, **D_i**: Local storage deficit, **q_v**: vertical drainage flux into local water table, **q_s**: subsurface saturated zone flux

Figure 2-2. Concept of TOPMODEL and its schematic diagram in r.TOPMODEL package. Modified from Jeziorska and Niedzielski (2018).

Table 2-2. Range of reasonable TOPMODEL parameter ranges (Cho *et al.*, 2019; Nan *et al.*, 2011; Sigdel *et al.*, 2011)

Parameter	Min	Max	Description	Sensitivity	Reference
Qso (m/h)	0.0005	0.00075	Initial subsurface flow per unit area	Insensitive	Sigdel et al., 2011
	0	0.0001			Cho et al., 2019
lnTe ($\ln(m^2/h)$)	-3.3	-1.5	Areal average of log-transformed soil surface transmissivity	More sensitive, peak flow	Sigdel et al., 2011
	-7	10			Cho et al., 2019
	0.5	1.5			Nan et al., 2011
m	0.054	0.085	Scaling parameter for transmissivity decline (Exponential storage)	Highly sensitive, base flow	Sigdel et al., 2011
	0.001	0.25			Cho et al., 2019
	0.0001	0.03			Nan et al., 2011
Sr0 (m)	0.00001	0.01	Initial root zone storage deficit	Insensitive	Sigdel et al., 2011
	0	0.01			Cho et al., 2019
Srmax (m)	0.02	0.1	Maximum root zone storage deficit	Sensitive, physically-based	Sigdel et al., 2011
	0.005	0.08			Cho et al., 2019
	0	0.5			Nan et al., 2011
Td (h/m)	10	40	Unsaturated zone time delay	Less Sensitive	Sigdel et al., 2011
	0.001	40			Cho et al., 2019
	0.001	50			Nan et al., 2011
vch (m/h)	2300	4000	Channel routing velocity	Sensitive, time to peak	Sigdel et al., 2011
	50	2000			Cho et al., 2019
	500	9000			Nan et al., 2011
vr (m/h)	50	2000	Surface routing velocity	Time to peak	Cho et al., 2019
	500	5000			Nan et al., 2011
k0 (m/h)	0.0011	0.1	Surface hydraulic conductivity	Physically based	Sigdel et al., 2011
	0.0001	0.2			Cho et al., 2019
CD-psi (m)	0.11	0.25	Wetting front suction head	Insensitive, Green-Ampt parameter	Sigdel et al., 2011
	0.01	0.5			Cho et al., 2019
dTheta	0.25	0.36	<i>Water content change in wetting front; not included in r.TOPMODEL</i>	<i>Insensitive, Green-Ampt parameter</i>	<i>Sigdel et al., 2011</i>
	0.01	0.6			<i>Cho et al., 2019</i>

2.3.4. Performance Evaluation, and Uncertainty/Sensitivity Analysis

In the coupled models, TOPMODEL parameters were optimized for the headwater catchment of the study area, even though a regionally calibrated NWM v1.2.2 configuration was used as a control that provides a performance baseline. Comparing models with different levels of calibration is unfair in terms of model prediction accuracy. However, the loose one-way coupling of a conceptual hydrological model simplifying the structure of NWM allows watershed-by-watershed parameter calibration and uncertainty/sensitivity analysis with minimal computation load, where such a level of calibration and analysis is unrealistic in NWM. Uncertainty analysis of a tight two-way coupled model is challenging due to heavy computational demand, even though the framework for such is in advancement (Moges et al., 2020). The ability to easily perform parameter optimization involving uncertainty and sensitivity analysis is one of the key advantages that a loose one-way coupling method can provide.

We applied conventional, random sampling-based methods for uncertainty estimation and parameter sensitivity analysis, to track how the model behavior changes between coupling methods. Nash-Sutcliffe Efficiency (Nash and Sutcliffe, 1970) was used as an objective function for model calibration. Parameter sets were sampled with a Quasi-Monte Carlo method (Sobol sequence; Sobol', 1967) to produce more evenly distributed parameter sets than would be obtained with pseudo-random sampling.

The choice of the objective function strongly influences calibrated models' behavior (Gupta et al., 1998; Yapo et al., 1996, 1998). For example, using NSE as an objective function tends to bias models toward capturing high flow (Legates and McCabe, 1999). Instead, we adopted an approach suggested by Seibert et al. (2018), comparing multiple metric scores

against benchmarks to evaluate the model performance. We investigated metric scores including NSE, root mean square error (RMSE), root mean square error to the standard deviation (RSR), Percent Bias (PBIAS), and Kling-Gupta Efficiency (KGE; Gupta et al., 2009) to compare with benchmark models (NWM and TOPMODEL). Moriasi et al. (2007) suggested that PBIAS lower than 25%, NSE over 0.5, and RSR lower than 0.7 can be considered as a minimum standard for satisfactory model performance.

Generalized Likelihood Uncertainty Estimation (GLUE) (Beven and Binley, 1992) was applied as an uncertainty analysis method for streamflow prediction. GLUE has been often criticized for its subjectivity and informality (Mantovan and Todini, 2006; Stedinger et al., 2008), but formal Bayesian (differential evolution adaptive metropolis, DREAM) and informal (GLUE) approaches can produce similar estimates of total uncertainty in streamflow (Vrugt et al., 2009). Further, Sadegh and Vrugt, (2013) showed that GLUE highly resembles the newer Approximate Bayesian Computation (ABC) uncertainty analysis method. Considering such, we consider the informal GLUE method sufficient to estimate total uncertainty for the model experiments in this study. If the purpose of uncertainty analysis is to dissect how forcing (input), parameter, and model structural error consist of total uncertainty, it is recommendable to use a formal Bayesian approach (Vrugt et al., 2009).

A behaviorability threshold and weighting model outputs by their NSE score were applied to generate uncertainty bounds for model streamflow prediction. The threshold of NSE was set to 0.7 for better performing coupled models and 0.55 for worse performing models, and we used values within a confidence interval of 90% from GLUE. The percentage of streamflow observations contained within the bounds is an indicator of the performance. However, to distinguish small differences in the range of these bounds, we adopted an

additional quality measure called “Average Relative Interval Length (ARIL)” (Jin et al., 2010).

$$ARIL = \frac{1}{n} \sum \frac{Limit_{Upper,t} - Limit_{Lower,t}}{Q_{obs,t}} \quad (\text{Eq. 2-2})$$

where n is the number of timesteps, $Limit_{Upper,t}$ and $Limit_{Lower,t}$ are upper and lower limits of the uncertainty bounds, and $Q_{obs,t}$ is observed value. ARIL indicates how narrow the bound is, with smaller values preferred (Jin et al., 2010).

We used the “Jansen 1999” (Jansen, 1999) method to retrieve first order and total sensitivity indices for parameters. Saltelli et al. (2010) and Sun et al., (2017) concluded that the “Jansen 1999” estimator is the most efficient and accurate among comparable global sensitivity techniques. Generally, NSE is a robust metric used within the sensitivity analysis method to quantify model performance, however, because it can range from $-\infty$ to $+1$, Sobol-like global sensitivity analysis methods can suffer from non-centered, extreme negative values (Nossent and Bauwens, 2012). To resolve this issue, we implement a bounded formulation of the NSE called C_{2M} suggested by Mathevet et al. (2006).

$$C_{2M} = \frac{NSE}{2 - NSE} \quad (\text{Eq. 2-3})$$

where NSE stands for Nash-Sutcliffe Efficiency. C_{2M} varies between -1 and $+1$ and has the same zero value as NSE, having a less skewed distribution, yet providing intuitively relevant scaling to the range of regular NSE values (Mathevet et al., 2006). C_{2M} metrics can resolve the criticism made by Garrick et al. (1978) that NSE produces misleadingly high values, however, we do not consider this aspect in this study and C_{2M} will only be used for sensitivity analysis purposes.

Hydrological signatures are a useful addition to statistical performance metrics for model evaluation, as they help evaluate the model’s ability to correctly represent hydrological

processes and flux partitioning (McMillan, 2020). One of the most widely used hydrologic signatures, the flow duration curve (FDC), was applied to review the model's capability to predict water availability in the watershed. FDC summarizes hydrological behavior by aggregating streamflow values over time and is not sensitive to timing errors (McMillan et al., 2017). However, quantifying FDC into a numerical signature value (e.g. with midsection slope) involves a complicated decision, because the shape of FDC is affected by multiple hydrologic processes (McMillan et al., 2017). Therefore, in this study, we limited the use of FDC to an informal graphical inspection of water availability.

2.3.5. Model Coupling Options

The six versions of LSM (Noah-MP) + TOPMODEL coupling proposed in this study have variations in their coupling interface corresponding to different levels of internal modifications and usage of coupling fluxes. The choice of version corresponds to a varying dependency of the coupled system on LSM-calculated fluxes.

The original configuration of TOPMODEL uses hourly rainfall and potential evapotranspiration rate (PET) as an input. In all our coupling options, we removed TOPMODEL's ET routine designed to scale PET input with user input parameter and estimate AET. This enabled us to use Noah-MP calculated actual evapotranspiration (input-equivalent flux) without inaccurate formulation. Hourly rainfall rate was substituted with water flux toward soil ($P - \Delta Can - \Delta Snw$), and potential evapotranspiration rate was substituted with LSM calculated actual evapotranspiration (ET_a). Additionally, counterpart fluxes derived from LSM calculated runoff or drainage value were transferred to TOPMODEL. These counterpart fluxes are equivalent to infiltration excess (Q_{sfc}) and vertical drainage in soil column (Q_{ugd}). Usage of counterpart fluxes involves modification and bypass of

TOPMODEL internal calculations. Detailed coupling options are as follows (Table 2-3). Refer to Figure 2 for details of how the implementation of each coupling option changes the internal processes of TOPMODEL.

Table 2-3. Summary of affected TOPMODEL structure and coupling flux usage for each NWM-TOPMODEL one-way coupling options.

Option	Coupling flux usage		Affected TOPMODEL structures	Affected TOPMODEL parameters
	Input equivalent	Counterpart		
1	Precip, ETa	None	ET scaling scheme in RZ removed. However, RZ structure constrains input equivalent fluxes	Reduced occurrence: Srmax
2	Precip, ETa	None	RZ structure removed. Local storage deficit in UZ constrains ET	Removed: Sr0, Srmax
3	Precip, ETa	Q_{ugd}	Addition to option 2: vertical drainage calculation is dynamically scaled by counterpart LSM flux	Removed: Sr0, Srmax, td
4	Precip, ETa	Q_{ugd}	Addition to option 2: Vertical drainage calculation is overridden by counterpart LSM flux	Removed: Sr0, Srmax, td
5	Precip, ETa	Q_{sfc}	Addition to option 2: Surface infiltration calculation is overridden by counterpart LSM flux	Removed: Sr0, Srmax, k0, CD Reduced occurrence: m
6	None	Q_{sfc} & Q_{ugd}	TOPMODEL exclusively relies on counterpart LSM fluxes to calculate runoff	Removed: Sr0, Srmax, k0, CD, td Reduced occurrence: m

Coupling option 1 (Turn off TOPMODEL’s ET scaling scheme: No ET scaling).

Removes the operation in TOPMODEL’s root zone structure adjusting the ET input, which is unnecessary and inaccurate in coupled models. Root zone structure of TOPMODEL is intended to simplify whole atmosphere-vegetation-soil interaction processes with single non-physically based and user defined parameter “Srmax” (Beven et al., 2020). Root zone layer

releases water down to unsaturated zone only when capacity is exceeded (fill-and-spill), but such process is not governed by physics related to field capacity. On the other hand, ET is scaled with fractional rootzone storage for each timestep, and it continues until depletion. As the coupled model uses actual evapotranspiration estimates (ETa) calculated from Noah-MP as input instead of potential evapotranspiration rate (PET), we removed the fractional ET scaling scheme from root zone to prevent duplicate calculation (Table 3). The root zone structure remains as a capacitor that limits and buffers water fluxes entering the unsaturated zone (Uz).

Coupling option 2 (Constraining ET with local storage deficit: Root zone removal).

Rootzone (Rz) structure is completely removed from TOPMODEL. The terms root zone and unsaturated zone imply their association with soil structure representation, however, their behavior in the TOPMODEL simulation does not correspond to how Noah-MP simulates soil hydraulics. An arbitrary characteristic of rootzone (Rz) is discussed in coupling option 1 description above. In coupling option 2, input equivalent fluxes (Precipitation and ETa) can directly interact with the unsaturated zone (Uz) of TOPMODEL without being affected by root zone (Rz) structure (Table 3). This allows TOPMODEL to constrain ET by local storage deficit (soil water status).

Coupling option 3 (Indirect reference of LSM subsurface flux: Dynamic vertical drainage). Branched from option 2 (rootzone structure removal). A dynamic unsaturated zone delay function that represents the interaction between soil moisture, field capacity, and gravitational drainage in Noah-MP was introduced to TOPMODEL. This modification induces the vertical drainage calculation of TOPMODEL to resemble Noah-MP's soil moisture status and hydraulics.

Counterpart flux (Q_{ugd}) from Noah-MP is referenced to establish a dynamic function to substitute the vertical drainage parameter of TOPMODEL. The original TOPMODEL governs vertical drainage from unsaturated zone (Uz) to saturated zone (Sz) with user input parameter "td", which is a fixed coefficient that requires calibration. This coupling option substitutes the td parameter with a simple dynamic delay function that references Noah-MP's subsurface fluxes changing over time. Dynamic delay function references underground runoff (Q_{ugd}) of Noah-MP which is calculated based on soil physics related to field capacity.

$$Qv = \frac{Suz}{S*td} \quad (\text{Eq. 2- 4})$$

where Qv is vertical drainage from unsaturated zone to saturated zone (meter), Suz is unsaturated zone storage (meter), S is local storage deficit (meter), dt is simulation timestep (hour), and td is an unsaturated zone time delay (hour/meter). Dynamic delay function was formulated by referencing Noah-MP flux as follows,

$$Qv = \frac{Suz}{S} * \left(0.02 + \left(\frac{Q_{ugd,t}}{Q_{ugd,max} - Q_{ugd,min}} \right)^{\frac{3}{2}} \right) \quad (\text{Eq. 2-5})$$

Where 0.02 is the minimum recommended value of $1/td$, $Q_{ugd,t}$ is LSM calculated gravitational vertical drainage at timestep, $Q_{ugd,max}$ is maximum value over time, and $Q_{ugd,min}$ is the minimum (usually 0). Introducing dynamic delay function delivers soil hydraulics characteristics of Noah-MP to TOPMODEL. However, vertical drainage from unsaturated zone to saturated zone groundwater is still driven by the TOPMODEL water table level relationship. The design of the non-linear vertical drainage function had subsurface preferential flow in mind, which was implicitly considered in TOPMODEL's root zone (Rz) structure that was removed in this coupling option (Beven et al., 2020).

Coupling option 4 (LSM subsurface vertical flux substitutes vertical drainage calculation in TOPMODEL: Vertical drainage Override). Developed from option 2 (rootzone structure removal), vertical drainage calculation in TOPMODEL is overridden by counterpart flux Q_{ugd} . The difference from option 3 (Dynamic unsaturated-zone delay) is that Q_{ugd} overrides the whole vertical drainage calculation processes. This option considers LSM's free gravitational drainage returns a "true" value; drains the water from unsaturated zone to saturated zone and contributes to baseflow runoff. By doing so, vertical movement of soil water in unsaturated zone is no longer simulated by the water-table level dynamics of TOPMODEL.

Coupling option 5 (LSM calculates soil water infiltration: Infiltration Override). Developed from option 2 (rootzone removal), surface infiltration calculation process in TOPMODEL is overridden by LSM flux. TOPMODEL takes in counterpart flux Q_{sfc} from LSM as an infiltration excess overland flow. TOPMODEL no longer uses soil hydraulics parameter and an occurrence of TOPMODEL's second most sensitive parameter m (scaling parameter for transmissivity decline) in the model simulation is reduced.

Coupling option 6 (TOPMODEL becomes reliant on LSM: full override). TOPMODEL does not receive any data related to meteorological inputs, but fully relies on runoff related counterpart fluxes from Noah-MP. Therefore, only subsurface flow rate calculation based on the distribution of topographic wetness index and surface/channel routing are functional in TOPMODEL.

2.4. Study Area

A well-studied and data-rich headwater catchment was chosen as a study site to test the validity of model coupling and compare coupling options. The study focused on the Angelo

Coast Range Reserve (39°43'47" N, 123°38'34" W), an area within the Eel River Critical Zone Observatory, which is one of the University of California's Natural Reserves in Northern California (Figure 2-3). The study area falls into "Elder Creek-South Fork Eel River" watershed area which is classified as HUC12 (hydrologic unit code) 180101060103, and modeling was done for the sub-catchment upstream of the USGS "Elder Creek" stream gage site (11475560). The study site has a steep hillslope (average 32°) that drains to the about 17-km² Elder Creek catchment at 392 m above sea level (University of California Natural Reserve System, Angelo Coast Range Reserve. Accessed June 2019 - July 2020, <https://angelo.berkeley.edu/>). The climate in the area is coastal Mediterranean with warm, dry summers and cold, wet winters, an annual average of 2042 mm of rain with very little snow with most of the precipitation falling between October and May (Oregon State University, PRISM Climate Group. Accessed June 2019 - July 2020, <https://prism.oregonstate.edu/>).

The study site has complex geology that is made up of the Coastal Belt of the Franciscan Formation. It is well-bedded, little sheared, has interbedded with local folded mudstone-rich turbidities, and some lenses of sandstone and conglomerate exist (M. C. Blake Jr., 1985; Mclaughlin et al., 2014; Rempe and Dietrich, 2018). Thick weathered bedrock (5-25 meters) is overlain by a thin soil layer (0.5–0.75 meters), and groundwater levels indicate that pervasive fracturing in the bed likely prevents the bedding from controlling the groundwater flow direction (Rempe and Dietrich, 2018). Rempe and Dietrich (2018) emphasize the role of water held in the weathered bedrock, referring as "rock moisture", which is unquantified, distinct from soil moisture or groundwater, and a stable source of water in the study site.

This application implemented a model simulation period from October 1st, 2015 to September 30th, 2019, covering 4 water years. An idealized uniform precipitation scenario

was used for model initialization to fill the soil column and groundwater reservoir as WRF-Hydro model recommends (Gochis et al., 2018). The model spin-up used four repetitive model runs using the first three months of the first water year 2015 (10/01/2014 – 12/31/2014) followed by a simulation of the whole water year 2015 for stabilization (10/01/2014 – 09/30/2015).

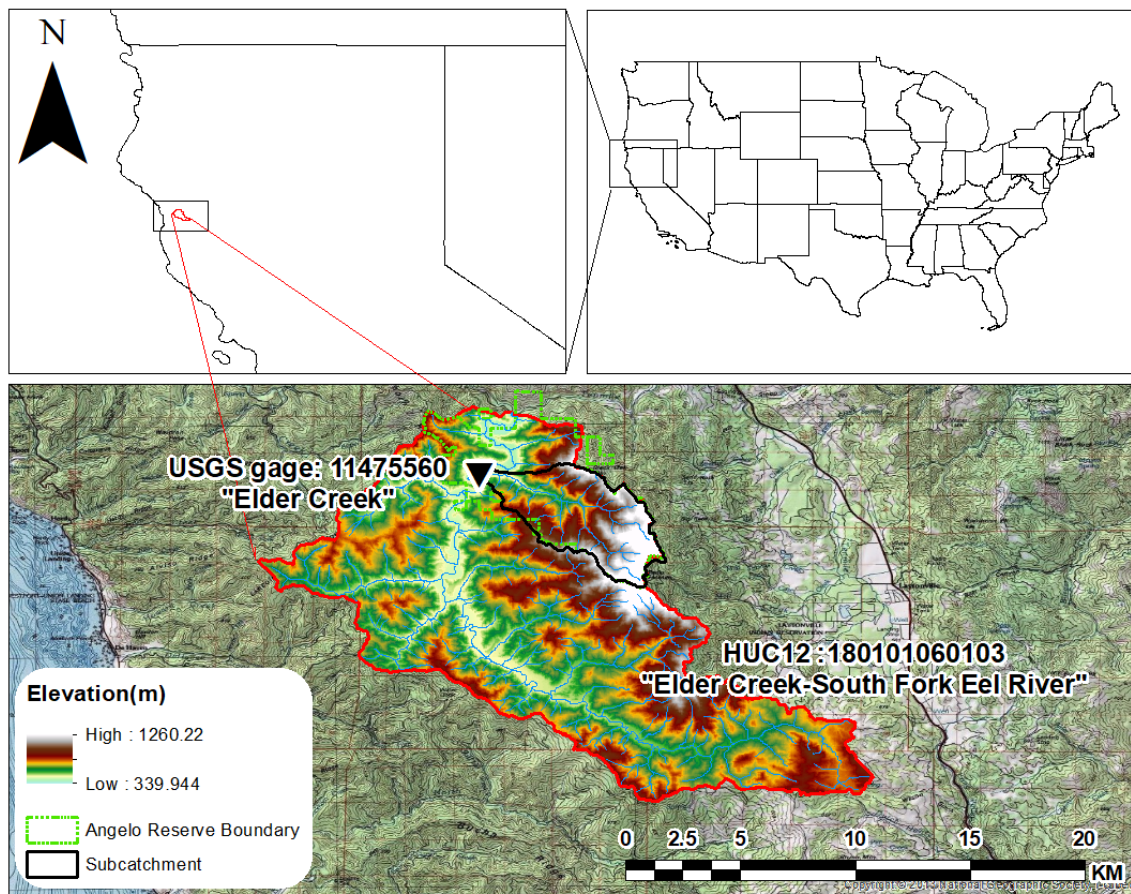


Figure 2-3. Study area: 17 km² Elder Creek-South Fork Eel River watershed in California in black outline.

2.5. Results

2.5.1. Model Performance Evaluation

In this section, we compared the model performance based on simulated streamflow of the original NWM, original TOPMODEL, and Noah-MP&TOPMODEL coupled versions. 26,000 parameter-sets sampled by Sobol sequence were used for all six coupling options and metrics are calculated from the whole simulation period (October 1st, 2015 to September 30th, 2019). However, the time windows for hydrograph figures are limited to the wet season of the water year 2017 (October 2016 to March 2017) for legibility. This period had a high number of events and hydrographs of each coupling option were easily distinguishable. We note that the water budget between NLDAS rainfall, USGS observed runoff, and actual evapotranspiration rate (AET) from Noah-MP was calculated at 1:0.94:0.27, but TOPMOELs' calibration in the coupled models did not consider such uncertainty from inputs.

Table 2-4. Statistical scores of NWM and NWM-TOPMODEL coupling options with the best parameter-set and GLUE bound related statistics (Simulation period Oct 01, 2015~Sep 30, 2019)

	NSE	RMSE	RSR	PBIAS	KGE	ARIL	% within bound
NWM	0.488	1.162	0.715	-32.5	0.597	-	-
TOPMODEL (Control)	0.749	0.812	0.500	-23.9	0.662	1.98	47.9
Option1	0.789	0.746	0.459	-14.5	0.766	2.28	45.7
Option2	0.792	0.742	0.457	5.4	0.829	2.69	29.9
Option3	0.806	0.715	0.440	3.3	0.821	2.58	30.7
Option4	0.599	1.028	0.633	25.3	0.676	3.03	15.6
Option5	0.616	1.007	0.620	-0.2	0.659	4.13	36.8
Option6	0.605	1.021	0.628	9.0	0.694	5.11	18.36

The NWM did not meet the minimum standard suggested by Moriasi et al. (2007) (PBIAS lower than 25%, NSE over 0.5, and RSR lower than 0.7). It performed poorly during wet seasons (October to March) failing to properly estimate the baseflow rate (Figure 4). During the events, NWM showed a very flashy hydrograph that had unrealistic slope and recession, and often overestimated the peak flowrate. During smaller events, NWM frequently missed peaks that appeared in the USGS observations. The FDC showed the strong tendency of NWM to underestimate the water availability in the watershed. This result highlights the potential drawbacks of applying the NWM in small headwater catchments, particularly concerning its spatial structure, representation of hydrological processes, and the challenges of calibrating the model to specific watersheds due to high computational demands.

The original standalone TOPMODEL that uses NLDAS precipitation and potential evapotranspiration rate as inputs (TOPMODEL-control) was tested as a second control for the experiment. It returned higher metric scores compared to NWM and shared similar characteristics with option 1 (Table 2-4). Even though scores were nearly good as some better-performing coupled models (1, 2, and 3), only 97 out of 26,000 parameter-sets satisfied GLUE thresholds of NSE 0.7. Better coupled options (1, 2, and 3) had over 2,000~4,000 surpassing the same threshold. We will discuss this aspect further in the following section “Behavioral changes in coupled TOPMODEL”.

Among the 6 different coupling options tested, moderate options (1, 2, and 3) showed reliable performance through varying years and seasons. The performance gap was larger between wet years and dry years, rather than wet seasons and dry seasons. More aggressive coupling cases (from option 4 to option 6) that relied more heavily on Noah-MP output fluxes produced relatively lacking performance and they were acceptable only during the wet season

of wet years, or dry season of dry years. Other than such periods, these aggressively coupled models did not have clear superiority over NWM in streamflow prediction.

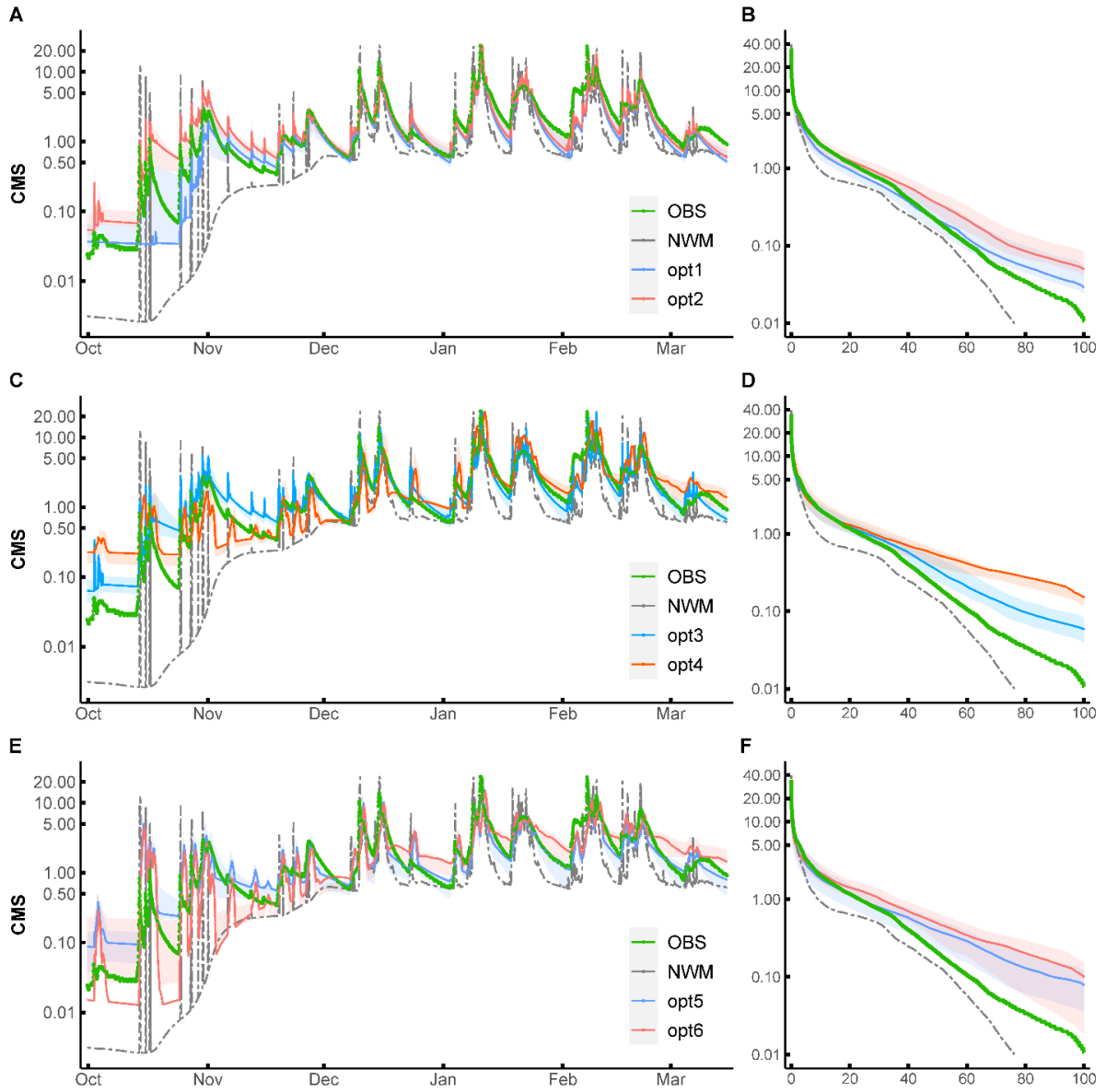


Figure 2-4. Comparison of hydrographs (the wet season of the water year 2017, Oct 2016 to Mar 2017), flow duration curve (FDC; whole simulation period, Oct 2015 to Sep 2019) from observation, National Water Model (NWM), and coupled models (with uncertainty bounds). Outputs from stand-alone TOPMODEL not included. A: Hydrograph of Option 1 and 2, B: FDC of Option 1 and 2, C: Hydrograph of Option 3 and 4, D: FDC of Option 3 and 4, E: Hydrograph of Option 5 and 6, F: FDC of Option 5 and 6.

Coupling Noah-MP and TOPMODEL with a minor change in ET scheme (Option 1, ET replacement) improved all the statistical scores and hydrographs from NWM or TOPMODEL-control (Table 2-4, Figure 2-4). These results demonstrated how simplification and calibration of subsurface model components can improve streamflow performance metrics where distributed flux forecasting is not required, while still benefiting from distributed LSM simulations. Option 1 consistently outperformed NWM except for the period when baseflow recesses near depletion during the dry season (April to September). Option 1 noticeably improved bias in TOPMODEL-control underestimating high flows, however, still tended to underestimate peak runoff and showed wider uncertainty bounds (ARIL) during early-season events. From the FDC, we saw that water availability in option 1 was closer to the observation than NWM, but it tended to underestimate the streamflow over the 40th percentile.

In coupling option 2 (Rootzone Removal), PBIAS and KGE noticeably improved compared to option 1 while improvement in NSE, RMSE, and RSR is minor. The median hydrograph from coupling option 2 shared a similar shape and timing for peaks, but values were higher. This higher streamflow value provided more accurate estimations of runoff and peak flow rate during events and compensates for the increased error during low flow conditions, resulting in higher score of evaluation metrics. Coupling option 2 had a recession curve that is closer to the observed recession shape and reproduced small peaks that previous coupling option 1 failed to capture. Metrics showed that coupling option 2 resolved underestimation of high flows. From FDC, option 2 generally overestimated the streamflow below the 20th percentile compared to option 1, however, slope and curvature were noticeably better than option 1 within the top 40th percentile. When evaluated for the entire simulation period, option 2 showed higher uncertainty; larger ARIL than option 1 and lower percentage

of observations within the model confidence bounds (Table 2-4). However, when those metrics were calculated only for the wet season of the WY 2017 (wettest year), ARIL became nearly identical and % of observation within bound was higher in option 2 than option 1 (49% vs 42%). Therefore, constraining AET with local storage deficit by removing root zone structure improved the coupled model's prediction and lowered uncertainty during wet season and high flow events but harmed low flow estimation with overestimation.

Coupling option 3 (Dynamic Unsaturated-zone Delay) produced the highest scores of all the options (Table 2-4). It showed an improvement in NSE, RMSE, RSR, and PBIAS, only the KGE exhibited a slight decrease. ARIL and % within bound improved from option 2 but worse than option 1 (Table 2-4). The simulated hydrograph and FDC were very similar to option 2, but baseflow increased and the recession curve fitted more closely to the observed streamflow with a flatter slope. This improvement in option 3 was less expected for two reasons. The derivation of dynamic vertical drainage delay function from LSM flux (Q_{ugd}) is simply an approximation of the gravitational drainage trend related to field capacity, and TOPMODEL is known to be relatively insensitive to the "td" parameter.

The more aggressive coupling options overrode TOPMODEL internal states with counterpart flux calculated from LSM (option 4, 5, and 6). In this case, statistical scores decreased sharply and required us to reduce the GLUE threshold value to an NSE of 0.55 (Table 2-4). These aggressive coupling options still outperformed NWM, but unlike previous options (1,2, and 3), they inherited the characteristics of NWM with lower predictive skill during the wet season showing “flashy runoff superimposed on slow recessions”. Overriding the vertical drainage and related underground runoff calculations with LSM flux caused extreme underestimation of baseflow even during wet seasons, demonstrating incompatibility

of the fluxes between the two models. We tested an alternative formulation, which became option 4 (Vertical Drainage Override), where the vertical drainage component was redirected to contribute to baseflow. It produced more realistic dynamic behavior but often generated more runoff than precipitation input and still performed poorly in estimating the peak flow rate or time-to-peak (Figure 2-4). Overall, option 4 was among the worst-performing coupled models.

Coupling option 5 (Infiltration Override) removes the surface infiltration calculation of TOPMODEL and force in LSM flux while maintaining other structures of option 2 (Rootzone Removal). This option 5 only overrode the surface infiltration process and showed better scores compared to options 4 that overrode vertical drainage calculation (Table 4). The hydrographs of option 5 suffered from delayed time-to-peak estimation, which extended in some extreme cases to over 24 hours (Figure 4). A comparable pattern of delayed peaks was also found in option 4 (Vertical Drainage Override). However, a similar delay to option 4 may be a coincidence because surface infiltration and subsurface vertical drainage are distinct and weakly related calculation processes. ARIL from options 5 was significantly larger than any previous options including option 4 which showed worse prediction scores. We infer that overriding an internal state of TOPMODEL with counterpart flux raises the incompatibility of TOPMODEL and its own routing scheme. Overriding the infiltration calculation brought high uncertainty into coupled model behavior.

Option 6 (Full Override) did not use any data that is equivalent to meteorological inputs of TOPMODEL. The shape of its hydrograph and FDC were similar to that of option 4 (Vertical Drainage Override), but peak discharge values were higher as TOPMODEL's infiltration calculation was overrode by the Noah-MP derived flux. Option 8 only uses runoff

related fluxes from Noah-MP but has higher scores in all evaluation metrics than option 4. This result suggests that varying levels of coupling fluxes utilization and model structure modification may not linearly affect models' prediction performances.

2.5.2. Behavioral Changes in Coupled TOPMODEL

The improvements in statistical metrics for streamflow prediction varied depending on coupling scenarios. To seek further how “coupling interface” affects models' overall behavior and streamflow prediction, we reviewed TOPMODELS' parameter sensitivity and water balance change.

In TOPMODEL-control, only 97 out of 26,000 parameter-sets satisfied GLUE thresholds of NSE 0.7. However, better performing coupled options (1, 2, and 3) had 2,000~4,000 surpassing the same threshold. This gap is vast compared to variation between statistical metrics (Table 2-4). We found these 97 parameter-sets specifically had a relatively narrow distribution of “m” parameter (transmissivity decline, 0.02~0.056) compared to the range of sampled space (0.0001 to 0.25). The most sensitive parameters in TOPMODEL are widely known to be LnTe (log-transformed soil surface transmissivity) and m (Exponential storage parameter) (Cho et al., 2019; Sigdel et al., 2011). None of coupled options had such a narrow range of “m” parameter value. TOPMODEL's reliance on the “m” parameter in the study area was resolved when LSM surficial fluxes were used as model input. This implies that the coupling simple hydrologic models with LSM may maintain their prediction performance under certain level of input/structural uncertainty.

Model's behavioral change due to coupling methods could be inferred from parameter sensitivity, and therefore, we analyzed total sensitivity indices for parameters by applying the “Jansen 1999” method (Jansen, 1999), excluding vch and dt parameters which are inactive in

the model due to its set-up. As coupling options more aggressively modify TOPMODEL structure and rely on LSM fluxes, sensitivity indices of multiple parameters declined regardless of their significance (Figure 2-5; A, B, D, E). In option 6, where LSM's underground and infiltration excess fluxes override calculation processes, sensitivity indices for LnTe and m became very small at 0.13 and 0.005 each. Meanwhile, vr (Surface routing velocity) became the most significant parameter for TOPMODEL. Level of reliance on LSM clearly affected TOPMODEL parameter sensitivities. However, more importantly, we found two notable trends in the changes to parameter sensitivity indices.

The first is that modification of model structure can significantly affect sensitivity indices of parameters that are not directly involved in the calculation. Removing rootzone structure naturally eliminated the involvement of Srmax and Sr0 parameters. Meanwhile, sensitivity indices increased for LnTe, but indices for m, k0, CD, and qs0 decreased noticeably in a similar trend (comparison between options 1, 2, and 3; Figure 2-5). None of these five parameters are directly involved in rootzone layer's operation based on Srmax capacity. However, modifying the model's structure alters the allocation of water throughout each calculation step and affects parameter sensitivity beyond its own domain. Similar effects happened to vr, k0, CD, and qs0 parameters when option 4 overrides vertical drainage calculation with LSM flux, where only m and td parameters were directly involved in vertical drainage calculation. We hypothesize small changes in coupling interface can accumulate through model processes and result in unpredictable shifts in model parameter sensitivity.

The second is that the significance of certain structures or functions in streamflow prediction may not be accurately reflected by the model's sensitivity to related parameters. For instance, even though TOPMODEL showed marginal sensitivity to td parameter,

substituting it with the dynamic scaling of Noah-MP flux in option 3 brought a noticeable change in streamflow estimation. This change improved streamflow prediction during a wet season in the dry year (WY 2018) from NSE 0.48 (option 2) to 0.63 (option 3). Therefore, coupling design cannot fully rely on knowledge from existing studies regarding the significance of certain parameters.

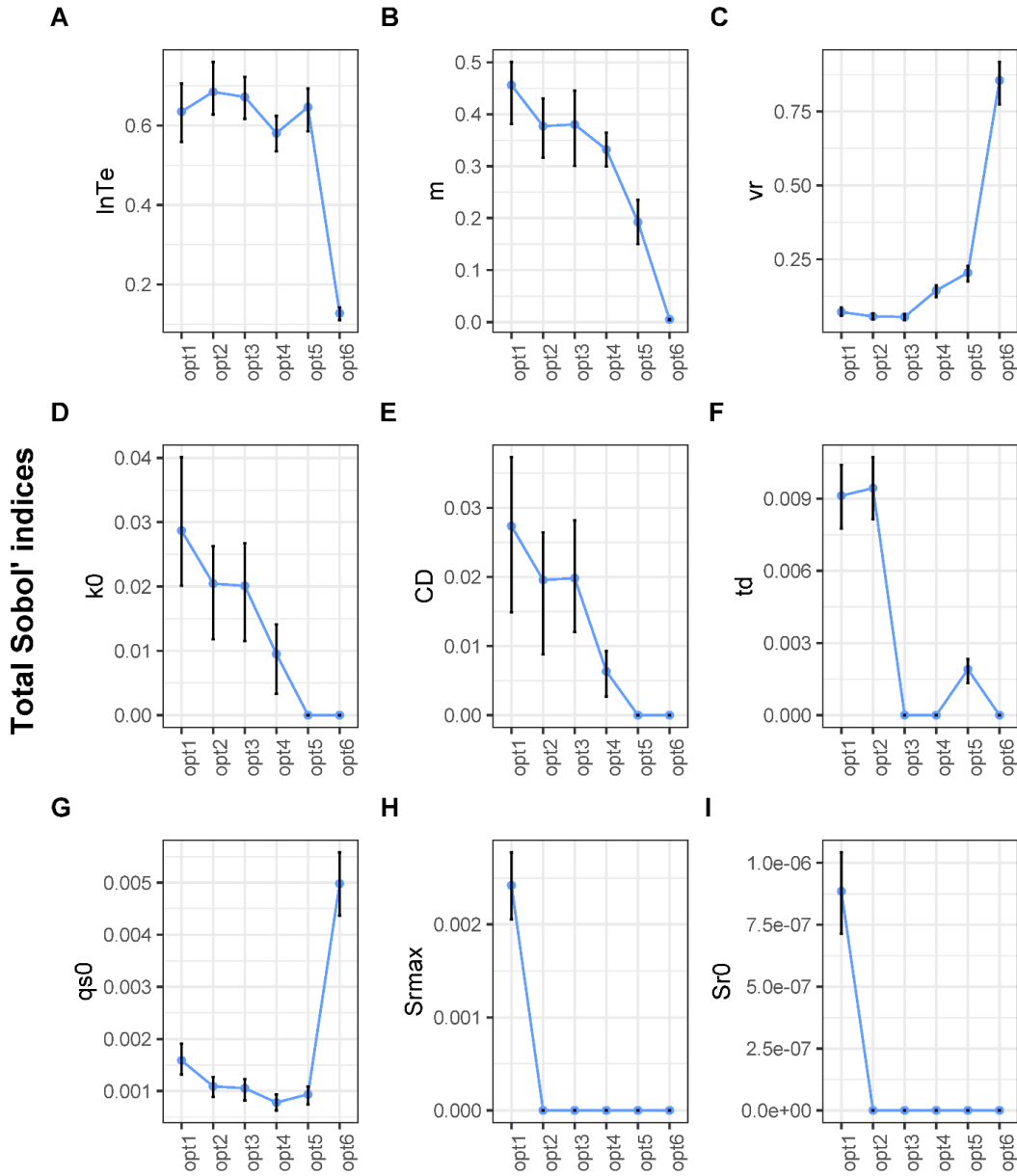


Figure 2-5. Total Sobol' indices of each TOPMODEL parameters in six coupled models. Parameter sensitivities are affected by varying coupling interface and modification of TOPMODEL structure.

Summarizing the flow components in coupled options can help visualize changes in TOPMODEL's process representation and highlight any incompatibility within coupling fluxes. (Figure 2-6). In particular, the figure shows changes in the runoff ratio between different options (Qsim value in Figure 2-6), and changes in the rainfall partitioning between overland flow and baseflow. Better performing options (1-3) maintain the strong reliance on subsurface flow, while more poorly performing options route a greater proportion of the flow via saturation (option 4) or infiltration (option 5 and 6) excess.

We can examine the causes of this difference by noting Noah-MP flux values. "Underground runoff" from Noah-MP represents free gravitational drainage and is comparable to TOPMODEL's vertical drainage in unsaturated zone. However, such flux was sufficiently small that it failed to create enough subsurface flow in TOPMODEL based on local water-table dynamics. When the vertical drainage was redirected to contribute straight into the subsurface runoff, watershed runoff was overestimated as shown in option 4 and 6 (Figure 2-6). Rainfall that was partitioned as "infiltration excess" using REFKDT function in Noah-MP was over 30% of observed runoff in the study area, which was not realistic based on expert knowledge of the watershed and is likely to be overestimated. The calibration of TOPMODEL parameters in these cases could not resolve the incompatibility of fluxes between Noah-MP and TOPMODEL.

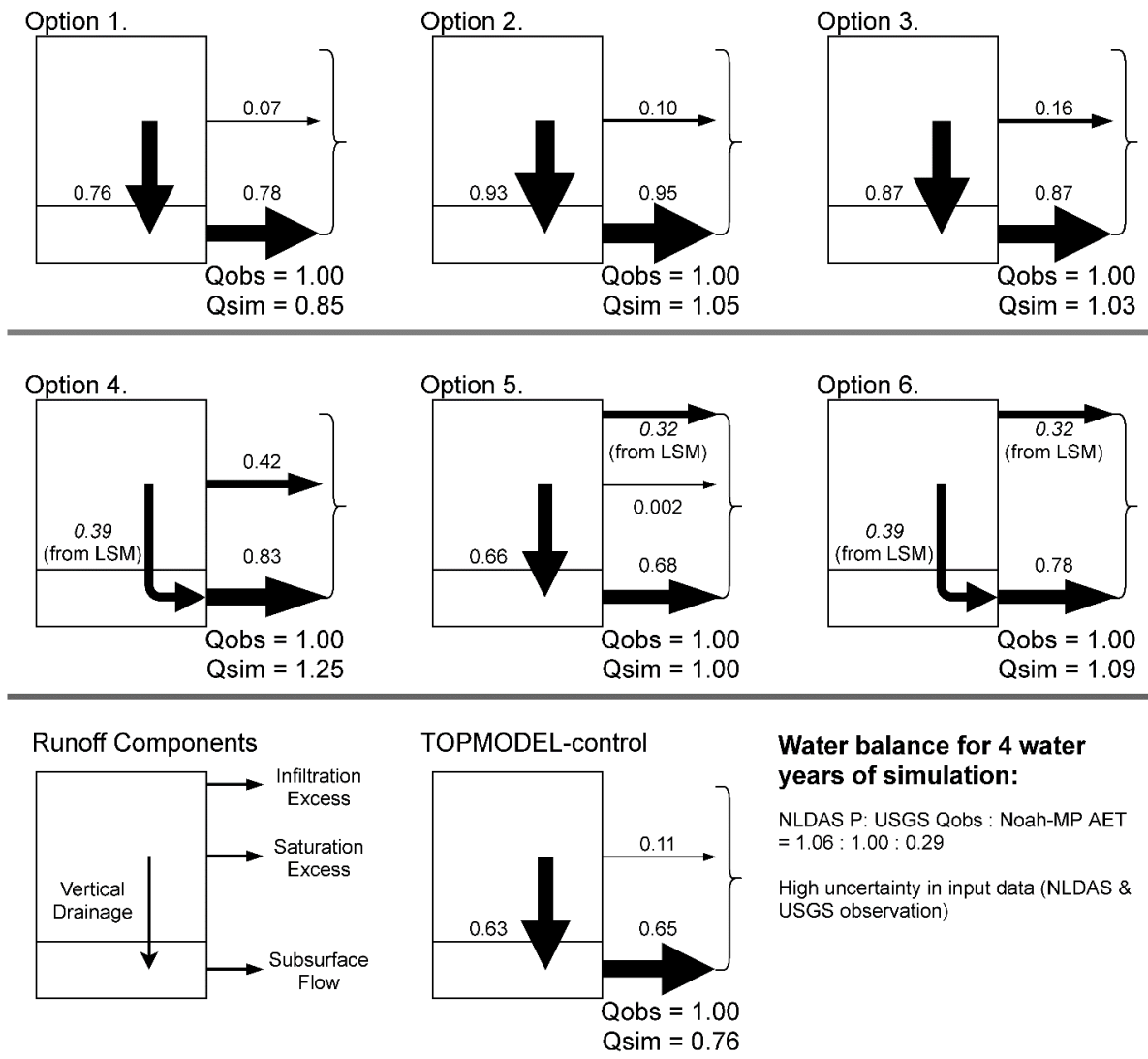


Figure 2-6. Flow components of TOPMODEL in six coupled models and TOPMODEL-control. The total observed runoff at the outlet of the catchment (Q_{obs}) through the simulation period (Oct 2015 to Sep 2019) is set to 1.00 as a standard. The Sum of each flow component is equal to simulated runoff (Q_{sim}).

2.6. Discussion

2.6.1. Improvement in Streamflow Predictive Performance

This experiment showed that a one-way coupling scheme with NWM’s Noah-MP coupled to a calibrated TOPMODEL outperformed the NWM v1.2 and original TOPMODEL (controls) in a headwater catchment, both in simulating flood peak magnitudes and in

simulating water availability. The improvement could be due to the different usage of topographic data, better representation of runoff and flow processes, or the model being highly capable of watershed-specific parameter calibration, or all of them combined. It could be seen as integrating strength of physics-based and conceptual model as Mendoza et al. (2015) suggested. Our results indicate that replacing the subsurface representation and runoff calculation of current NWM configuration with a conceptual model (TOPMODEL) better characterized hydrologic processes in the study watershed.

The water balance in study watershed implied high level of input uncertainty or error in meteorological forcing (NLDAS) and/or USGS streamflow observation. The calibration process of TOPMODEL is affected by erroneous input and biased toward creating high flows. Coupling TOPMODEL with Noah-MP allowed model to produce hydrograph and water balance that better fit given data with larger number of parameter-sets in the behavioral ensemble. The impact of input uncertainty was evident in our results, as NSE performance increased from Option 1 to 3 due to improved performance during high flows when using the LSM-based fluxes for soil moisture calculations. However, input bias caused a lower performance in the low-flow tail of the FDC for Options 2 and 3, as excess water caused a high bias in these flows. Coupling models do not resolve input uncertainty, but was able to improve predictive performance compared to the TOPMODEL-control model.

2.6.2. Coupling Interface Strongly Affects Hydrologic Model Behavior

Varying the details in the coupling interface strongly affected the performance of the coupled model and was evidenced through uncertainty and parameter sensitivity analysis. Various metrics showed that moderate coupling options performed better, and option 3 (Dynamic unsaturated-zone delay) performed the best among all the coupling schemes we

tested (NSE and KGE over 0.8 for 4 water years in hourly timestep simulation). It is a moderate option based on limited trust on non-surface LSM flux (Q_{ugd}) but allows it to adjust/constrain TOPMODEL's vertical drainage calculation to emulate the changing trend in internal state of LSM. On the other hand, when internal states and calculation were aggressively overridden by the non-surface/runoff-related Noah-MP fluxes, TOPMODEL showed a poor flow prediction and/or irregular parameter sensitivity. We found no evidence that the number of parameters remaining in the TOPMODEL has a meaningful impact on model performance. We did find that when substantial parts of TOPMODEL were replaced by LSM states, the physical integrity of the hydrologic model was impacted.

Tracking parameter sensitivity flagged an abnormal behavior in coupled TOPMODEL. It was found that coupling interface can affect some parameters in a way neither intended nor expected, even when they were remote from the location of coupling or modified components. This occurs regardless of modifying TOPMODEL to be compatible with non-surface coupling fluxes from Noah-MP. We note that the coupling scheme's prediction performance metrics cannot completely indicate the soundness of coupling behavior. The parameter sensitivity can and did diverge rapidly even when model performance metrics or hydrographs were similar. Therefore, parameter sensitivity analysis represents valuable additional tools to trace the impact of coupling options on the model function.

The results have shown that some incompatibility is inherent between model fluxes and can affect the model's hydrologic integrity when applying override-type coupling with internal states. Therefore, each sub-model might calculate a different internal value for certain hydrological variables used as coupling fluxes even when they are theoretically identical. Such structural differences between sub-models are due to differing process delineation and

assumptions rather than one model being purely “wrong”. In our case study, the structural incompatibility was not mitigated by parameter calibration and prevented the coupled model from maintaining sound behavior.

2.6.3. Implications in coupling method

Our results show profound differences between model behavior and parameter sensitivity under coupling options that appear superficially similar. Structural uncertainty is one of the major sources of modeling uncertainty and significantly affects the prediction outcome (Butts et al., 2004; Refsgaard et al., 2006). We, therefore, propose that coupling method uncertainty should be considered as a major source of model structural uncertainty when developing model coupling options. This consideration becomes especially important given recent proposals to develop a more flexible, modular, and modern NWM framework (Johnson et al., 2019).

Lower reliance on LSM fluxes and re-constraining them under TOPMODEL structure with minor modification resulted in better performance in options 1, 2, and 3 with less aggressive coupling. On the other hand, dynamic scaling from option 3 shown that allowing TOPMODEL’s soil moisture status to emulate that of LSM with indirect use of coupling flux outperformed any other options. These suggest that constraints between LSM fluxes and a hydrologic model's internal state allow the hydrologic model to selectively emulate the trend of LSM status while transforming it into compatible value, and ultimately lead to better results. Such an approach can be viewed as establishing a consistent constraint and allowing model to avoid incompatibility issues.

Based on the findings, we propose general principles for developing effective coupling methods in hydrologic modeling. When models have some incompatibility in process

representation, sub-models can keep cohesion within calculation processes by avoiding the forced override of internal states with coupling fluxes. Allowing independence to sub-models' internal processes can prevent the coupled model from failing with structural uncertainty. The indirect use of coupling fluxes, for instance, option 3 in the study, or Hydroblocks (Chaney et al., 2016) that uses changes in water table depth from Noah-MP as recharge rate, could address incompatibility issues. In summary 1) maintain integrity of sub-models' key structures/processes, and 2) carefully arrange coupling fluxes in a compatible way that establish consistency between sub-models' internal status.

Two-way coupling must be treated differently from one-way coupling due to its complexity and feedback loops, however, such general principles could still apply. If each sub-models' design shares a common assumption or representation of hydrological process and space (vertical and horizontal), such caution may not be necessary. It is the strategy taken in LSM based hydrologic modeling. In typical cases where models have some incompatibility in process representation, it would be better to consider indirect use of coupling fluxes first. We suppose that extracting one sub-model's key component and embedding it into the other sub-model can also reduce incompatibilities. This would help to avoid structural uncertainty from the coupling interface, despite potentially compromising the goal of retaining model independence in a modular modeling framework.

2.6.4. Limitations

In this study, we took advantage of a one-way coupling approach (easy calibration and uncertainty/sensitivity analysis) to test out the impact of details in the coupling interface (type of coupling flux, location of coupling, and model's internal process modification) over coupled models' behavior. On the contrary, two-way coupled models require an advanced

approach such as uncertainty propagation framework (Moges et al., 2020) to investigate uncertainty/parameter sensitivity. Input or observational uncertainties are one of the major model uncertainties (McMillan et al., 2012) and such misinformation in data can easily fail the model (Beven and Westerberg, 2011). Neither analysis to assess the uncertainty from input data nor model calibration technique to resolve errors in input/observation data was considered due to the limited scope of the study.

One-way coupling scheme set up in the study is relatively simple and this approach prevents the need for a detailed understanding of WRF-Hydro's internal structure to synthesize or disintegrate internal variables. However, it is only targeted for an experiment in a single headwater catchment and was not designed for applying on a large scale. Applying this to multiple watersheds over large areas will require dedicated watershed boundary delineation and embedding an NWM-compatible channel routing scheme into hydrologic models. Lastly, as mentioned earlier in the methods section, data handling was done externally using the model outputs in the study. However, any operational model must include a data management module that can efficiently transfer/exchange model fluxes while keeping software coupling levels low.

2.6.5. Broader applications

The modular approach in hydrological modeling is becoming more common. The results of this study support the proposal that a loose, one-way coupling scheme can bring practical benefits over a more complex model. Butts et al. (2004) suggested that the model structure has a strong influence on model performance, and complexity does not necessarily increase performance. Frameworks that evaluate the applicability of various hydrological models such as Framework for Understanding Structural Errors (FUSE; Clark et al., 2008) and Modular

Assessment of Rainfall-Runoff Models Toolbox (MARRMoT; Knoben et al., 2019) can support “mix-and-match” approach of hydrological models for varying purpose and environment (McMillan et al., 2009). This “mix-and-match” style approach allows an application of different formulation based on physics-based solutions, but also an incorporation of existing model conceptualization or code, such as is possible in the DECIPHeR framework (Coxon et al., 2019) or Delft-FEWS system (Werner et al., 2013). This patchwork approach promotes modular model structure and might prevent “reinvention of the wheel” by making use of already established successful model structures. Our study showed that it is important to account for the structural uncertainty from coupling in such an approach, and a one-way coupling enables such with minimal effort due to its simple structure and high understandability. For future modular design in hydrological modeling, our results provide evidence that one-way coupling can be a useful method for “mix-and-match” approaches.

2.7. Conclusions

The successful application of a one-way coupling of TOPMODEL with the Noah-MP demonstrated in this study illustrates that simplification of the NWM subsurface structure in headwater catchments produced desirable results. The conclusions can be summarized as follows:

- 1) One-way coupling resulted in increased predictive skill compared to controls (NWM and original TOPMODEL). This implies substituting LSMs' 1-D soil column-based subsurface representation with a conceptual model structure can better upscale the runoff processes into watershed behavior and improve streamflow forecast.

2) One-way coupling scheme facilitated conventional model calibration, performance evaluation, and uncertainty-sensitivity analysis methods to examine how the coupling interface affects the coupled hydrologic model's behavior.

3) Coupling interface strongly affected prediction performance. A moderate coupling option represented the most successful approach; Using LSM surface components with TOPMODEL subsurface structure, and indirectly referencing LSM subsurface flux with limited trust. Changes in the coupling interface also led to unexpected shifts in TOPMODEL parameter sensitivity or water balance even when performance metrics were similar.

4) Coupling interface should be considered as the source of structural uncertainty in coupled models. Incompatibility can exist between sub-models' internal fluxes even when they are theoretically identical because of varying process delineation and assumptions.

5) It is recommendable to maintain the independence of sub-models' key structures/processes and to arrange coupling fluxes to establish consistency between sub-models' internal status unless each sub-model specifically shares an assumption and structure.

The study contributes towards the potential of extending a modular approach in hydrologic modeling toward a pragmatic “mix-and-match” design linking large-scale physical process-based models and various conceptual hydrological models by needs or geographical locations with one-way or two-way coupling.

2.8. References

1. Alghamdi, J.S., 2008. MEASURING SOFTWARE COUPLING. *Arabian Journal for Science & Engineering* (Springer Science & Business Media BV) 33.
2. Archfield, S.A., M. Clark, B. Arheimer, L.E. Hay, H. McMillan, J.E. Kiang, J. Seibert, K. Hakala, A. Bock, T. Wagener, W.H. Farmer, V. Andréassian, S. Attinger, A. Viglione, R. Knight, S. Markstrom, and T. Over, 2015. Accelerating Advances in Continental Domain Hydrologic Modeling. *Water Resources Research* 51:10078–10091.

3. Arnault, J., S. Wagner, T. Rummeler, B. Fersch, J. Bliefernicht, S. Andresen, and H. Kunstmann, 2016. Role of Runoff-Infiltration Partitioning and Resolved Overland Flow on Land-Atmosphere Feedbacks: A Case Study with the WRF-Hydro Coupled Modeling System for West Africa. *Journal of Hydrometeorology* 17:1489–1516.
4. Beven, K., 1984. Infiltration into a Class of Vertically Non-Uniform Soils. *Taylor & Francis* 29:425–434.
5. Beven, K., 1997. TOPMODEL: A Critique. *Hydrological Processes* 11:1069–1085.
6. Beven, K., 2012. *Rainfall-Runoff Modelling*. John Wiley & Sons, Ltd, Chichester, UK. doi:10.1002/9781119951001.
7. Beven, K. and A. Binley, 1992. The Future of Distributed Models: Model Calibration and Uncertainty Prediction. *Hydrological Processes* 6:279–298.
8. Beven, K.J. and M.J. Kirkby, 1977. Towards a Simple, Physically Based, Variable Contributing Area Model of Catchment Hydrology. *Bulletin of the International Association of Scientific Hydrology* 24:43–69.
9. Beven, K.J. and M.J. Kirkby, 1979. A Physically Based, Variable Contributing Area Model of Basin Hydrology. *Hydrological Sciences Bulletin* 24:43–69.
10. Beven, K.J., R. Lamb, M.J. Kirkby, and J.E. Freer, 2020. A History of TOPMODEL. *Hydrol. Earth Syst. Sci. Discuss.*:1–44.
11. Beven, K.J., R. Lamb, P.F. Quinn, R. Romanowicz, and J.E. Freer, 1995. *Topmodel. Computer Models of Watershed Hydrology*.
12. Beven, K. and I. Westerberg, 2011. On Red Herrings and Real Herrings: Disinformation and Information in Hydrological Inference. *Hydrological Processes* 25:1676–1680.
13. Bilal, H. and S. Black, 2006. Computing Ripple Effect for Object Oriented Software. *Quantitative Approaches in Object-Oriented Software Engineering (QAOOSE)*.
14. Bouilloud, L., K. Chancibault, # Bé, A. Vincendon, R. Ducrocq, F. Habets, G.-M. Saulnier, S. Anquetin, E. Martin, and J. Noilhan, 2010. Coupling the ISBA Land Surface Model and the TOPMODEL Hydrological Model for Mediterranean Flash-Flood Forecasting: Description, Calibration, and Validation. *Journals.Amet Soc. Org* 11:315–333.
15. Butts, M.B., J.T. Payne, M. Kristensen, and H. Madsen, 2004. An Evaluation of the Impact of Model Structure on Hydrological Modelling Uncertainty for Streamflow Simulation. *Journal of Hydrology. Elsevier*, pp. 242–266.
16. Buytaert, W., 2011. Topmodel: Implementation of the Hydrological Model TOPMODEL in R. *Global Change Biology* 13:679–706.
17. Castronova, T. and D. Tijerina, 2019. CUAHSI/Nwm_subsetting: CUAHSI Subsetter. doi:10.5281/ZENODO.3343763.
18. Chaney, N.W., P. Metcalfe, and E.F. Wood, 2016. HydroBlocks: A Field-Scale Resolving Land Surface Model for Application over Continental Extents. *Hydrological Processes* 30:3543–3559.
19. Cho, H., 2000. *GIS Hydrological Modeling System by Using Programming Interface of GRASS*. Kyungpook National University, Korea.
20. Cho, H., J. Park, and D. Kim, 2019. Evaluation of Four GLUE Likelihood Measures and Behavior of Large Parameter Samples in ISPSO-GLUE for TOPMODEL. *Water (Switzerland)* 11. doi:10.3390/w11030447.

21. Clark, M.P., Y. Fan, D.M. Lawrence, J.C. Adam, D. Bolster, D.J. Gochis, R.P. Hooper, M. Kumar, L.R. Leung, D.S. Mackay, R.M. Maxwell, C. Shen, S.C. Swenson, and X. Zeng, 2015. Improving the Representation of Hydrologic Processes in Earth System Models. *Water Resources Research* 51:5929–5956.
22. Clark, M.P., B. Nijssen, J.D. Lundquist, D. Kavetski, D.E. Rupp, R.A. Woods, J.E. Freer, E.D. Gutmann, A.W. Wood, D.J. Gochis, R.M. Rasmussen, D.G. Tarboton, V. Mahat, G.N. Flerchinger, and D.G. Marks, 2015. The Structure for Unifying Multiple Modeling Alternatives (SUMMA), Version 1.0: Technical Description. doi:10.5065/D6WQ01TD.
23. Clark, M.P., A.G. Slater, D.E. Rupp, R.A. Woods, J.A. Vrugt, H. V. Gupta, T. Wagener, and L.E. Hay, 2008. Framework for Understanding Structural Errors (FUSE): A Modular Framework to Diagnose Differences between Hydrological Models. *Water Resources Research* 44. doi:10.1029/2007WR006735.
24. Coxon, G., J. Freer, R. Lane, T. Dunne, W.J.M. Knoben, N.J.K. Howden, N. Quinn, T. Wagener, and R. Woods, 2019. DECIPHr v1: Dynamic FluxEs and Connectivity for Predictions of HydRology. *Geosci. Model Dev* 12:2285–2306.
25. Cronshey, R.G., R.T. Roberts, and N. Miller, 1985. URBAN HYDROLOGY FOR SMALL WATERSHEDS (TR-55 REV.).
26. Decharme, B. and H. Douville, 2006. Introduction of a Sub-Grid Hydrology in the ISBA Land Surface Model. *Climate Dynamics* 26:65–78.
27. Deng, H.P. and S.F. Sun, 2012. Incorporation of TOPMODEL into Land Surface Model SSiB and Numerically Testing the Effects of the Corporation at Basin Scale. *Science China Earth Sciences* 55:1731–1741.
28. Fan, Y., M. Clark, D.M. Lawrence, S. Swenson, L.E. Band, S.L. Brantley, P.D. Brooks, W.E. Dietrich, A. Flores, G. Grant, J.W. Kirchner, D.S. Mackay, J.J. McDonnell, P.C.D. Milly, P.L. Sullivan, C. Tague, H. Ajami, N. Chaney, A. Hartmann, P. Hazenberg, J. McNamara, J. Pelletier, J. Perket, E. Rouholahnejad-Freund, T. Wagener, X. Zeng, E. Beighley, J. Buzan, M. Huang, B. Livneh, B.P. Mohanty, B. Nijssen, M. Safeeq, C. Shen, W. van Verseveld, J. Volk, and D. Yamazaki, 2019. Hillslope Hydrology in Global Change Research and Earth System Modeling. *Water Resources Research* 55:1737–1772.
29. Fenton, N. and A. Melton, 1990. Deriving Structurally Based Software Measures. *The Journal of Systems and Software* 12:177–187.
30. Gan, Y., X.Z. Liang, Q. Duan, F. Chen, J. Li, and Y. Zhang, 2019. Assessment and Reduction of the Physical Parameterization Uncertainty for Noah-MP Land Surface Model. *Water Resources Research* 55:5518–5538.
31. Garrick, M., C. Cunnane, and J.E. Nash, 1978. A Criterion of Efficiency for Rainfall-Runoff Models. *Journal of Hydrology* 36:375–381.
32. Gharari, S., M.P. Clark, N. Mizukami, W.J.M. Knoben, J.S. Wong, and A. Pietroniro, 2020. Flexible Vector-Based Spatial Configurations in Land Models. *Hydrology and Earth System Sciences* 24:5953–5971.
33. Gharari, S., M.P. Clark, N. Mizukami, J.S. Wong, A. Pietroniro, and H.S. Wheatler, 2019. Improving the Representation of Subsurface Water Movement in Land Models. *Journal of Hydrometeorology* 20:2401–2418.

34. Givati, A., D. Gochis, T. Rummeler, and H. Kunstmann, 2016. Comparing One-Way and Two-Way Coupled Hydrometeorological Forecasting Systems for Flood Forecasting in the Mediterranean Region. *Hydrology* 3:19.
35. Gochis, D.J., M. Barlage, A. Dugger, K. FitzGerald, L. Karsten, M. McAllister, J. McCreight, J. Mills, A. RafieeiNasab, L. Read, K. Sampson, D. Yates, and W. Yu, 2018. WRF-Hydro V5 Technical Description The NCAR WRF-Hydro Modeling System Technical Description Until Further Notice, Please Cite the WRF-Hydro Modeling System as Follows: WRF-Hydro V5 Technical Description WRF-Hydro V5 Technical Description.
36. Gochis, D.J., W. Yu, and D. Yates, 2015. The WRF-Hydro Model Technical Description and User's Guide, Version 3.0. NCAR Technical Document.
37. Gupta, H. V., H. Kling, K.K. Yilmaz, and G.F. Martinez, 2009. Decomposition of the Mean Squared Error and NSE Performance Criteria: Implications for Improving Hydrological Modelling. *Journal of Hydrology* 377:80–91.
38. Gupta, H.V., S. Sorooshian, and P.O. Yapo, 1998. Toward Improved Calibration of Hydrologic Models: Multiple and Noncommensurable Measures of Information. *Water Resources Research* 34:751–763.
39. Habets, F. and G.M. Saulnier, 2001. Subgrid Runoff Parameterization. *Physics and Chemistry of the Earth, Part B: Hydrology, Oceans and Atmosphere* 26:455–459.
40. Hay, L.E., M.P. Clark, M. Pagowski, G.H. Leavesley, and J.J. Gutowski, 2006. One-Way Coupling of an Atmospheric and a Hydrologic Model in Colorado. *Journal of Hydrometeorology* 7:569–589.
41. Van Den Hurk, B., M. Best, P. Dirmeyer, A. Pitman, J. Polcher, and J. Santanello, 2011. Acceleration of Land Surface Model Development over a Decade of Glass. *Bulletin of the American Meteorological Society* 92:1593–1600.
42. Jansen, M.J.W., 1999. Analysis of Variance Designs for Model Output. *Computer Physics Communications* 117:35–43.
43. Jeziorska, J. and T. Niedzielski, 2018. Applicability of TOPMODEL in the Mountainous Catchments in the Upper Nysa Kłodzka River Basin (SW Poland). *Acta Geophysica* 66:203–222.
44. Jin, X., C.Y. Xu, Q. Zhang, and V.P. Singh, 2010. Parameter and Modeling Uncertainty Simulated by GLUE and a Formal Bayesian Method for a Conceptual Hydrological Model. *Journal of Hydrology* 383:147–155.
45. Johnson, D.W., N.J. Frazier, F.L. Ogden, S. Cui, D.L. Blodgett, J.D. Hughes, I. Norton, P. A., R. Cabell, D.W. Johnson, N.J. Frazier, F.L. Ogden, S. Cui, D.L. Blodgett, J.D. Hughes, I. Norton, P. A., and R. Cabell, 2019. Next Generation National Water Model Architecture: Organizing Principles to Support Evolving Capabilities. AGUFM 2019:H43I-2145.
46. Kirkby, M.J., 1975. Hydrograph Modelling Strategies. *Processes in Physical and Human Geography*, pp. 69–90.
47. Kirkby, M.J. and D. Weyman, 1974. Measurements of Contributing Area in Very Small Drainage Basins. Department of Geography, University of Bristol No. 3.
48. Knoben, W.J.M., J.E. Freer, K.J.A. Fowler, M.C. Peel, and R.A. Woods, 2019. Modular Assessment of Rainfall-Runoff Models Toolbox (MARRMoT) v1.2: An Open-Source, Extendable Framework Providing Implementations of 46 Conceptual

- Hydrologic Models as Continuous State-Space Formulations. *Geoscientific Model Development* 12:2463–2480.
49. Lahmers, T.M., C.L. Castro, and P. Hazenberg, 2020. Effects of Lateral Flow on the Convective Environment in a Coupled Hydrometeorological Modeling System in a Semiarid Environment. *Journal of Hydrometeorology* 21:615–642.
 50. Legates, D.R. and G.J. McCabe, 1999. Evaluating the Use of “Goodness-of-Fit” Measures in Hydrologic and Hydroclimatic Model Validation. *Water Resources Research* 35:233–241.
 51. Linton, J., 2008. Is the Hydrologic Cycle Sustainable? A Historical-Geographical Critique of a Modern Concept. *Annals of the Association of American Geographers* 98:630–649.
 52. Mantovan, P. and E. Todini, 2006. Hydrological Forecasting Uncertainty Assessment: Incoherence of the GLUE Methodology. *Journal of Hydrology* 330:368–381.
 53. Mathevet, T., C. Michel, V. Andréassian, and C. Perrin, 2006. A Bounded Version of the Nash-Sutcliffe Criterion for Better Model Assessment on Large Sets of Basins. *IAHS-AISH Publication*:211–219.
 54. McManamay, R.A. and C.R. Derolph, 2019. Data Descriptor: A Stream Classification System for the Conterminous United States. *Scientific Data* 6. doi:10.1038/sdata.2019.17.
 55. McMillan, H., 2020. Linking Hydrologic Signatures to Hydrologic Processes: A Review. *Hydrological Processes* 34:1393–1409.
 56. Mcmillan, H., M. Clark, R. Woods, M. Duncan, M.S. Srinivasan, A. Western, and D. Goodrich, 2009. Improving Perceptual and Conceptual Hydrological Models Using Data from Small Basins. *IAHS Publ.* <https://opensky.ucar.edu/islandora/object/articles%3A19040/>. Accessed 8 Sep 2020.
 57. McMillan, H., T. Krueger, and J. Freer, 2012. Benchmarking Observational Uncertainties for Hydrology: Rainfall, River Discharge and Water Quality. *Hydrological Processes* 26:4078–4111.
 58. McMillan, H., I. Westerberg, and F. Branger, 2017. Five Guidelines for Selecting Hydrological Signatures. *Hydrological Processes* 31:4757–4761.
 59. Mendoza, P.A., M.P. Clark, M. Barlage, B. Rajagopalan, L. Samaniego, G. Abramowitz, and H. Gupta, 2015. Are We Unnecessarily Constraining the Agility of Complex Process-Based Models? *Water Resources Research* 51:716–728.
 60. Moges, E., Y. Demissie, and H. Li, 2020. Uncertainty Propagation in Coupled Hydrological Models Using Winding Stairs and Null-Space Monte Carlo Methods. *Journal of Hydrology* 589:125341.
 61. Mölders, N., 2001. Concepts for Coupling Hydrological and Meteorological Models.
 62. Moore, R.J., 1985. The Probability-Distributed Principle and Runoff Production at Point and Basin Scales. *Hydrological Sciences Journal* 30:273–297.
 63. Moriasi, D.N., J.G. Arnold, M.W. Van Liew, R.L. Bingner, R.D. Harmel, and T.L. Veith, 2007. Model Evaluation Guidelines for Systematic Quantification of Accuracy in Watershed Simulations. *Transactions of the ASABE* 50:885–900.
 64. Morita, M. and B.C. Yen, 2000. Numerical Methods for Conjunctive Two-Dimensional Surface and Three-Dimensional Sub-Surface Flows. *International Journal for Numerical Methods in Fluids* 32:921–957.

65. Myers, G.J., 1975. *Reliable Software Through Composite Design*. Mason. Charter PublisheTS. S 197.
66. Nan, Z., L. Shu, Y. Zhao, X. Li, and Y. Ding, 2011. Integrated Modeling Environment and a Preliminary Application on the Heihe River Basin, China. *Science China Technological Sciences* 54:2145–2156.
67. Nash, J.E. and J. V. Sutcliffe, 1970. River Flow Forecasting through Conceptual Models Part I - A Discussion of Principles. *Journal of Hydrology* 10:282–290.
68. NCAR Research Application Laboratory, 2015. Rwrhydro. https://ral.ucar.edu/projects/wrf_hydro/rwrhydro. Accessed 18 Mar 2020.
69. Nguyen, P., A. Thorstensen, S. Sorooshian, K. Hsu, A. AghaKouchak, B. Sanders, V. Koren, Z. Cui, and M. Smith, 2016. A High Resolution Coupled Hydrologic–Hydraulic Model (HiResFlood-UCI) for Flash Flood Modeling. *Journal of Hydrology* 541:401–420.
70. Niu, G.-Y., Z.-L. Yang, R.E. Dickinson, and L.E. Gulden, 2005. A Simple TOPMODEL-Based Runoff Parameterization (SIMTOP) for Use in Global Climate Models. *Journal of Geophysical Research* 110:D21106.
71. Niu, G.-Y., Z.-L. Yang, R.E. Dickinson, L.E. Gulden, and H. Su, 2007. Development of a Simple Groundwater Model for Use in Climate Models and Evaluation with Gravity Recovery and Climate Experiment Data. *Journal of Geophysical Research* 112:D07103.
72. Nossent, J. and W. Bauwens, 2012. Application of a Normalized Nash-Sutcliffe Efficiency to Improve the Accuracy of the Sobol’ Sensitivity Analysis of a Hydrological Model. *EGUGA* 14:237.
73. Offutt, A.J., M.J. Harrold, and P. Kolte, 1993. A Software Metric System for Module Coupling. *The Journal of Systems and Software* 20:295–308.
74. Page-Jones, M., 1988. *The Practical Guide to Structured Systems Design*. Yourdon Press.
75. Rahman, M. and R. Rosolem, 2017. Towards a Simple Representation of Chalk Hydrology in Land Surface Modelling. *Hydrology and Earth System Sciences* 21:459–471.
76. Refsgaard, J.C., J.P. van der Sluijs, J. Brown, and P. van der Keur, 2006. A Framework for Dealing with Uncertainty Due to Model Structure Error. *Advances in Water Resources* 29:1586–1597.
77. Rempe, D.M. and W.E. Dietrich, 2018. Direct Observations of Rock Moisture, a Hidden Component of the Hydrologic Cycle. *Proceedings of the National Academy of Sciences of the United States of America* 115:2664–2669.
78. Sadegh, M. and J.A. Vrugt, 2013. Approximate Bayesian Computation in Hydrologic Modeling: Equifinality of Formal and Informal Approaches. *Hydrology and Earth System Sciences Discussions* 10:4739–4797.
79. Saltelli, A., P. Annoni, I. Azzini, F. Campolongo, M. Ratto, and S. Tarantola, 2010. Variance Based Sensitivity Analysis of Model Output. Design and Estimator for the Total Sensitivity Index. *Computer Physics Communications* 181:259–270.
80. Schaake, J.C., V.I. Koren, Q.Y. Duan, K. Mitchell, and F. Chen, 1996. Simple Water Balance Model for Estimating Runoff at Different Spatial and Temporal Scales. *Journal of Geophysical Research Atmospheres* 101:7461–7475.

81. Seaber, P.R., F.P. Kapinos, and G.L. Knapp, 1987. Hydrologic Unit Maps (USA). US Geological Survey Water-Supply Paper 2294. doi:10.3133/wsp2294.
82. Seibert, J., M.J.P. Vis, E. Lewis, and H.J. van Meerveld, 2018. Upper and Lower Benchmarks in Hydrological Modelling. *Hydrological Processes* 32:1120–1125.
83. Senatore, A., G. Mendicino, D.J. Gochis, W. Yu, D.N. Yates, and H. Kunstmann, 2015. Fully Coupled Atmosphere-Hydrology Simulations for the Central Mediterranean: Impact of Enhanced Hydrological Parameterization for Short and Long Time Scales. *Journal of Advances in Modeling Earth Systems* 7:1693–1715.
84. Shen, C. and M.S. Phanikumar, 2010. A Process-Based, Distributed Hydrologic Model Based on a Large-Scale Method for Surface-Subsurface Coupling. *Advances in Water Resources* 33:1524–1541.
85. Sigdel, A., R. Jha, D. Bhatta, R.A. Abou-Shanab, V.R. Sapireddy, and B.H. Jeon, 2011. Applicability of TOPMODEL in the Catchments of Nepal: Bagmati River Basin. *Geosystem Engineering* 14:181–190.
86. Sobol', I., 1967. On the Distribution of Points in a Cube and the Approximate Evaluation of Integrals. *USSR Computational Mathematics and Mathematical Physics* 7:86–112.
87. Stedinger, J.R., R.M. Vogel, S.U. Lee, and R. Batchelder, 2008. Appraisal of the Generalized Likelihood Uncertainty Estimation (GLUE) Method. *Water Resour. Res* 44:0–06.
88. Stieglitz, M., D. Rind, J. Famiglietti, and C. Rosenzweig, 1997. An Efficient Approach to Modeling the Topographic Control of Surface Hydrology for Regional and Global Climate Modeling. *Journal of Climate* 10:118–137.
89. Sun, X., S. Roberts, B. Croke, and A. Jakeman, 2017. A Comparison of Global Sensitivity Techniques and Sampling Method. doi:10.36334/modsim.2017.a1.sun.
90. Tarboton, D.G., 2015. Terrain Analysis Using Digital Elevation Models (TauDEM). Terrain Analysis Using Digital Elevation Models (TauDEM).
91. Vincendon, B., V. Ducrocq, G.M. Saulnier, L. Bouilloud, K. Chancibault, F. Habets, and J. Noilhan, 2010. Benefit of Coupling the ISBA Land Surface Model with a TOPMODEL Hydrological Model Version Dedicated to Mediterranean Flash-Floods. *Journal of Hydrology* 394:256–266.
92. Vrugt, J.A., C.J.F. ter Braak, H. V Gupta, and B.A. Robinson, 2009. Equifinality of Formal (DREAM) and Informal (GLUE) Bayesian Approaches in Hydrologic Modeling? *Stochastic Environmental Research and Risk Assessment* 23:1011–1026.
93. Walko, R.L., L.E. Band, J. Baron, T.G.F. Kittel, R. Lammers, T.J. Lee, D. Ojima, R.A. Pielke, C. Taylor, C. Tague, C.J. Treback, and P.L. Vidale, 2000. Coupled Atmosphere-Biophysics-Hydrology Models for Environmental Modeling. *Journal of Applied Meteorology* 39:931–944.
94. Werner, M., J. Schellekens, P. Gijsbers, M. van Dijk, O. van den Akker, and K. Heynert, 2013. The Delft-FEWS Flow Forecasting System. *Environmental Modelling and Software* 40:65–77.
95. Xue, Z.G., D.J. Gochis, W. Yu, B.D. Keim, R. V. Rohli, Z. Zang, K. Sampson, A. Dugger, D. Sathiaraj, and Q. Ge, 2018. Modeling Hydroclimatic Change in Southwest Louisiana Rivers. *Water (Switzerland)* 10. doi:10.3390/w10050596.

96. Yapo, P.O., H.V. Gupta, and S. Sorooshian, 1996. Automatic Calibration of Conceptual Rainfall-Runoff Models: Sensitivity to Calibration Data. *Journal of Hydrology* 181:23–48.
97. Yapo, P.O., H.V. Gupta, and S. Sorooshian, 1998. Multi-Objective Global Optimization for Hydrologic Models. *Journal of Hydrology* 204:83–97.
98. Yourdon, E. and L. Constantine, 1979. *Structured Design: Fundamentals of a Discipline of Computer Program and Systems Design*. <https://dl.acm.org/citation.cfm?id=578522>. Accessed 13 Jul 2020.
99. Zhao, W. and A. Li, 2015. A Review on Land Surface Processes Modelling over Complex Terrain. *Advances in Meteorology* 2015. doi:10.1155/2015/607181.

Chapter 3. Untangling the impacts of land cover representation and resampling in distributed hydrological model predictions.

Abstract

Accurate land cover information is essential for hydrometeorological modeling, as it defines parameters governing land-atmosphere-vegetation interactions, water partitioning, and routing. This study presents a controlled sensitivity analysis that evaluated the impact of land cover resampling methods on hydrologic simulations within the WRF-Hydro/NWM framework. The choice of resampling algorithms affected simulations, but such influence was only prominent in arid environments, catchments featuring land cover classes that covers small fraction of the areas but with high hydrologic impact, or low-flow predictions. The study tested two distinct spatial aspects: areal proportions of land cover classes and spatial patterns in land cover. Areal proportions influenced vertical hydrologic fluxes at the catchment scale and subsequently affected streamflow characteristics. In contrast, spatial arrangement alone had a marginal impact on vertical fluxes but could still induce limited alterations in streamflow characteristics through routing processes. These results suggest that spatially distributed land cover, as used in physics-based model structures, has a limited impact on watershed-scale hydrologic simulations.

3.1. Introduction

Hydrologic information, such as prediction of streamflow and other water fluxes, is essential for managing water resources and mitigating flood and drought hazards. Increasingly, hydrologic information is required across national to continental domains to support federal policy-making, planning and hazard response (Alley et al., 2013; Demeritt et

al., 2013). Distributed hydrologic models provide this information by simulating the terrestrial water cycle at high resolutions across continental domains, driven by meteorological observations or predictions (Archfield et al., 2015; Bierkens, 2015; Wood et al., 2011). Distributed hydrologic models are complex and include many choices of model structure, parameters and settings that could be optimized to improve model accuracy. In practice, however, many such choices are rarely investigated and therefore their potential importance is unknown. This article investigates one such choice: the resampling scheme used to calculate the model's land cover classes, based on observed land cover data.

The study focus on the WRF-Hydro modelling system, a popular and open-source distributed hydrologic model developed by the U.S. National Center for Atmospheric Research (Gochis et al., 2018). WRF-Hydro has gained prominence as the core model for the National Water Model (NWM), which is operated by U.S. National Oceanic and Atmospheric Administration to provide flood forecasting across the US territories (Johnson et al., 2019). WRF-Hydro blends approaches to continental domain hydrologic modeling from the catchment modelling and land surface modelling communities, by integrating the gridded Noah-MP land surface model (Niu et al., 2011) with hydrologic routing and groundwater modules. The NWM long-range implementation of WRF-Hydro uses a 1 km land surface model grid and 1 km surface flow routing grid.

Accurate land cover information is important in WRF-Hydro/NWM, which uses land cover classes to define the model parameters that control land-atmosphere-vegetation interaction, vertical water partitioning and routing (Gochis et al., 2018). An evaluation of the historical simulation of NWM v2.1 across over 3,500 gages revealed that the composition of land cover classes affects both model accuracy and bias (Johnson et al., 2023). Similarly, the

importance of land cover data source and resolution has been shown for other distributed hydrologic models (Alawi and Özkul, 2023; Jin et al., 2019). The strong influence of land cover on model behavior can be explained by the importance of vertical land-surface fluxes and water partitioning in shaping watershed runoff behavior. For example, sensitivity analyses show that evapotranspiration, quickflow, infiltration and percolation are the processes that most strongly control runoff generation (Mai et al., 2022; Markstrom et al., 2016). All these near-surface processes are controlled by land cover parameters in WRF-Hydro and other similar frameworks based on land surface models.

Despite the important of land cover representation, the calibration of WRF-Hydro in the NWM prioritizes a set of hydraulic and user-defined partitioning parameters, and the land cover-derived spatial parameters are often used as-is due to their high dimensionality. Land cover parameters are derived from National Land Cover Database input data layers, requiring resampling to transform high-resolution input data (~10-30 m) to lower-resolution model grid scale (~1 km). Resampling methods used in the hydrology community include Majority Rule (each grid cell is allocated to the most popular land cover class within it) and Nearest Neighbor (each grid cell is allocated to the land cover class at its center), which preserve spatial pattern while allowing changes in the areal percentage of each class. The Area Preservation method alternatively preserves class percentage, while allowing some changes in spatial pattern (Johnson and Clarke, 2021). While it is known that resampling methods affect the spatial patterns of land cover, and the accuracy in terms of percentage area in each land cover category (Johnson and Clarke, 2021), the impacts of resampling method choice on catchment water balance or streamflow simulations has not been examined for distributed hydrologic models such as WRF-Hydro.

The objective of the paper is therefore to evaluate whether the choice of resampling (upsampling finer resolution dataset to coarser model resolution) method has a consequential impact on hydrologic simulation in the WRF-Hydro/NWM modeling system. The results of the study will guide hydrologic modelers as to whether it is important to evaluate resampling method choice as part of model set-up, and which aspects of hydrologic simulations may be affected. Using a sensitivity analysis approach, the study varied the resampling method to change either the percentage area assigned to each land cover class, or the spatial pattern of land cover classes within the watershed. The choice of resampling methods included schemes currently used by the hydrological community, and schemes designed to remove information about land cover proportion or spatial pattern. Using six watersheds across the U.S., the study analyzed the difference in simulated vertical water fluxes and streamflow characteristics between each resampling method. Initial hypotheses were that: 1) Changes in land cover class proportions will affect near-surface vertical water fluxes, primarily impacting catchment water balance with lesser influence on streamflow simulation, 2) Changes in the spatial pattern of land cover will affect lateral hydrologic processes in addition to near-surface vertical fluxes, and will therefore impact streamflow simulations in addition to catchment water balance.

3.2. Study Area

3.2.1. Selection Criteria

We selected U.S. basins as follows. We chose headwater basins with area between 400 and 1000 km², at least two US Geological Survey (USGS) gages and no large dams (height > 50m or storage > 10,000 Acre Feet). These conditions facilitated inspection of streamflow records and a smoother closure of the catchment water balance based on observations. Basins

should contain at least 3 land cover classes each covering at least 10% of the basin area, with no single land cover class exceeding 55% area. The areal proportion of water, barren, and wetland NLCD land cover types should be below 5% each, because the Noah-MP land surface model is unreliable for these types, lacking representation of groundwater and soil moisture interaction in wetlands (Li et al., 2022; Zhang et al., 2021). Subsequently, we selected six watersheds from an initial pool of 20 candidates, using the following criteria: 1) avoidance of highly elongated shapes, as channel routing can dominate the hydrologic response, and 2) avoidance of watersheds with excessive developed and agricultural land use to minimize potential disruptions from extensive groundwater pumping or water imports.

3.2.2. Study Watersheds

Of the six selected basins, three had significant developed land uses (Figure 3-1). We assigned the name of the basins by the county containing of each catchment outlet location. Detailed watershed information is summarized in Table 3-1.

Table 3-1. Catchment information

Name	Outlet NHDPlusV2 Common Identifier (COMID)	USGS National Water Information System ID	Total Drainage Area (km²)	Mean Annual Rainfall (mm)
Douglas	191739	06709000	712	435
Caldwell	1631587	08173000	800	852
Berkeley	5894384	01616500	704	1037
Travis	5781369	08159000	831	862
Stark	19389766	03118500	445	1012
Polk	23762661	14190500	622	1527

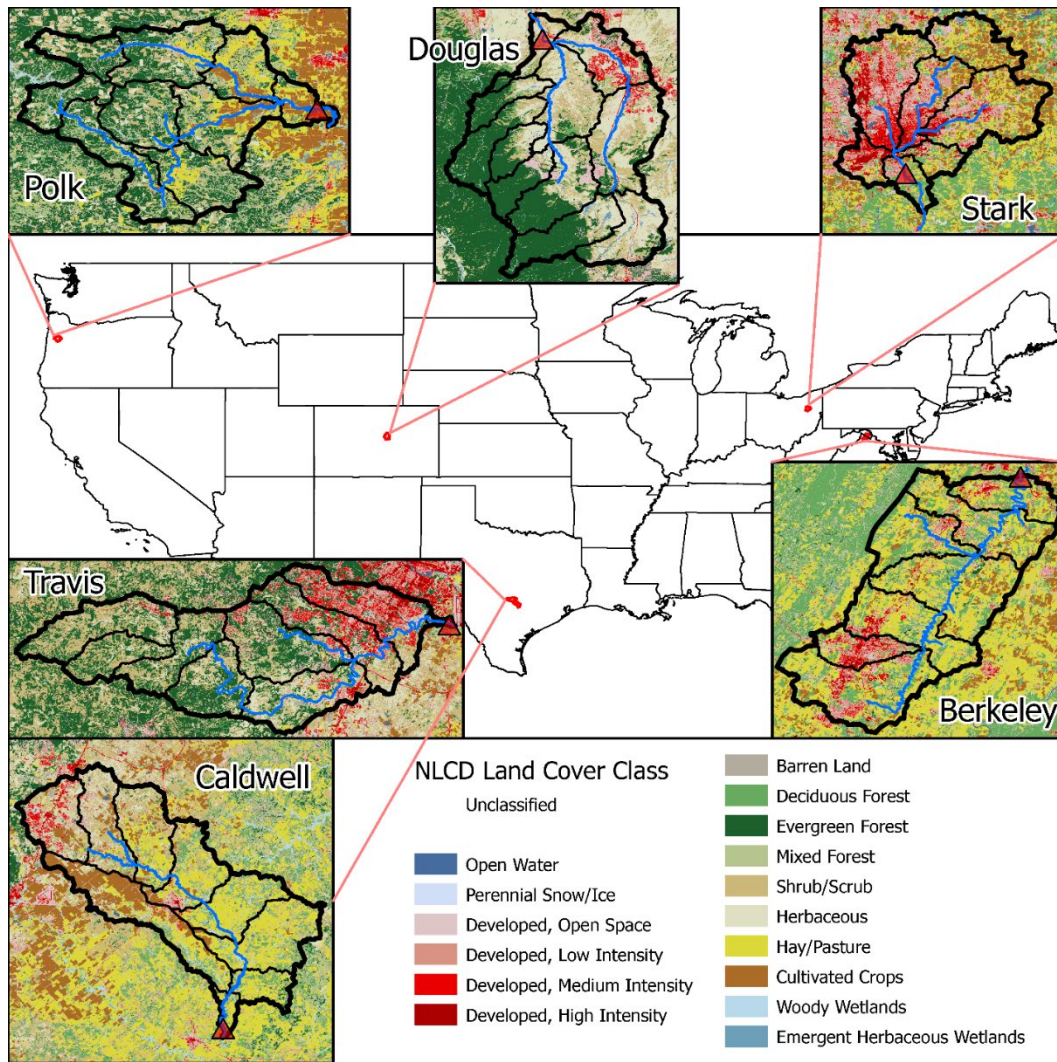


Figure 3-1. Location of six study basins. The names are assigned by the county containing the catchment outlet gage.

3.3. Methods

3.3.1. Overview of Study Design

This research applied a model experiment to evaluate how different land cover resampling methods affect the simulated water balance and streamflow (Figure 3-2). We employed the stand-alone WRF-Hydro model v5.1.2 (McCreight et al., 2020) with NWM-configured inputs and physics options. Our two original resampling schemes were the operational NWM land

cover input (NWM on Figure 2), and the recent Area Preservation scheme (AP) that preserves class areas (Johnson and Clarke, 2021). To test the impact of land cover spatial pattern, each of these schemes was compared with a ‘shuffled’ version in which the class areas were preserved, but the spatial pattern was assigned randomly (NWM-SHUF and AP-SHUF). To test the impact of removing information on land cover class areas, we tested a ‘lumped’ scheme in which each HUC 12 sub-basin was assigned to only one land cover class (HUC12L). Although many other schemes could be devised, the schemes we tested were designed to compare current schemes with maximal changes in spatial pattern or class area. The schemes are described in more detail in Section 3.2. WRF-Hydro was run for a 20-year period with each scheme, the model implementation is described in Section 3.3.3. To determine the hydrologic impacts of the resampling schemes, we examined changes in the catchment water balance (Section 3.3.4) and changes in streamflow characteristics (Section 3.3.5).

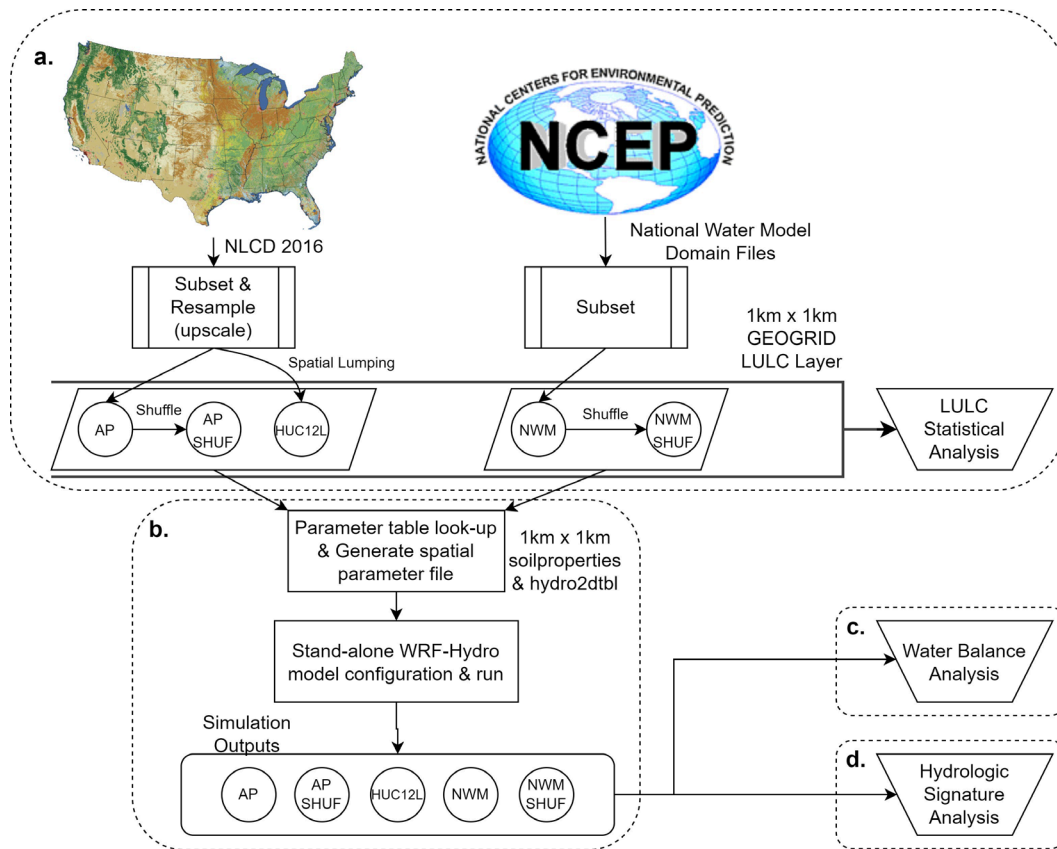


Figure 3-2. Model experiment overview. (a) LULC subset/resampling and statistical analysis. Discussed in section 3.3.2. (b) Detailed WRF-Hydro set up under National Water Model configuration. Discussed in section 3.3.3. (c) Catchment scale water balance analysis. Discussed in section 3.3.4. (d) Analyzing simulated streamflow characteristics using hydrologic signatures. Discussed in section 3.3.5.

3.3.2. Land Cover Resampling (Upscaling) Schemes

This section presents the five resampling schemes used to create model land cover input layers (Figure 3-2a), along with the rationale for these choices, and the statistical methods used to analyze the resulting differences in land cover inputs. Workflows for each scheme can be replicated by using the R package and scripts developed by the authors (Johnson & Kim, 2023; <https://github.com/mikejohnson51/wrfhydroSubsetter>).

Our first scheme (“NWM scheme”) used the land cover inputs from the NWM v2.2. These data are publicly available from the NOAA repository (NCEP, 2023; <https://www.nco.ncep.noaa.gov/pmb/codes/nwprod/>). We subset the land cover input layer

for the study basins using the R package developed by the authors (J. M. Johnson & Kim, 2023). This NWM land cover input is derived from NLCD 2016 dataset (Farrar, 2021; https://www.weather.gov/media/notification/pdf2/scn20-119nwm_v2.1_aad.pdf) and underwent a custom masking process to prevent oversampling of water. Subsequently, it was resampled using the mode (majority rule) and involved interpolation with Moderate Resolution Imaging Spectroradiometer (MODIS) land cover data (B. Cosgrove - NOAA, personal communication, August 31, 2023). Our analysis identified that NWM's LULC bivariate raster correlation (Clifford et al., 1989; Dutilleul et al., 1993) averaged at 0.67 and 0.41 with majority rule and nearest neighbor. We exclusively used NLCD 2016 dataset in our study, aligning with our goal of assessing the influence of different land cover spatial representations on model behavior, rather than evaluating the effect of actual land cover changes (e.g., NLCD 2019) on model prediction accuracy.

Our second scheme ("AP scheme") was generated using the Area Preservation resampling algorithm which was previously developed by one of the authors (Johnson, 2021; <https://github.com/mikejohnson51/resample>). This method draws from traditional methods such as nearest neighbor and majority rule, while better retaining minority classes and producing higher class area accuracy.

Our third scheme ("HUC12L") applied a sub-catchment lumping by assigning the single largest land cover type to each HUC12 (hydrologic unit code 12) watershed from the Watershed Boundary Dataset (WBD) within each study basin. Our basins usually consisted of five to ten HUC12 watersheds. This scheme was designed to create large changes in the areal proportions of land cover classes, while retaining some realism as the NOAA Next-

Generation Water Resource Modeling Framework will accommodate lumped configurations based on the users' need or watershed characteristics (Johnson et al., 2023).

Our fourth and fifth schemes (“SHUF-NWM”, “SHUF-AP”) randomly shuffle (uniform distribution, no supervised rules) the land cover grid cells of the “NWM” and “AP” schemes within each basin. These schemes were designed to create large changes in the spatial pattern of land cover classes, while preserving the same class areas. The comparison between the shuffled and original schemes enabled us to assess the isolated impact of land cover spatial pattern on model simulation.

Prior to any model runs, we conducted three statistical and spatial analyses to examine how these five land cover schemes differ. First, we assessed the basin-scale global accuracy of categorical land cover class fractions (areal proportion) in resampled schemes by comparing them to the high-resolution NLCD 2016 dataset, which served as the reference (Appendix). To assess accuracy, we computed root mean square error (RMSE) and mean absolute error (MAE) as metrics in each study basin, and presented the average (avg) values for the five study basins, along with the standard deviation (SD) values.

$$RMSE = \sqrt{\frac{\sum_{i=1}^N (Fraction_{NLCD,i} - Fraction_{resampled,i})^2}{N}}$$

$$\& MAE = \frac{\sum_{i=1}^N |Fraction_{NLCD,i} - Fraction_{resampled,i}|}{N} \quad (Eq. 3-1)$$

Second, we examined the count of cells (1km resolution model grid) that overlap with an identical land cover class between each scheme. Third, we investigated Dutilleul’s moving window bivariate raster correlation (Clifford et al., 1989; Dutilleul et al., 1993) between schemes to quantify differences in spatial pattern. This metric was calculated using the “spatialEco” R-package (Evans et al., 2022).

3.3.3. WRF-Hydro Implementation

The study ran WRF-Hydro for 20 water years (2001 to 2020) with 1-hour NLDAS meteorological forcing with the settings as used for the NWM long-range configuration (hourly timestep for the Noah-MP module, 10 and 300 second timestep for terrain and channel routing). This configuration uses 1km resolution terrain and subsurface routing options which gives a 1:1 spatial correspondence between LSM/routing grids and downscaled NLDAS forcing. This configuration was selected to avoid uncertainty that can be caused by spatial aggregation of parameters and fluxes between multiscale model grids. To stabilize the internal state of model beforehand, initialization was conducted using an idealized uniform precipitation scenario (Gochis et al., 2018), followed by four repetitive spin-up runs using water years 1999 and 2000.

A short discussion is warranted on the role that land cover parameters play in controlling hydrologic processes within WRF-Hydro. Our resampling schemes alter the land cover layer in the “geogrid” input file. These changes are propagated into parameters that control soil-vegetation-atmosphere interactions, because these parameter grids are generated by table look-up from the land cover input during pre-processing with WRF-Hydro tools (NCAR, 2023a; https://ral.ucar.edu/projects/wrf_hydro/pre-processing-tools). Parameters affected include: 1) Spatial parameters governing interception, evapotranspiration, and snow/ice processes, leading to potential changes in soil moisture conditions. 2) Surface roughness of the terrain routing grid, which can affect the re-infiltration of overland flow. 3) Soil hydraulic parameters (saturation, field capacity and wilting point) in urban areas which are overwritten with prescribed values. Some sensitive parameters of WRF-Hydro are not affected by land cover changes: these include “slope” (coefficient for soil drainage to linear reservoir which

may derive from topographic data, but often empirically calibrated) and “refkdt” (empirical infiltration partitioning parameter; Schaake et al., 1996). Both parameters are spatially variable in the NWM, and have strong impacts on runoff simulations (Silver et al., 2017), we retained original NWM values in all cases.

3.3.4. Catchment-scale Water Balance Analysis

Volumetric changes in vertical water flux and partitioning can be analyzed by evaluating catchment water balance in the WRF-Hydro simulations described in the previous section. We used the “rwrhydro” package in R (NCAR, 2023b) to aggregate model output fluxes into evapotranspiration, surface runoff, subsurface runoff, and change in soil moisture storage (as a percentage of precipitation). We then compared the water balance between land cover schemes with absolute and proportional (percent) differences. We compared the water balance of the three schemes that modify land cover class areas (NWM and HUC12L against AP), and then compared the shuffled schemes (SHUF-NWM/AP) against their non-shuffled original (NWM/AP).

3.3.5. Analyzing Simulated Streamflow Characteristics Using Hydrologic Signatures

In this section, we examined the differences in streamflow regime arising from different land cover resampling schemes. We used a visual inspection of the flow duration, which allows us to assess changes in the overall distribution of streamflow magnitudes. We do not include “goodness-of-fit” model evaluation or calibration, because our focus is on how land cover resampling influences model behavior, rather than accuracy of streamflow simulations in a particular time period or basin. The accuracy of WRF-Hydro simulations is often influenced by various factors including basin and climate characteristics and NOAA’s

national calibration strategy, which may interact with or offset land cover errors (Johnson et al., 2023). However, we include plots of the observed USGS flow duration curve, which both enables a brief comparison of WRF-Hydro results with observed flow data, and provides context regarding the magnitude of land cover impact in comparison with deviations from observed flow.

To further understand changes in simulated streamflow, we used suites of hydrologic signatures. Hydrologic signatures are metrics that quantify various watershed response characteristics, and often relate to hydrologic processes in the upstream watershed (McMillan, 2020; McMillan, 2021). When analyzing hydrologic signatures, researchers aim to use a well-rounded set that covers various aspects of streamflow such as magnitude, frequency, duration, timing, and rate of change to characterize watershed flow regime and hydrologic phenomena (Gnann et al., 2021; Poff et al., 1997; Richter et al., 1996). In this study, we focused on signatures that are linked to the process represented in WRF-Hydro structure (near-surface vertical processes, and lateral aggregation/distribution) to investigate their association with areal proportion and spatial patterns of land cover. These include:

- 1) $Sig_{sfc-vrt}$ set consists of signatures that are linked to near-surface vertical flux exchange or water partitioning processes (e.g., infiltration, evaporation, transpiration) at the soil column (grid-cell) level. Hydrologic fluxes from such near-surface vertical processes may control watershed runoff response depending on model structures.
- 2) Sig_{lat} set includes signatures relevant to lateral aggregation/distribution of water at the hillslope/watershed scale which is represented as terrain routing in the model.

Hydrologic signatures were calculated from 6-hourly streamflow simulation outputs using the TOSSH toolbox (Gnann et al., 2022). We excluded “frequency” and “duration” signatures

as they were unreliable due to the iconic streamflow pattern of LSM-based hydrologic models (“flashy runoff superimposed on slow recessions”; Gharari et al., 2019). Hydrologic signatures were calculated from two separate multi-year periods (WY 2001~2010, WY 2011~2020) for more reliable timing and rate of change signatures. We note that such measures did not skew the interquartile range of signatures, but only smoothed out some extreme values and outliers.

- 1) **The *Sig_{sfc-vrt}* set** consists of 8 signatures (Table 3-2). The low-flow magnitude signatures provide evidence of how changes in ET and soil water availability affect slow flow (subsurface runoff) responses. We analyzed the lowest 7-day average flow that occurs once every 10 years (7Q10) and 5th percentile streamflow (Q5). The mean- and high-flow magnitude signatures provide evidence of how changes in rainfall partitioning affect quick flow (surface runoff) responses during larger events. We analyzed 50th and 95th percentile streamflow (Qmean and Q95) and flood magnitude corresponding to 1, 2, and 5-year recurrence interval floods. The rate of change signature links to partitioning between quick and slow runoff (McMillan, 2020; Yilmaz et al., 2008), and provides evidence of how changes in land cover resampling alter the dominant runoff generation processes in the WRF-Hydro model. We analyzed the mid-section slope of the flow duration curve.
- 2) **The *Sig_{lat}* set** consists of four signatures (Table 3-2). A baseflow index (BFI) is widely used to quantify the significance of baseflow processes. The gradient of the mid-section of the master recession curve (MRC) is linked with the water retention capacity of the watershed. These two signatures are not closely related to near-surface vertical processes or water partitioning, but are more related to geological, soil, and

topographical characteristics of the watershed (Estrany et al., 2010). Rising limb density (RLD) is related to lateral processes and can indicate whether watershed responses are dominated by hillslope process or delay in channel routing (McMillan, 2020; Shamir et al., 2005).

Table 3-2. Selected hydrologic signatures for each signature set.

	<i>Sig_{sfc-vrt}</i>	<i>Sig_{lat}</i>
Magnitude	- Q5, 7Q10, Qmean, Q95 - 1, 2 & 5 Year Flood Magnitude	- Base Flow Index (BFI)
Timing		- Mean Half Flow Interval (HFI)
Rate of Change	- Mid-section Slope of Flow Duration Curve (FDC)	- Mid-section Slope of Master Recession Curve (MRC) - Rising Limb Density (RLD)

To evaluate the impact of land cover resampling on our 2 sets of hydrologic signatures, we examined four comparison cases; (1) NWM to AP, (2) HUC12L to AP, (3) SHUF-AP to AP, (4) SHUF-NWM to NWM. Comparing NWM and HUC12L to AP shows how minor or major changes in areal proportion of land cover classes affect streamflow prediction. Comparing shuffled schemes to their original shows how major changes in spatial pattern of land cover but identical areal proportions affect streamflow prediction.

3.4. Results

Results will be presented in the following order: 1) a statistical and spatial analysis of resampled land cover grids; 2) a comparison of the simulated catchment water balance between land cover resampling schemes; and 3) an evaluation of simulated hydrologic signatures characterizing streamflow between land cover resampling schemes.

3.4.1. Land Cover Statistics and Spatial Correlation

Figure 3-3 presents the original high-resolution land cover data (NLCD2016) against the results of each lower-resolution resampling scheme. The NWM and AP schemes show similarities in overall structure, however, the AP scheme shows more local spatial variability. The HUC12L scheme shows land cover lumped by subcatchment, and the shuffled schemes show arbitrarily dispersed land cover classes.

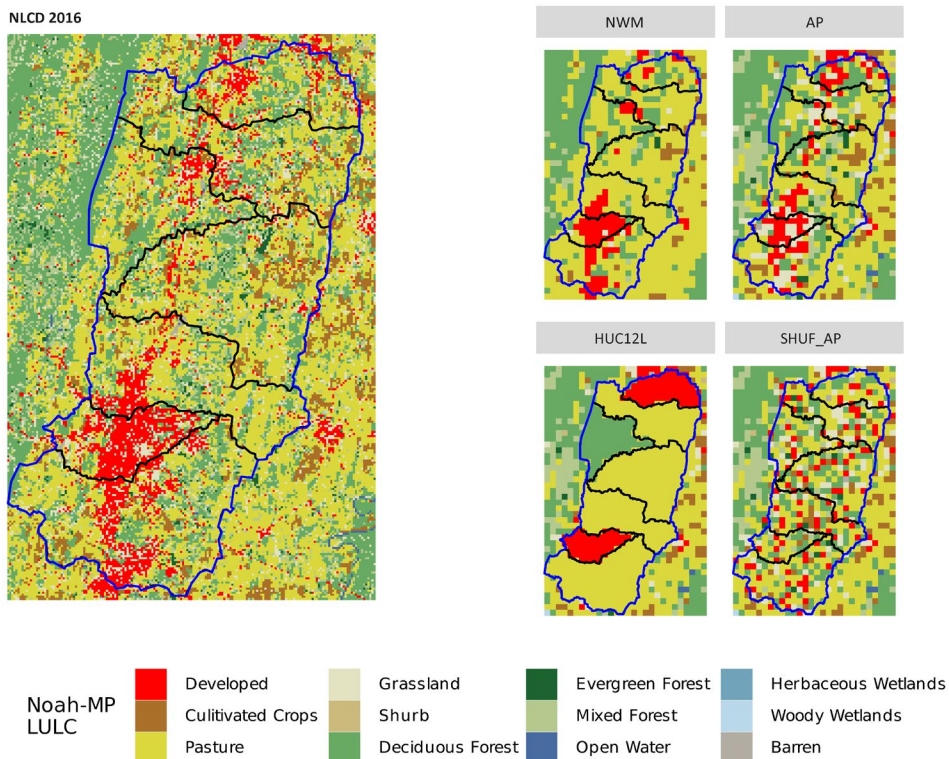


Figure 3-3. Comparison of NWM, AP, HUC12L, and SHUF against NLCD 2016 at “Berkeley” basin (Opequon Creek watershed in West Virginia). SHUF-NWM is not presented as it shares arbitrary spatial pattern similar to SHUF-AP.

This work evaluated basin-scale global accuracy of land cover class fractions (areal proportion) across six study watersheds, and the outcome summarizes as follows. AP scheme was most accurate (RMSE: avg 0.9%, sd 0.3%; MAE: avg 0.6%, sd 0.2%) and was able to count scattered land covers classes (developed or forest) into global fraction while preventing

the over-representation of the most prominent classes (pasture/hay in study basins). The NWM scheme showed inferior metrics compared to the AP scheme (RMSE: avg 4.6% sd 2.4%; MAE avg 2.8%, sd 1.4%), and over-represented the most prominent classes when compared to AP. HUC12L ranked the lowest with respect to global areal accuracy (RMSE avg 8.0%, sd 3.8%; MAE avg 4.9%, sd 2.0%), while SHUF-NWM and SHUF-AP shared identical land cover class fractions (areal proportion) to their unshuffled counterparts NWM and AP. The HUC12L scheme over-represents the fraction of land cover classes that were highly clustered in small areas (e.g., developed areas or evergreen forests) making HUC12L substantially different from the NLCD 2016 reference (see 3.8. Appendix).

An investigation of the proportion of cells having identical land cover classes, and spatial correlation derived from Dutilleul's algorithm (Clifford et al., 1989; Dutilleul et al., 1993) showed that the land cover schemes have substantial differences in spatial patterns (Table 3). NWM and AP have 66% of identical cells, but spatial correlation is lower at 0.58. Meanwhile, HUC12L showed a higher similarity to AP (74% identical cells; 0.5 spatial correlation), than to NWM (60% 74% identical cells; 0.35 spatial correlation). The lower spatial correlations demonstrate the inaccurate clustering of land cover classes in HUC12L.

When the shuffled schemes (SHUF-NWM/SHUF-AP) compared against their originals (NWM/AP), 55%/61% respectively of cells had identical land cover classes. As expected, spatial correlations are low (0.23) in both cases, indicating the significant difference in spatial patterns caused by random shuffling.

Table 3-3. (A) Ratio of cells overlap with identical values and (B) spatial correlation (raster modified T-test; Clifford et al., 1989; Dutilleul et al., 1993) between different land cover schemes.

(A) Percentage of cells with identical values (%)					
	NWM	AP	HUC12L	SHUF (NWM)	SHUF (AP)
NWM	100				
AP	66	100			
HUC12L	60	74	100		
SHUF (NWM)	61	42	47	100	
SHUF (AP)	42	55	58	42	100
(B) Spatial Correlation					
	NWM	AP	HUC12L	SHUF (NWM)	SHUF (AP)
NWM	1.00				
AP	0.58	1.00			
HUC12L	0.35	0.50	1.00		
SHUF (NWM)	0.23	0.14	0.16	1.00	
SHUF (AP)	0.14	0.23	0.25	0.12	1.00

3.4.2. Water Balance Analysis

In this section, study watersheds are listed in order of aridity defined by the proportion of actual ET and runoff simulated in the NWM configuration of WRF-Hydro. Two drier basins (Douglas and Caldwell) had very high actual ET (over 85%) and low runoff ratio (below 0.1). Berkeley and Travis basins had relatively high actual ET (over 70%), however, their runoff ratio exceeded 0.2. Stark and Polk basins had a relatively high runoff ratio exceeding 0.5 (mostly as subsurface runoff), and lost less than 45% of actual ET (Table 3-4).

For all basins, the NWM and AP resampling schemes produced less than a 3-percentage point difference in all water budget components (evapotranspiration, surface runoff, subsurface runoff; see Water Budget Components section of Table 3-4). This is reasonable considering the high spatial correlation and number of identical cells between two schemes.

Generally, the percentage point differences were greater in ET and subsurface runoff (corresponding to “slow flow” and sometimes referred as “underground runoff” in the WRF-Hydro system) than in surface runoff (corresponding to “quick flow”). The difference in water budget components between HUC12L and AP was much greater than that between NWM and AP. For Stark basin, which has a high urban land cover, the lumped HUC12L scheme had over a 10-percentage point difference in ET when compared to AP. Absolute changes in water balance components were always the greatest in ET, followed by subsurface runoff, and then surface runoff. Change in soil storage was insignificant in both comparison cases (less than 1 percentage point) and is not shown. Although the percentage point changes in surface and subsurface runoff were small, their proportional changes (Proportional difference against AP section of Table 3-4) were often significant in the drier Douglas and Caldwell basins where these fluxes are small.

Table 3-4. Water balance components in NWM, AP, and HUC12L (left), and proportional differences against AP in % (right). ET: Evapotranspiration, SFC: surface runoff, GW: subsurface runoff.

		Water budget components (%)			Proportional difference against AP		
		ET	SFC	GW	Δ ET (%)	Δ SFC(%)	Δ GW(%)
Douglas	AP	89.47	0.48	10.36			
	NWM	91.8	0.36	8.09	2.58	-29.09	-24.6
	HUC12L	85.74	0.99	13.63	-4.25	70.13	27.27
Caldwell	AP	85.56	4.72	9.43			
	NWM	88.13	4.55	7.19	2.96	-3.72	-26.91
	HUC12L	80.44	6.19	13.3	-6.17	26.99	34.07
Berkeley	AP	77.37	3.27	19.49			
	NWM	78.2	3.63	18.28	1.07	10.32	-6.41
	HUC12L	75.57	2.33	22.39	-2.35	-33.56	13.85
Travis	AP	72.84	3.51	22.18			
	NWM	72.61	3.64	22.31	-0.33	3.66	0.62
	HUC12L	74.42	3.63	20.38	2.14	3.4	-8.46
Stark	AP	45.85	0.21	54.24			
	NWM	45.95	0.21	54.15	0.2	-0.17	-0.17
	HUC12L	34.62	0.25	65.42	-27.92	17.45	18.68
Polk	AP	44.47	14.87	41.19			
	NWM	44.14	14.76	41.64	-0.74	-0.78	1.1
	HUC12L	42.82	14.64	43.08	-3.78	-1.54	4.49
Average	AP						
	NWM				0.96	-3.30	-9.40
	HUC12L				-7.06	13.81	14.98

Comparing the shuffled schemes (SHUF-NWM/SHUF-AP) against their originals (NWM/AP) resulted in changes below 1 percentage point for all water budget components (Table 3-5). Compared to differences among the unshuffled schemes (NWM, AP, HUC12L), shuffling made greater changes to surface runoff and lesser changes to ET. This trend was most prominent in the drier Douglas, Berkeley, and Travis basins. Even though the shuffled

schemes introduced an arbitrary spatial pattern for land cover that should have disturbed the interaction with soil texture and topography in model calculations, the changes in water balance components aside from surface runoff were minimal.

Table 3-5. Comparison of water balance components between original and shuffled schemes. Percent-point difference in percent-point (left), and proportional difference in % (right). ET: Evapotranspiration, SFC: surface runoff, GW: subsurface runoff (“underground runoff”).

		Percentage-point difference in water budget components			Proportional difference in each water budget component		
		Δ ET (p.p.)	Δ SFC (p.p.)	Δ GW (p.p.)	Δ ET (%)	Δ SFC (%)	Δ GW (%)
Douglas	SHUF(AP)-AP	-0.8	-0.15	1.1	-0.9	-36.87	10.06
	SHUF(NWM)-NWM	-1.34	-0.09	1.3	-1.47	-28.81	14.84
Caldwell	SHUF(AP)-AP	0.41	0.24	-0.36	0.48	5.05	-3.88
	SHUF(NWM)-NWM	0.06	0.1	-0.07	0.07	2.24	-1.05
Berkeley	SHUF(AP)-AP	0.77	0.17	-0.91	0.99	5.04	-4.77
	SHUF(NWM)-NWM	0.95	-1.08	0.05	1.2	-34.89	0.29
Travis	SHUF(AP)-AP	0.62	-0.83	0.19	0.84	-26.8	0.87
	SHUF(NWM)-NWM	0.28	-0.9	0.64	0.39	-28.35	2.8
Stark	SHUF(AP)-AP	1.34	-0.003	-1.11	2.87	-1.23	-2.07
	SHUF(NWM)-NWM	0.94	0.01	-1.02	2.03	3.39	-1.9
Polk	SHUF(AP)-AP	0.04	0.003	0.02	0.08	0.02	0.05
	SHUF(NWM)-NWM	-0.14	0.04	0.13	-0.31	0.29	0.31
Average	SHUF(AP)-AP	0.40	-0.10	-0.18	0.73	-9.13	0.04
	SHUF(NWM)-NWM	0.13	-0.32	0.17	0.32	-14.36	2.55

In summary, water balance components showed some sensitivity to change in the areal proportion of land cover classes, as found in the comparison between NWM, AP, and HUC12L. In this case, ET and subsurface runoff showed the most significant changes, and particularly in drier watersheds. In contrast, water balance components showed little

sensitivity to change in the spatial pattern of land cover classes, as found in the comparison between shuffled schemes and their originals.

3.4.3. Hydrologic Signature Analysis

We plotted modelled flow duration curves from each resampling scheme together with the observed USGS flows, to summarize water availability and flow distribution (Figure 3-4). Basins are arranged from the driest (Figure 3-4a, Douglas) to the wettest (Figure 3-4f, Polk). Comparison with USGS historical flow data suggests that NWM simulations exhibited relatively low accuracy in reproducing the flow regime. In basins Douglas, Caldwell, Berkeley and Stark, differences in flow duration curves between land cover schemes are of similar magnitude to differences between modelled and observed flow duration curves. In basins Travis and Polk, differences in flow duration curves between land cover schemes are small. Overall, the largest impacts of land cover scheme occur in low-flow conditions in drier basins.

The flow duration curves were nearly indistinguishable between the NWM and AP resampling schemes in the four wettest watersheds (Figure 3-4; c to f), and only the two driest watersheds (Figure 3-4; a and b) showed variation. In these two basins, the AP scheme produced higher flow than the NWM scheme reflecting changes in water balance as also shown in Table 3-4. This may be related to AP better capturing the proportion of pasture classes (3.8. Appendix) which were often over-represented in the NWM scheme. The flow duration curve from the lumped HUC12L scheme was clearly distinguishable from the AP and NWM schemes for moderate and low flows, except for two basins (Figure 3-4; d and f).

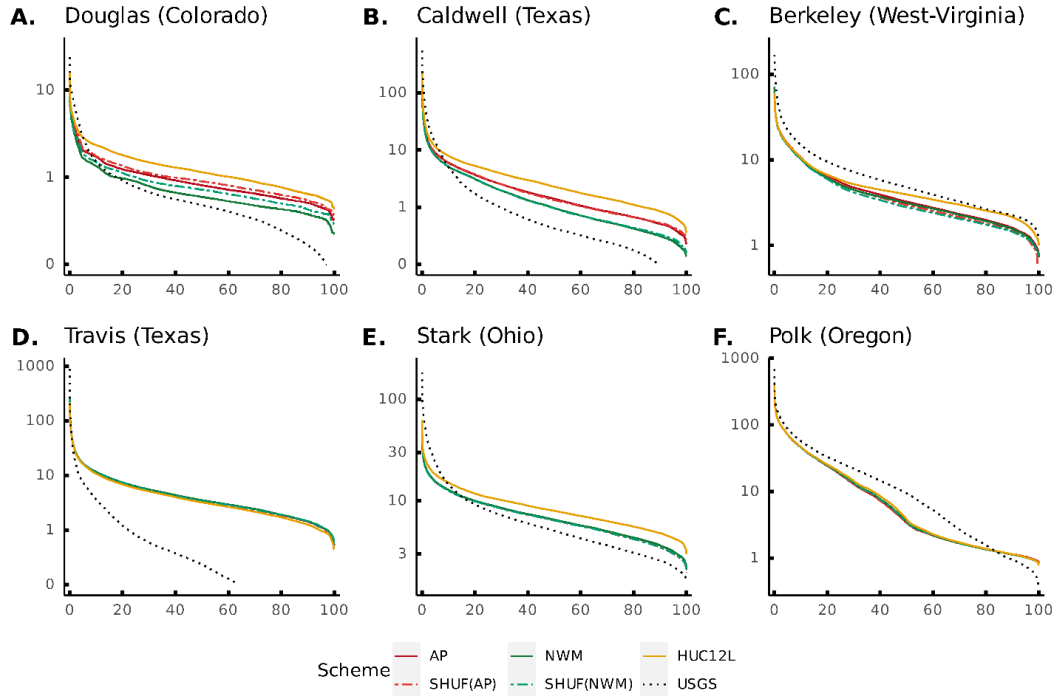


Figure 3-4. Flow Duration Curve (FDC) from each scheme and USGS observation in six study basins. The X-axis is exceedance probability in percent (%), and Y-axis is catchment discharge in cubic meters per second. USGS observation provides the context regarding the magnitude of impact of LULC on simulated water availability.

Shuffling the spatial pattern of land cover alone had minimal impact on streamflow distribution. The only exception was the driest watershed (Douglas) when the flowrate fell below $2m^3/s$ (Figure 3-4a). This result aligns with our previous water balance analysis and implies that the spatial pattern of land cover has a limited impact on streamflow simulation in WRF-Hydro.

Next, we analyzed the percent difference distribution in selected sets of hydrologic signatures. Comparisons between pairs of schemes are shown in Figure 3-5.

Sig_{sfc-vt}, magnitude signatures related to low flow condition and water availability (7Q10, Q5, Qmean, and Q95; yellow labels in Figure 3-5): In every case, low flow signatures (7Q10, Q5) were more affected than medium/high flow signatures (Qmean, Q95).

Similarly, most of the minimums or outliers were from drier periods in the driest basins (Douglas and Caldwell) where small volumetric changes in runoff presented as large proportional changes. It is notable that the percentage differences in these low flow signatures were much greater than the percentage differences in water balance components described in the previous section. Therefore, the choice of land cover scheme has the potential to impact low flow analyses, even when overall water balance is similar.

Magnitude signatures from the NWM-AP comparison (Figure 3-5a) showed that the NWM scheme underestimates streamflow compared to the AP scheme. The HUC12L-AP comparison (Figure 3-5b) showed that the HUC12L scheme overestimated streamflow compared to AP, and the increase was most noticeable in low flow signatures (e.g., 7Q10, Q5). Median proportional differences between HUC12L and AP were noticeably larger than between NWM and AP, agreeing with the water balance analysis from the previous section.

In a comparison of shuffled schemes with their originals (Figure 3-5; c and d), Q_{mean} , Q5, and Q95 showed almost no change, but 7Q10 increased in most cases. Some basins showed changes in composition between surface and groundwater runoff in water balance analysis, but it was not enough to explain the consistent trend in 7Q10.

***Sig_{sfc-vt}*, flood magnitude signatures (1, 2, and 5-Yr):** For the comparisons NWM-AP and HUC12L-AP, changes in flood magnitude mirrored the changes in other magnitude signatures. However, the differences between schemes decreased for larger recurrence intervals. The driest watersheds (Douglas and Caldwell) generally exhibited the largest differences in flood magnitude between land cover schemes, with most values appearing outside the interquartile range (not shown). Shuffling the spatial pattern of land cover classes significantly reduced the 2-year flood magnitude, while the 1 and 5-year flood magnitudes

were minorly affected. Such selective impact only occurring on “median-sized”/bank-full level flood events was independent of water balance changes. We hypothesize this is caused by the interaction between terrain routing and re-infiltration since runoff volume during flood events are more controlled by the partitioning of precipitation, not by a spatial aggregation and redistribution function.

***Sig_{sfc-vt}*, rate of change signatures (FDC Mid-section slope, FDC_MD):** The proportional change of the FDC mid-section slope was moderate (interquartile range within 5~10%) in the NWM-AP and HUC12L-AP comparisons (Figure 3-5; a and b). However, the shuffled cases showed minimal difference (less than 3%) (Figure 3-5; c and d). FDC mid-section slope relates to the partitioning of quick and slow runoff, and therefore, our results indicated that the spatial pattern of land cover had a limited impact on this behavior.

***Sig_{lat}*, timing signatures (mean half flow interval, HFI):** The mean HFI only showed noticeable differences in the HUC12L-AP comparison, while the other experiments showed less than 2% differences. HUC12L schemes have a unique clustered land cover pattern, but there is no evidence to correlate this to a shift in HFI, as HFI remained insensitive to the shuffled land cover patterns. This implies the seasonal/annual flow regime was more affected by a change in proportional area of land cover classes than their spatial pattern.

***Sig_{lat}*, magnitude signatures (Baseflow Index, BFI):** The baseflow index showed almost no differences in all experiments and was insensitive to changes in water balance and the spatial representation of land cover. This occurs despite multiple basins experiencing considerable change in composition between simulated surface and groundwater runoff, especially in HUC12L schemes.

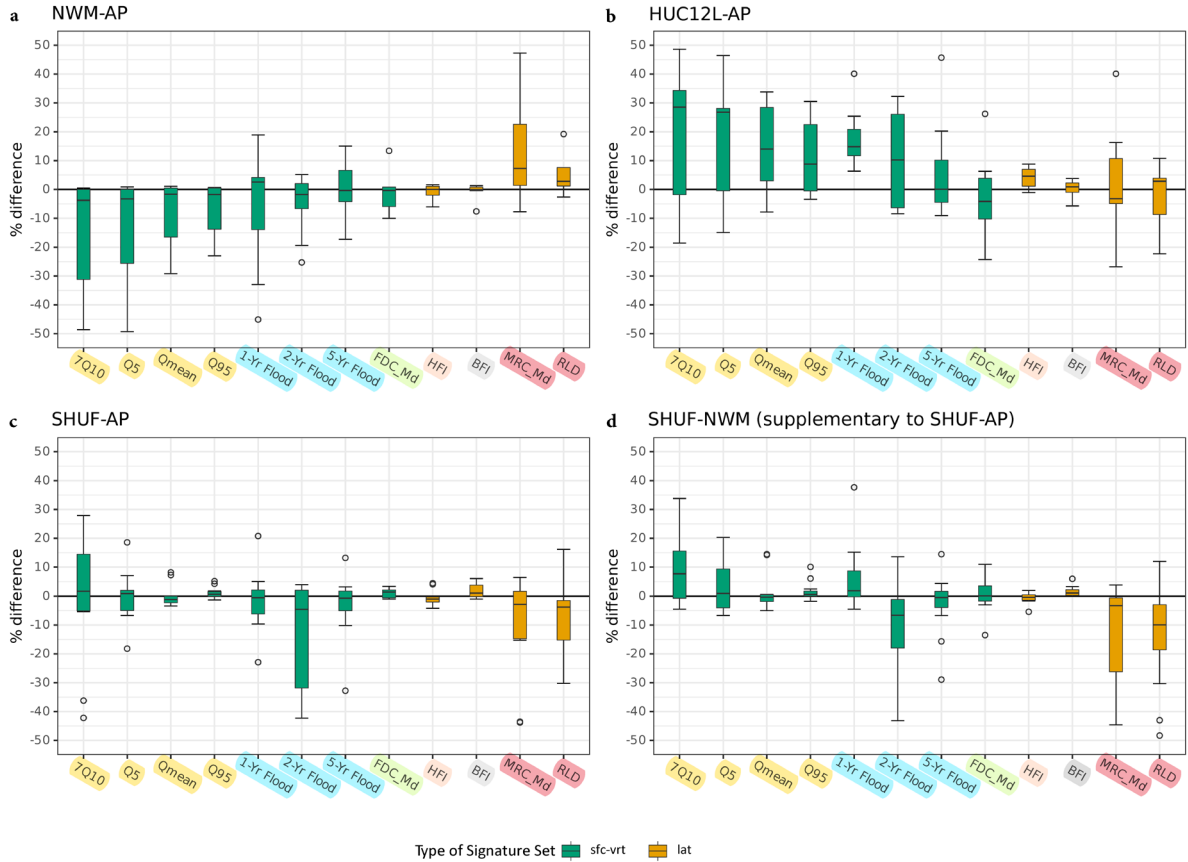


Figure 3-5. Summary of percent difference in hydrologic signatures comparing NWM-AP, HUC12L-AP, and SHUF-AP (and SHUF-NWM). The highlights on X-axis labels correspond to how the hydrologic signatures were reviewed together in section 4.3. Y-axis represents the proportional change in %. (a) Comparison of NWM and AP (b) Comparison of HUC12L and AP (c) Comparison of SHUF-AP and AP (d) Comparison of SHUF-NWM and NWM.

Sig_{lat}, rate of change signatures (Master Recession Curve mid-section slope, **MRC_Md**; & Rising Limb Density, **RLD**): Although the mid-section slope of the master recession curve is supposed to represent the water retention capacity of the watershed, volumetric changes in water balance between NWM, AP and HUC12L schemes did not result in consistent changes to the MRC signature. NWM schemes had higher ET and lower groundwater runoff compared to AP resulting in higher MRC mid-section gradient (quicker recession). In contrast, the lumped HUC12L scheme had lower ET and higher groundwater

runoff than AP, but changes in the mid-section gradient of the MRC were variable between watersheds. Both shuffled cases had a lower MRC mid-section gradient, showing a slower recession regardless of changes in water balance. Rising Limb Density (RLD) showed similar results to MRC, and similar inconsistency in correspondence to changes in water balance. Shuffled land cover schemes have lower RLD than their originals, which combined with a lower MRC slope show a consistent pattern that shuffling reduces the flashiness of watershed response to produce a smoother hydrograph.

Table 6 provides qualitative summary of the outcomes by interpreting which spatial aspect of LULC had a primary control over different hydrologic components and processes in the model simulation. The changes in vertical hydrologic fluxes, and the Sig_{sfc-vt} (vertical) signatures, were dominated by the areal proportion of land cover. However, critically low flow condition (7Q10) and the 2-year flood were particularly sensitive to the land cover spatial pattern. In the Sig_{lat} (lateral) signature set, we only could distinguish the primary control factor within the signatures that are most relevant to lateral processes; catchment water retention capacity and hillslope process signatures were most affected by land cover spatial pattern.

Table 3-6. Qualitative summary and interpretation of relationship between LULC spatial representation aspects (areal Proportion and spatial pattern), model vertical water fluxes (catchment water balance), watershed response characteristics observed from streamflow hydrologic signatures (*Sig_{sfc-vt}*: hydrologic signatures linked to near-surface vertical flux exchange, and *Sig_{lat}*: hydrologic signatures linked to lateral processes). X indicates the primary influencing factor, and (x) indicates potential influence may be present but its impact was insignificant (median change less than 5%) or highly variable.

Group	Hydrologic variable	Primary Influencing Factor	
		Areal Proportion	Spatial pattern
Catchment water balance	Evapotranspiration	X	
	Groundwater runoff	X	
	Surface runoff		X
<i>Sig_{sfc-vt}</i>	Critically low flow conditions		X
	General low flow conditions	X	
	General water availability	X	
	1-year & 5-year flood	X	
	Median-sized (2-year) flood		X
	Runoff partitioning	X	
<i>Sig_{lat}</i>	Seasonal/annual flow regime	(x: insignificant)	
	Baseflow processes	Indistinguishable	
	Catchment water retention capacity	(x: highly variable)	X
	Hillslope process		X

3.5. Discussion

We first note that the analysis of resampled LULC grids showed that AP most accurately captures the global areal proportion of landcover classes from the input source, while preserving minority LULC classes. This result suggests that an advanced resampling algorithm can improve the global areal and local accuracy of distributed model’s static input that are upscaled from categorical raster datasets. In the following sections, we delve deeper into the relationship between LULC characteristics (areal class proportions and spatial organization) and hydrologic processes in the model.

3.5.1. Basin-scale Water Balance: Land Cover Influence on Vertical Processes

When comparing NWM, AP, and HUC12L resampling schemes, basin-scale water balance showed low differences despite substantial changes in land cover areal class proportions and spatial patterns. Differences were larger for drier basins but were negligible in watersheds where modeled runoff coefficient exceeded 0.2. Comparing shuffled schemes with their originals showed that spatial pattern of land cover had a very low impact on basin-scale water balance. This result was unexpected because WRF-Hydro model design is rooted in understanding the interplay among spatially distributed forcing, land cover, soil properties, and topography. Our initial hypothesis that spatial pattern of land cover influences vertical water fluxes and that this influence extends to the basin-scale water balance, was disproven at the given catchment size and model resolution.

Our results agree with research that has shown changes in water balance (ET and runoff) caused by land cover change were noticeable at the cell scale, but became negligible at the basin scale using the Variable Infiltration Capacity (VIC) model (Patidar and Behera, 2018). Likewise, the dynamic feedback from a land-use change model to a semi-distributed eco-hydrologic model had a negligible impact on watershed runoff prediction (Yalew et al., 2018).

3.5.2. Land Cover Influence on Simulated Streamflow Characteristics

The two aspects of land cover spatial representation that we tested (areal proportions, and spatial pattern) affected simulated streamflow characteristics differently. The areal proportion of land cover classes impacted near-surface vertical water fluxes at catchment scale, and the cumulative effect of these volumetric changes in fluxes subsequently reflected on the streamflow simulation. This aligns with earlier studies that found near-surface vertical processes dominating the runoff generation process in various model structures (Mai et al.,

2022; Markstrom et al., 2016). In contrast, the spatial organization of land cover had a limited influence on catchment water balance, and its impact on simulated streamflow characteristics was small and primarily occurred through lateral processes (redistribution of water via routing).

Comparing NWM, AP, and HUC12L showed us how differences in areal proportions of land cover in common resampling schemes drive volumetric changes in near-surface vertical water fluxes and therefore cascading changes in streamflow characteristics. Signatures of flow magnitude from the ***Sig_{sf_{c-vt}}*** set (linked to near-surface/vertical processes) detected changes in runoff characteristics that aligned with changes in catchment water balance. Low flow signatures (7Q10, Q5) and floods with lower recurrence intervals were more sensitive to land cover changes than higher flow condition signatures (Q_{mean}, Q95) and larger floods. This trend was particularly pronounced in drier basins.

Comparing shuffled schemes against their originals (comparison of NWM/AP against NWM-SHUF/AP-SHUF) showed that spatial pattern of land cover impacts simulated flow characteristics despite having a small impact on basin water balances. The shuffled schemes with lower spatial coherence of land cover class produce a dampened runoff response with less extreme low or high flows. This is evidenced in higher values of the 7Q10 signature (for critically low flow conditions), lower values of 2-Yr floods, slower recession and longer time-to-peak. The dispersed land cover pattern likely increased re-infiltration and altered lateral surface and subsurface routing. This result suggests that the limited hydrologic impacts of land cover spatial pattern primarily occur through their interaction with routing scheme.

3.5.3. Recommendations on Land Cover Input Practices for WRF-Hydro

We make the following recommendations on land cover input practices for hydrologic prediction using WRF-Hydro or similarly structured LSM-based distributed hydrologic models:

1) **Resampling method of land cover input:** Achieving accurate land cover class areal proportion should be the priority when resampling higher resolution data to a coarser model input, as WRF-Hydro is more sensitive to areal proportion than to spatial pattern of land cover at catchment scales. Applying a resampling method such as AP (Johnson and Clarke, 2021) is recommended when minor land cover classes with high hydrological impact (e.g., developed land use, post-fire land cover) are present within the watershed area.

2) **The importance of land cover resampling varies by region and modeling purpose:** Accurate representation of land cover is particularly important in drier catchments where ET is significant and strongly controls soil moisture conditions. Dry catchments were more sensitive to land cover resampling scheme, and wet or subsurface-processes dominated catchments were less sensitive to both areal proportion and spatial pattern. This relates to findings that the NWM overestimates ET in dry climates where barren land cover type is prominent (Johnson et al., 2023). Land cover resampling is more important when the modeling purpose includes estimating low flow conditions such as the 7Q10 signature which measures very low flows that are crucial for water quality and water supply managements (Blum et al., 2019; EPA, 1986; Poshtiri and Pal, 2016). In contrast, land cover resampling is less important when using WRF-Hydro to predict the magnitude of larger floods, confirming established knowledge that land cover impacts are lower for large flood flows (Dunne and Leopold, 1978).

3) **Using lumped land cover representation:** Assigning a single representative land cover for subcatchments within the target watershed (e.g., our HUC12L scheme) may be acceptable when following conditions are met; runoff ratio of the watershed exceeds 0.2, subsurface processes dominate runoff response, no significant development exists in a watershed, and flood forecasting is the main objective. Yet, in such cases, it would be more reasonable to couple a simpler runoff/routing module (more flexible in calibration capacity) with Noah-MP instead of relying on WRF-Hydro's routing module (Kim et al., 2021).

3.5.4. Implications for Land Cover Resampling in LSM-based Distributed Hydrologic Modeling

Our study findings revealed that the spatial information in land cover input has limited influence on watershed-scale hydrologic processes in WRF-Hydro. Our results show that the land cover resampling method can impact the calculation of vertical hydrologic fluxes within each 1-D soil column (LSM grid cell), but its significance diminishes when fluxes are aggregated into watershed-scale runoff responses. This is more likely if the model architecture is inclined to representing vertical process complexity than horizontal (lateral) complexity (Newman et al., 2014). We would expect similar results for LSM-based or hydrometeorological models that share common architectures and spatial representation to WRF-Hydro (Gochis et al., 2018); i.e. they use rather coarse 1-D soil column focused on vertical process complexity as a fundamental hydrologic unit, solve subsurface flow with Darcy-Richards equation (Richards, 1931), and route overland flow with kinematic/diffusive waves.

Recent research has hinted at the potential insensitivity of such models to non-climatic inputs. Gharari et al. (2020) showed that the discretization level of static inputs had limited

influence on soil moisture and streamflow predictions in Variable Infiltration Capacity (VIC) model (Liang et al., 1994), in contrast to the pronounced influence from scaling of climatic forcing. When implementing the vector-based river network routing scheme in WRF-Hydro, it exhibited greater sensitivity to the coupling interface between the LSM grid and vectorized network than to the LSM grid resolution (Lin et al., 2018). Similarly, Kim et al. (2021) demonstrated that subsurface representation in NWM was inadequate for organizing hillslope/watershed-scale processes in a smaller headwater catchment, and outperformed by simpler topography-based TOPMODEL (Beven and Kirkby, 1979) that was one-way coupled with Noah-MP. These observations align with the idea that a reductionist modeling approach (spatially distributed and physically based) may not always be the most effective means of comprehending hydrological behavior at the catchment scale (McDonnell et al., 2007; Savenije, 2010). However, it is worthwhile to note that real-world runoff response can exhibit insensitivity to land cover changes. For instance, Anderson et al. (2022) found that the correlation between hydrological changes and alteration in urban/tree cover changes can be weak, opposed to common knowledge, especially with smaller proportional changes. Therefore, while enhancing land cover inputs (such as applying AP resampling) or parameterization can improve model realism, these efforts may not significantly improve hydrologic prediction capability of LSM-based models. Further investigation on these insensitivities in both model and real watersheds could offer valuable insights for advancing model architectures.

3.6. Conclusions

Overall, the study offers insight into the impact of two distinct aspects of spatial representation in land cover (areal proportion and spatial arrangement), which can greatly vary

depending on resampling methods, on hydrologic simulation in WRF-Hydro/NWM. The findings can be summarized as follows:

- 1) The areal proportion of land cover classes within a catchment significantly influences volumetric changes in vertical hydrologic fluxes (catchment-scale water balance), which subsequently affect simulated streamflow characteristics.
- 2) In contrast, the spatial arrangement of land cover had a marginal impact on catchment-scale water balance but could still pose limited alteration in simulated streamflow characteristics primarily through routing processes.
- 3) Utilizing the AP algorithm, which better preserve minority classes and produces higher class area accuracy, for land cover resampling in WRF-Hydro can enhance model realism and offer benefits, particularly in arid environment, catchments featuring minor land cover classes with high hydrological impact (such as developed land use and post-fire land cover), or when predicting low-flow conditions.
- 4) The study suggests that reductionist approach of LSM-based hydrologic modeling (physics-based and spatially distributed) may not be necessary for simulating the hydrological impact of land cover on macroscale processes (hillslope, sub-catchment, catchment). This provides a promising foundation for model development with more flexible spatial configurations within the NOAA Next Generation Water Resource Modeling Framework.

The findings of the study encourage the advancement of land surface modelling frameworks towards a direction where spatial information is effectively employed to establish a well-balanced representation of both vertical and lateral processes, using fundamental unit that is beyond 1-D soil columns (e.g., Hillslope-scale; Fan et al., 2019).

3.7. References

1. Alawi, S.A., Özkul, S., 2023. Evaluation of land use/land cover datasets in hydrological modelling using the SWAT model. *H2Open Journal* 6, 63–74. <https://doi.org/10.2166/H2OJ.2023.062>
2. Alley, W.M., Evenson, E.J., Barber, N.L., Bruce, B.W., Dennehy, K.F., Freeman, M., Freeman, W.O., Fischer, J.M., Hughes, W.B., Kennen, J., Kiang, J.E., 2013. Progress Toward Establishing a National Assessment of Water Availability and Use.
3. Anderson, B.J., Slater, L.J., Dadson, S.J., Blum, A.G., Prosdocimi, I., 2022. Statistical attribution of the influence of urban and tree cover change on streamflow: a comparison of large sample statistical approaches. *Water Resour Res* e2021WR030742. <https://doi.org/10.1029/2021WR030742>
4. Archfield, S.A., Clark, M., Arheimer, B., Hay, L.E., McMillan, H., Kiang, J.E., Seibert, J., Hakala, K., Bock, A., Wagener, T., Farmer, W.H., Andréassian, V., Attinger, S., Viglione, A., Knight, R., Markstrom, S., Over, T., 2015. Accelerating advances in continental domain hydrologic modeling. *Water Resour Res* 51, 10078–10091. <https://doi.org/10.1002/2015WR017498>
5. Beven, K.J., Kirkby, M.J., 1979. A physically based, variable contributing area model of basin hydrology. *Hydrological Sciences Bulletin* 24, 43–69. <https://doi.org/10.1080/02626667909491834>
6. Bierkens, M.F.P., 2015. Global hydrology 2015: State, trends, and directions. *Water Resour Res* 51, 4923–4947. <https://doi.org/10.1002/2015WR017173>
7. Blum, A.G., Archfield, S.A., Hirsch, R.M., Vogel, R.M., Kiang, J.E., Dudley, R.W., Volpi, E., 2019. Updating estimates of low-streamflow statistics to account for possible trends. <https://doi.org/10.1080/02626667.2019.1655148>
8. Clifford, P., Richardson, S., Hemon, D., 1989. Assessing the Significance of the Correlation between Two Spatial Processes. *Biometrics* 45, 123. <https://doi.org/10.2307/2532039>
9. Demeritt, D., Nobert, S., Cloke, H.L., Pappenberger, F., 2013. The European Flood Alert System and the communication, perception, and use of ensemble predictions for operational flood risk management. *Hydrol Process* 27, 147–157. <https://doi.org/10.1002/HYP.9419>
10. Dunne, T., Leopold, L.B. (Luna B., 1978. *Water in environmental planning* 818.
11. Dutilleul, P., Clifford, P., Richardson, S., Hemon, D., 1993. Modifying the t Test for Assessing the Correlation Between Two Spatial Processes. *Biometrics* 49, 305. <https://doi.org/10.2307/2532625>
12. EPA, 1986. *Technical Guidance Manual for Performing Wasteload Allocations, Book VI: Design Conditions-Chapter 1: Stream Design Flow for Steady-State Modeling.*
13. Estrany, J., Garcia, C., Batalla, R.J., 2010. Hydrological response of a small mediterranean agricultural catchment. *J Hydrol (Amst)* 380, 180–190. <https://doi.org/10.1016/J.JHYDROL.2009.10.035>
14. Evans, J.S., Murphy, M.A., Ram, K., 2022. *Spatial Analysis and Modelling Utilities [R package spatialEco version 2.0-0].*
15. Fan, Y., Clark, M., Lawrence, D.M., Swenson, S., Band, L.E., Brantley, S.L., Brooks, P.D., Dietrich, W.E., Flores, A., Grant, G., Kirchner, J.W., Mackay, D.S.,

- McDonnell, J.J., Milly, P.C.D., Sullivan, P.L., Tague, C., Ajami, H., Chaney, N., Hartmann, A., Hazenberg, P., McNamara, J., Pelletier, J., Perket, J., Rouholahnejad-Freund, E., Wagener, T., Zeng, X., Beighley, E., Buzan, J., Huang, M., Livneh, B., Mohanty, B.P., Nijssen, B., Safeeq, M., Shen, C., van Verseveld, W., Volk, J., Yamazaki, D., 2019. Hillslope Hydrology in Global Change Research and Earth System Modeling. *Water Resour Res* 55, 1737–1772.
<https://doi.org/10.1029/2018WR023903>
16. Farrar, M., 2021. Upgrade of National Water Model on NCEP’s WCOSS System, and its Post-Processing Application on the Integrated Dissemination Platform (IDP): Effective [WWW Document]. URL
https://www.weather.gov/media/notification/pdf2/scn20-119nwm_v2.1_aad.pdf
 (accessed 10.18.23).
 17. Gharari, S., Clark, M.P., Mizukami, N., Knoben, W.J.M., Wong, J.S., Pietroniro, A., 2020. Flexible vector-based spatial configurations in land models. *Hydrol Earth Syst Sci* 24, 5953–5971. <https://doi.org/10.5194/hess-24-5953-2020>
 18. Gharari, S., Clark, M.P., Mizukami, N., Wong, J.S., Pietroniro, A., Wheeler, H.S., 2019. Improving the representation of subsurface water movement in land models. *J Hydrometeorol* 20, 2401–2418. <https://doi.org/10.1175/JHM-D-19-0108.1>
 19. Gnann, S.J., Coxon, G., Woods, R.A., Howden, N.J.K., McMillan, H.K., 2022. TOSSHtoolbox/TOSSH: First release - minor update.
<https://doi.org/10.5281/ZENODO.6462813>
 20. Gnann, S.J., Coxon, G., Woods, R.A., Howden, N.J.K., McMillan, H.K., 2021. TOSSH: A Toolbox for Streamflow Signatures in Hydrology. *Environmental Modelling & Software* 138, 104983.
<https://doi.org/10.1016/J.ENVSOFT.2021.104983>
 21. Gochis, D.J., Barlage, M., Dugger, A., FitzGerald, K., Karsten, L., McAllister, M., McCreight, J., Mills, J., RafieeiNasab, A., Read, L., Sampson, K., Yates, D., Yu, W., 2018. WRF-Hydro V5 Technical Description The NCAR WRF-Hydro Modeling System Technical Description Until further notice, please cite the WRF-Hydro modeling system as follows: WRF-Hydro V5 Technical Description WRF-Hydro V5 Technical Description.
 22. Jin, X., Jin, Y., Yuan, D., Mao, X., 2019. Effects of land-use data resolution on hydrologic modelling, a case study in the upper reach of the Heihe River, Northwest China. *Ecol Modell* 404, 61–68.
<https://doi.org/10.1016/J.ECOLMODEL.2019.02.011>
 23. Johnson, J.M., 2021. mikejohnson51/resample: Area Preserving Raster Resampling.
<https://doi.org/10.5281/zenodo.4543984>
 24. Johnson, J.M., Clarke, K.C., 2021. An area preserving method for improved categorical raster resampling. *Cartogr Geogr Inf Sci* 48, 292–304.
<https://doi.org/10.1080/15230406.2021.1892531>
 25. Johnson, J.M., Fang, S., Sankarasubramanian, A., Modaresi Rad, A., Kindl da Cunha, L., Clarke, K.C., Mazrooei, Amirhossein, Yeghiazarian, L., Mazrooei, Amir, Collins, F.C., 2023. Comprehensive analysis of the NOAA National Water Model: A call for heterogeneous formulations and diagnostic model selection. *Authorea Preprints*. <https://doi.org/10.22541/ESSOAR.167415214.45806648/V1>

26. Johnson, J.M., Kim, D.-H. (Donny), 2023. wrfhydroSubsetter: v1.0. <https://doi.org/10.5281/ZENODO.7651625>
27. Johnson, J.M., Munasinghe, D., Eyclade, D., Cohen, S., 2019. An integrated evaluation of the National Water Model (NWM)-Height above nearest drainage (HAND) flood mapping methodology. *Natural Hazards and Earth System Sciences* 19, 2405–2420. <https://doi.org/10.5194/nhess-19-2405-2019>
28. Kim, D.-H., Naliaka, A., Zhu, Z., Ogden, F.L., McMillan, H.K., 2021. Experimental Coupling of TOPMODEL with the National Water Model: Effects of Coupling Interface Complexity on Model Performance. *J Am Water Resour Assoc.* <https://doi.org/10.1111/1752-1688.12953>
29. Li, J., Miao, C., Zhang, G., Fang, Y.H., Shangguan, W., Niu, G.Y., 2022. Global Evaluation of the Noah-MP Land Surface Model and Suggestions for Selecting Parameterization Schemes. *Journal of Geophysical Research: Atmospheres* 127, e2021JD035753. <https://doi.org/10.1029/2021JD035753>
30. Liang, X., Lettenmaier, D.P., Wood, E.F., Burges, S.J., 1994. A simple hydrologically based model of land surface water and energy fluxes for general circulation models. *J Geophys Res* 99, 415–429. <https://doi.org/10.1029/94JD00483>
31. Lin, P., Yang, Z.L., Gochis, D.J., Yu, W., Maidment, D.R., Somos-Valenzuela, M.A., David, C.H., 2018. Implementation of a vector-based river network routing scheme in the community WRF-Hydro modeling framework for flood discharge simulation. *Environmental Modelling and Software* 107, 1–11. <https://doi.org/10.1016/j.envsoft.2018.05.018>
32. Mai, J., Craig, J.R., Tolson, B.A., Arsenault, R., 2022. The sensitivity of simulated streamflow to individual hydrologic processes across North America. *Nature Communications* 2022 13:1 13, 1–11. <https://doi.org/10.1038/s41467-022-28010-7>
33. Markstrom, S.L., Hay, L.E., Clark, M.P., 2016. Towards simplification of hydrologic modeling: Identification of dominant processes. *Hydrol Earth Syst Sci* 20, 4655–4671. <https://doi.org/10.5194/HESS-20-4655-2016>
34. McCreight, J., Mills, T.J., FitzGerald, K., Fersch, B., donaldwj, Cabell, R., Dugger, A., Fanfarillo, A., laurareads, Barlage, M., Dan, logankarsten, McAllister, M., Dunlap, R., McCreight, J., weiyuncar, Nels, arezoorn, jdmattern-noaa, wrf-hydro-nwm-bot, champham, aheldmyer, 2020. NCAR/wrf_hydro_nwm_public: WRF-Hydro® v5.1.2. <https://doi.org/10.5281/ZENODO.3678643>
35. McDonnell, J.J., Sivapalan, M., Vaché, K., Dunn, S., Grant, G., Haggerty, R., Hinz, C., Hooper, R., Kirchner, J., Roderick, M.L., Selker, J., Weiler, M., 2007. Moving beyond heterogeneity and process complexity: A new vision for watershed hydrology. *Water Resour Res.* <https://doi.org/10.1029/2006WR005467>
36. McMillan, H., 2020. Linking hydrologic signatures to hydrologic processes: A review. *Hydrol Process* 34, 1393–1409. <https://doi.org/10.1002/hyp.13632>
37. McMillan, H.K., Hilary McMillan, C.K., 2021. A review of hydrologic signatures and their applications. *Wiley Interdisciplinary Reviews: Water* 8, e1499. <https://doi.org/10.1002/WAT2.1499>
38. NCAR, 2023a. WRF-Hydro® Pre-processing Tools | Research Applications Laboratory [WWW Document]. URL https://ral.ucar.edu/projects/wrf_hydro/pre-processing-tools (accessed 10.18.23).

39. NCAR, 2023b. NCAR/rwrhydro: A community-contributed tool box for managing, analyzing, and visualizing WRF Hydro (and NWM) input and output files in R. [WWW Document]. URL <https://github.com/NCAR/rwrhydro> (accessed 10.18.23).
40. NCEP, 2023. NCEP Model Source Codes [WWW Document]. URL <https://www.nco.ncep.noaa.gov/pmb/codes/nwprod/> (accessed 10.18.23).
41. Newman, A.J., Clark, M.P., Winstral, A., Marks, D., Seyfried, M., 2014. The Use of Similarity Concepts to Represent Subgrid Variability in Land Surface Models: Case Study in a Snowmelt-Dominated Watershed. *J Hydrometeorol* 15, 1717–1738. <https://doi.org/10.1175/JHM-D-13-038.1>
42. Patidar, N., Behera, • M D, 2018. How Significantly do Land Use and Land Cover (LULC) Changes Influence the Water Balance of a River Basin? A Study in Ganga River Basin, India. <https://doi.org/10.1007/s40010-017-0426-x>
43. Poff, N.L.R., Allan, J.D., Bain, M.B., Karr, J.R., Prestegard, K.L., Richter, B.D., Sparks, R.E., Stromberg, J.C., 1997. The natural flow regime: A paradigm for river conservation and restoration. *Bioscience* 47, 769–784. <https://doi.org/10.2307/1313099>
44. Poshtiri, M.P., Pal, I., 2016. Patterns of hydrological drought indicators in major U.S. River basins. *Clim Change* 134, 549–563. <https://doi.org/10.1007/s10584-015-1542-8>
45. Richards, L.A., 1931. Capillary conduction of liquids through porous mediums. *J Appl Phys* 1, 318–333. <https://doi.org/10.1063/1.1745010>
46. Richter, B.D., Baumgartner, J. V, Powell, J., Braun, D.P., 1996. A Method for Assessing Hydrologic Alteration within Ecosystems STOR. *Conservation Biology* 10, 1163–1174.
47. Savenije, H.H.G., 2010. HESS Opinions “Topography driven conceptual modelling (FLEX-Topo).” *Hydrol Earth Syst Sci* 14, 2681–2692. <https://doi.org/10.5194/hess-14-2681-2010>
48. Schaake, J.C., Koren, V.I., Duan, Q.Y., Mitchell, K., Chen, F., 1996. Simple water balance model for estimating runoff at different spatial and temporal scales. *Journal of Geophysical Research Atmospheres* 101, 7461–7475. <https://doi.org/10.1029/95JD02892>
49. Shamir, E., Imam, B., Morin, E., Gupta, H. V., Sorooshian, S., 2005. The role of hydrograph indices in parameter estimation of rainfall–runoff models. *Hydrol Process* 19, 2187–2207. <https://doi.org/10.1002/HYP.5676>
50. Silver, M., Karnieli, A., Ginat, H., Meiri, E., Fredj, E., 2017. An innovative method for determining hydrological calibration parameters for the WRF-Hydro model in arid regions. *Environmental Modelling & Software* 91, 47–69. <https://doi.org/10.1016/J.ENVSOFT.2017.01.010>
51. Wood, E.F., Roundy, J.K., Troy, T.J., van Beek, L.P.H., Bierkens, M.F.P., Blyth, E., de Roo, A., Döll, P., Ek, M., Famiglietti, J., Gochis, D., van de Giesen, N., Houser, P., Jaffé, P.R., Kollet, S., Lehner, B., Lettenmaier, D.P., Peters-Lidard, C., Sivapalan, M., Sheffield, J., Wade, A., Whitehead, P., 2011. Hyperresolution global land surface modeling: Meeting a grand challenge for monitoring Earth’s terrestrial water. *Water Resour Res* 47, 1–10. <https://doi.org/10.1029/2010WR010090>
52. Yalaw, S.G., Pilz, T., Schweitzer, C., Liersch, S., van der Kwast, J., van Griensven, A., Mul, M.L., Dickens, C., van der Zaag, P., 2018. Coupling land-use change and

- hydrologic models for quantification of catchment ecosystem services.
Environmental Modelling and Software 109, 315–328.
<https://doi.org/10.1016/J.ENVSOFT.2018.08.029>
53. Yilmaz, K.K., Gupta, H. V., Wagener, T., 2008. A process-based diagnostic approach to model evaluation: Application to the NWS distributed hydrologic model. Water Resour Res 44. <https://doi.org/10.1029/2007WR006716>
54. Zhang, Z., Bortolotti, L.E., Li, Z., Armstrong, L.M., Bell, T.W., Li, Y., 2021. Heterogeneous Changes to Wetlands in the Canadian Prairies Under Future Climate. Water Resour Res 57, e2020WR028727. <https://doi.org/10.1029/2020WR028727>

3.8. Appendix

Comparison of areal proportion of land use land cover (LULC) classes in NLCD 2016, NWM, AP, and HUC12L. Shuffled schemes are not presented as they share identical areal proportion to their material schemes (NWM and AP)

Land cover classes	Douglas				Caldwell				Berkeley				Travis				Stark				Polk			
	HUC12L	AP	NWM	NLCD	HUC12L	AP	NWM	NLCD	HUC12L	AP	NWM	NLCD	HUC12L	AP	NWM	NLCD	HUC12L	AP	NWM	NLCD	HUC12L	AP	NWM	NLCD
Developed	9.8	5.7	3.3	4.9	10.5	6	3	4.7	15	12.7	12.2	13.1	14.1	16.1	16.1	15.1	47.2	31.2	31.3	34.8	-	0.3	-	1.2
Cultivated Crops	-	-	-	-	15.8	12.3	14.1	13.3	0.5	5.9	3	6.4	0.1	0.3	0.3	0.6	36.7	18.1	18.8	15.6	5.2	6.1	7.7	6.4
Pasture	-	-	-	-	43.6	30.5	46.2	31	70.3	41.6	64.6	41.6	-	0.2	0.3	0.5	3.6	18.7	23.8	17.9	10.2	13.4	15.8	12.7
Grassland	26.5	32.7	38	32.8	13	16.5	12.6	14.2	0.4	11.2	0.8	9.2	13.5	18.4	16.8	18.5	2	16.1	15.7	16.2	2.6	10.3	3.3	10.1
Shrub	16.8	20.6	19.8	21.3	14.1	18.5	16.5	20.5	-	-	-	0.2	32.4	29	35.2	28.6	-	-	-	0.1	1.2	14.9	7	13.2
Deciduous Forest	0.1	3.4	0.7	3.9	1.3	10.1	6.3	9.3	13.1	22.3	18.2	20.8	0.3	5	1.3	4.9	8.3	11.3	9.5	10.9	0.5	1.8	0.3	1.8
Evergreen Forest	46.7	35.9	38.3	34.7	0.7	1.4	0.2	1	0.1	1.9	0.3	1.7	39.3	29.8	29.4	30.3	-	-	-	0.1	78	35.5	56.6	35.5
Mixed Forest	-	-	-	0.2	0.8	1.7	0.7	2.2	0.4	4.2	0.8	6.5	-	-	-	0.2	1.6	2.8	0.4	2.1	2	15.8	9.3	16.4
Open Water	-	-	-	0.1	-	1	-	0.7	-	-	-	0.1	-	-	-	0.2	-	0.6	-	0.6	-	-	-	0
Herbaceous Wetlands	0.1	1.6	-	1.4	-	-	-	0.1	-	-	-	0	-	-	-	-	0.2	0.8	0.4	0.6	-	0.2	-	1
Woody Wetlands	-	0.1	-	0.8	0.1	2	0.3	2.9	-	-	-	0.1	0.1	0.8	0.2	0.7	0.4	0.6	-	0.9	0.5	1.8	-	1.8
Barren	-	-	-	-	-	0.2	0.1	0.2	0.1	0.3	-	0.2	0.2	0.4	0.3	0.3	-	-	-	0.1	-	-	-	-
Elevation Max/Min (m)	1747			2971	101	271			105	496			138	509			298	404			54			1011
Slope (%)		12				1.6				3.2				3.3				2.2				15.9		
Stream density (km/km ²)			0.52			0.59				0.69				0.54				0.59				0.89		

Chapter 4. Landscape-based Conceptual Modeling Framework to Delineate Urban Impact on Runoff Processes and Hydrological Pathways using Effective Impervious Area

Abstract

This study explored the integration of urbanization impacts into landscape-oriented FLEX-Topo hydrologic models. It particularly incorporated spatially variable effective impervious area (EIA) estimation technique that uses publicly available spatial dataset (imperviousness and soil hydraulics), and its effects on runoff processes across diverse hydrologic landscape units. Two watersheds with contrasting climates and urbanization patterns were modeled to explore 1) how different complexity levels of urban impact representation in model adjustment, and 2) spatial resolution influence model performance and behavior. Incorporating EIA significantly enhanced model accuracy, outperforming the original configuration in streamflow prediction performance in every metric used in the study. However, including additional representations of subsurface urban impacts that mainly relies on empirical approximation derived from other case studies, did not consistently enhance performance and sometimes underperformed compared to the simpler EIA-only adjustment. This suggests that, in the absence of dataset that directly support the physical representation or statistical approximation, modifications or constraints applied to the model may not improve its realism as expected and could instead introduce unnecessary additional uncertainties. A comparative analysis of spatial resolution revealed that a coarser 1 km resolution model often outperformed a finer 90 m resolution model, regardless of urban adjustment level. While it is not uncommon for coarser resolutions to perform better in similar

studies, this finding challenges the assumption that representing detailed spatial arrangement between impervious surfaces and hydrologic landscapes is important in urban hydrologic modeling. Instead, the findings suggest that focusing on spatial aspect most relevant to hydrological flux calculations can be more important than retaining full spatial details. Certain parameters involved with distribution function interact with spatial resolution, and their outcomes can be chaotic, making it challenging to identify optimal combination of parameter value and spatial resolution. The study underscores the importance of balancing model complexity with practical applicability in urban hydrology, where both oversimplification and overcomplication present challenges. The urban-adjusted FLEX-Topo model shows potential for landscape management and urban planning, offering a robust framework for understanding the interplay between urbanization, landscape characteristics, and hydrological changes across scales.

4.1. Introduction

4.1.1. Urbanization impact on watershed hydrological processes

Urbanization can affect both vertical (e.g. evaporation, percolation) and lateral (e.g. interflow, runoff) hydrological processes in watersheds (Becker & Braun, 1999). These changes alter the essential catchment functions of partitioning, storing, and releasing water (Wagener et al., 2007). Urban development shifts water partitioning towards increased surface runoff, thereby diminishing subsurface processes and enhancing the hydraulic efficiency of a catchment (Johnson & Sayre, 1973; Putnam, 1972). This shift combined with enhanced hydrologic connectivity, drives the “flashy” hydrologic responses in urban watersheds (Dunne & Leopold, 1978; Kaushal et al., 2015; Leopold, 1968; Wolman, 1967). Impervious surfaces

play a critical role in altering hydrological cycles. However, factors such as drainage network efficiency, the spatial distribution of impervious areas, antecedent soil moisture, and the spatial and temporal patterns of rainfall are equally critical in determining flood characteristics like peak magnitude, lag time, and recession periods in urbanized catchments (Ogden et al., 2011; Shuster et al., 2005; Smith et al., 2002).

Urbanization alters the water balance and natural hydrological processes, but these changes are often overlooked in modeling (Fletcher et al., 2013; Van De Ven, 1990). Planning-centric specialized models typically focus on event-based approaches and require intensive spatial data, while forecasting models lack consistent representation of urban impacts, failing to effectively capture the highly variable interactions between natural and artificial hydrologic processes. Key components such as urban groundwater and evapotranspiration often receive insufficient attention in conventional stormwater management approaches, which may fail to fully account for the intricate dynamics of urban watersheds (Van De Ven, 1990). Case studies from urban catchments have demonstrated that antecedent soil moisture conditions significantly influence watershed responses, particularly under wet conditions or extreme events (Boyd et al., 1993; Smith et al., 2002). Saadi et al. (2020) analyzed 852 catchments across the U.S. with varying degrees of impervious surface cover and confirmed that antecedent soil moisture is a pivotal factor in determining runoff ratios, even in the most highly urbanized catchments. These insights highlight the need for advanced modeling tools that integrate both natural and urban-specific hydrological factors. This approach is beneficial, as urban hydrology, while distinct, still shares fundamental principles with natural hydrology, as proposed by Fletcher et al. (2013).

Numerous concepts have been developed to explain how urbanization modifies natural hydrology. Urban Variable Source Area (UVSA) concept (Miles & Band, 2015) acknowledges that quick flow response in urban areas is determined by a combination of infiltration excess overland flow from impervious surfaces and the dynamics stemming from topographic and impervious run-on induced soil water concentration (Schwartz & Smith, 2014). Lim (2016) demonstrated that total impervious area (TIA) typically exhibits a negative effect on VSA response. The concept of effective impervious area (EIA) integrates imperviousness with hydrologic connectivity, and advances the potential of the UVSA concept. Defined as the fraction of impervious surfaces hydraulically connected to the drainage system, EIA often showed strongest correlations with runoff response behavior in urban watersheds (Lee & Heaney, 2003; Shuster et al., 2005) and is frequently used as a static watershed descriptor or to parameterize urban rainfall-runoff models (Epps & Hathaway, 2019). Building on these ideas, the watershed capacitance concept considers how the fate of runoff from impervious to pervious surfaces varies according to a watershed's inherent natural hydrologic characteristics (Miles & Band, 2015). High complexity ecohydrological model with very fine spatial resolution showed the clear importance of considering hydrologic connectivity of impervious surfaces, not only for runoff prediction but also for soil moisture conditions in surrounding pervious areas (Shields and Tague, 2015). Therefore, integrating this series of concepts at intermediate complexity that focus on landscape control of natural hydrologic processes could be highly beneficial.

4.1.2. Landscape-based FLEX-Topo model

Landscape dynamics play a crucial role in natural hydrological processes, serving as the foundation for various theories and models (Gharari et al., 2011). Notable examples include

the Topographic Wetness Index and TOPMODEL (Beven & Kirkby, 1979). Winter (2001) introduced the concept of the hydrologic landscape as a unit characterized by distinct vertical positions and common hydrologic processes. Another recent and significant contribution is the Height Above Nearest Drainage (HAND; Renno et al., 2008), which calculates the elevation difference between a given location and the nearest drainage network. HAND demonstrated a strong correlation with the depth of the water table, making it a simple yet reliable spatial representation of soil water environments (Nobre et al., 2011; Renno et al., 2008). Additionally, HAND directly links to hydraulic gradient and normalized draining potential of the location, making it an excellent predictor of runoff generation processes (Gharari et al., 2011).

Savenije (2010) recognized HAND as a robust classifier of “hydrologic landscape” which can be implemented as Hydrological Response Units (HRUs) in the design of a landscape-based oriented hydrological model (FLEX-Topo). The FLEX-Topo model typically classifies different landscape types using HAND and slope as criteria to define Hydrological Response Units (HRUs) such as Wetland, Hillslope, and Plateau. The model allows each HRU to exhibit distinct runoff mechanisms and operate in parallel without interaction and supports both lumped and fully-distributed spatial configurations while offering various routing options. FLEX-Topo has demonstrated promising results in various applications and its adaptable structure is suited for representing diverse impacts on hydrological processes (Ekka et al., 2022; Gao et al., 2014; Gharari et al., 2014).

Despite its potential, the FLEX-Topo model has not yet been applied to urban watersheds or used to assess the effects of urbanization. This study seizes the unique opportunity to adjust the model for urban applications. By integrating concepts concerning imperviousness and its

hydrologic connectivity to the drainage network and surrounding pervious surfaces, the FLEX-Topo model can provide a comprehensive framework to assess urban impacts on runoff processes and hydrological pathways. This approach is essential for understanding and managing the complex dynamics of urban watersheds.

4.1.3. Scope of the Study

This study aims to explore simple methods for incorporating urban influences into the FLEX-Topo landscape-based hydrologic model (Savenije, 2010). As discussed above, we selected this model due to its balance of simplicity and flexibility, which enables it to capture the spatial variability of runoff generation mechanisms across watershed landscapes, despite the inherent limitations in fully representing all physical processes. The study hypothesizes that introducing tailored model adjustments aimed to represent urban impact (which will be referred as “urban adjustments”) to landscape classes across the watershed, accounting for spatial variability in dominant hydrologic processes and urbanization levels, will improve prediction accuracy and reduce model parameter sensitivity.

The study aims to test the effectiveness of explicitly delineating the hydrologic impact of urban imperviousness in the FLEX-Topo process-oriented watershed model. Given these considerations, our study addresses the following specific research questions:

- 1) How does the level of detail in representing urban-induced changes in runoff processes affect the accuracy and behavior of the model?
- 2) How does spatial resolution affect the implementation and outcomes of urban adjustments in the model?

4.2. Study Area

Two watersheds with distinct climate conditions and runoff seasonality were selected (Table 4-1, Figure 4-1), one being dry and another being wet. These variations in climate affect natural hydrologic processes and streamflow seasonality, resulting in different levels of urbanization impact. For example, hydrologic simulations have shown greater sensitivity to land use and land cover in drier catchments, as observed in studies using the distributed Noah-MP land surface model (D.-H. Kim et al., 2021).

The following criteria were applied in selecting the study areas:

1) **Complex Urbanscape Requirement:** The selected watersheds exhibit a complex relationship between topography and urban development patterns. Topography not only influences natural watershed characteristics but also shapes urban development patterns. We targeted watersheds where over 30% of the area is classified as "Hillslope" landscape type (see Methods section for classification criteria). This approach helps avoid watersheds that are predominantly flat and have urban development restricted to specific landscape types. The watersheds also had 20-50% urban cover to ensure a meaningful investigation of the interaction between urban and natural hydrologic processes. Additionally, each landscape type within the watershed had to have at least 10% imperviousness. Around 10 watersheds were initially filtered based on these criteria, then manually reviewed and selected.

2) **Manageability Considerations:** To maintain the study's focus on urbanization and avoid conflicting effects of other human impacts, additional criteria were considered: The watersheds had to be headwater catchments without major inflowing rivers, and free from significant upstream reservoirs or dams. Furthermore, we excluded areas with major aquifers or significant active groundwater pumping, based on municipal water usage datasets (Dieter

et al., 2018; Luukkonen et al., 2023). Lastly, the watershed size was limited to approximately 100km^2 to keep computational costs reasonable.

The first watershed is located in San Diego County, California, and covers the drainage area of Los Penasquitos Creek (Table 4-1). It will be referred to as “SD.” The SD watershed has a hot-summer Mediterranean climate (Köppen classification Csa) with highly seasonal streamflow patterns. It features a highly complex urbanscape where various densities of urban development are situated among geomorphology characterized by significant elevation differences and steep slopes (e.g., mesa, valley, and mountain). The diverse urban developments are interspersed with the natural topography, providing a challenging yet informative landscape for hydrologic modeling (Figure 4-1).

The second watershed is in Fulton and Dekalb County, Georgia, near Atlanta, covering the drainage area of Nancy Creek and will be referred to as the “Fulton” watershed (Table 4-1). The Fulton watershed has a humid subtropical climate (Köppen classification Cfa) and exhibits a streamflow pattern with minor seasonality, remaining relatively stable throughout the year. The topography consists of rolling hills with moderate elevation changes, but less steep hillslope gradient compared to the SD watershed. Despite these differences, the Fulton watershed also presents a complex urbanscape with diverse development densities spread across the different hydrologic landscapes (Figure 4-1).

Table 4-1. Basic information on the SD and Fulton Watershed

Name	Outlet NHDPlusV2 Common Identifier (COMID)	Outlet USGS gage National Water Information System ID	Total Drainage Area (km ²)	Regional Mean Annual Rainfall (mm)
San Diego (CA)	20331196	11023340	109.04	336
Fulton (GA)	2047963	02336410	97.64	1318

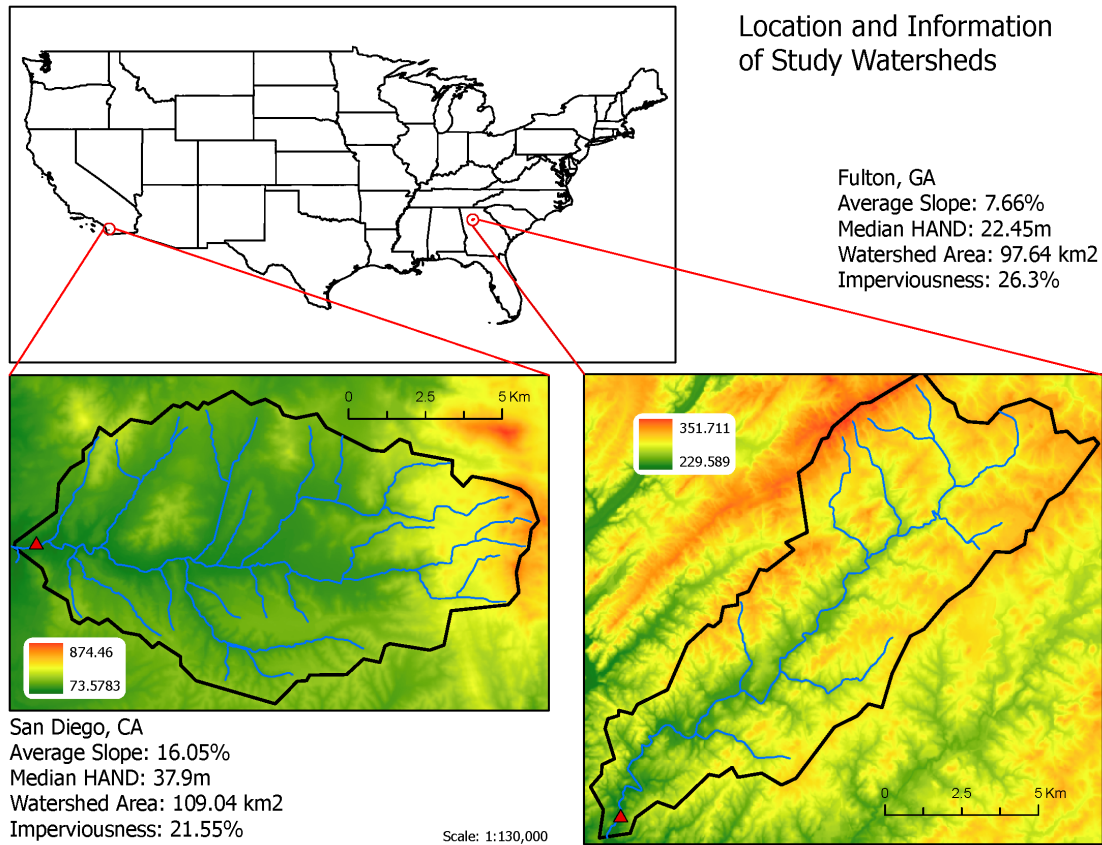


Figure 4-1. Location of the watersheds and their landscape statistics (average slope in %, median HAND value, watershed area, and imperviousness). The legend of the maps indicates the elevation in meters.

To further characterize the hydrological conditions and seasonality of the selected watersheds, we examined the Pardé coefficient (Figure 4-2), which is the ratio of the monthly mean discharge to the mean annual discharge throughout 10 water years (Water Year 2012 ~ 2021). This metric provides insights into the variability of streamflow within a year, offering a comparison of hydrological responses between different climates. The SD watershed showed high monthly streamflow variability, with high flows mainly occurring between January and March, indicating a pronounced seasonal hydrological pattern typical of Mediterranean climates. Conversely, the Fulton watershed's Pardé coefficient remained stable throughout the year, with only a slight uptick in February, reflecting the more consistent streamflow characteristic of humid subtropical climates.

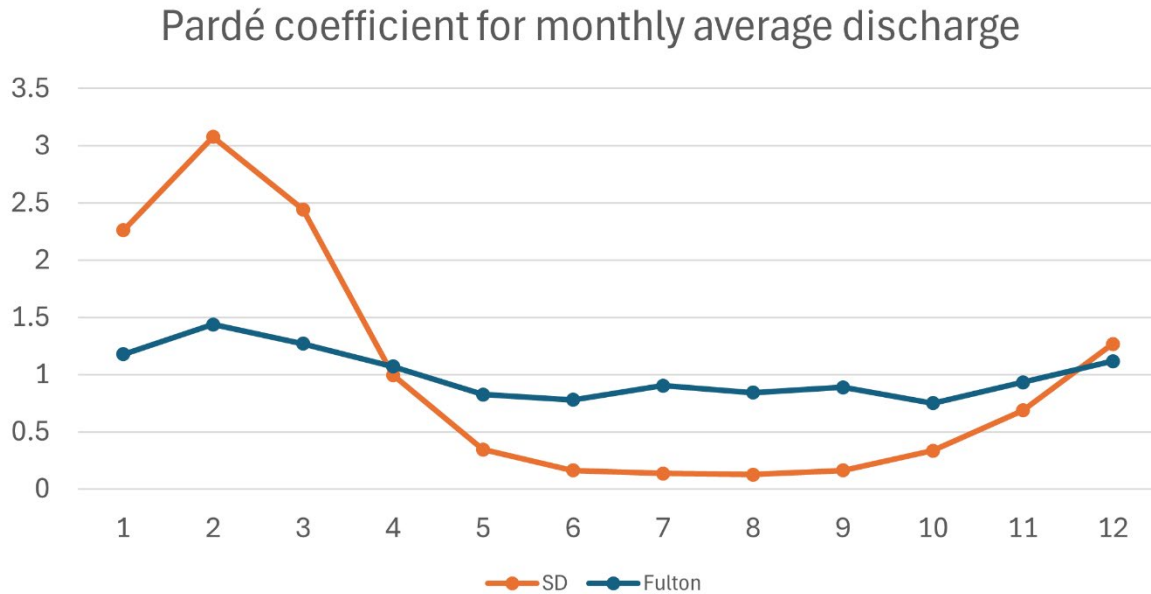


Figure 4-2. Streamflow seasonality quantified with Pardé coefficient for monthly average discharge. X-axis as a month where 1=January.

In summary, the SD watershed provides a case study in a Mediterranean climate with highly seasonal hydrological conditions in steep and complex topography, while the Fulton watershed offers a scenario in a humid subtropical climate with more stable hydrological conditions under relatively less steep topography with moderate complexity.

Static model inputs for these watersheds, including flow direction and stream path, were derived from the National Hydrography Dataset Plus (NHDPlus) and 3D Elevation Program (3DEP; previously National Elevation Dataset, NED) dataset (US Geological Survey).

4.3. Methods

The study aims to explore how the urban adjustment of the FLEX-Topo affects the model behavior and performance. In the following section, we discuss 1) the basic set up and preparation of the model input data, 2) the concept of urban adjustment and details, which introduces spatial variability into subsurface processes through parameter-scaling strategies,

3) calculation method of effective impervious area (EIA) utilizing the publicly available land data, and 4) model experiment design that investigates the influence of urban adjustment level and spatial resolution.

4.3.1. The FLEX-Topo model configurations and preparations

The FLEX-Topo model was originally designed to focus on the dominant runoff mechanisms across different landscapes, primarily using the HAND metric to categorize them into three primary types: Wetland, Hillslope, and Plateau. However, in this study, we indicate them as Lowland, Hillslope, and Upland as they do not typically match the perceived geomorphological image of “wetland” or “plateau” and could be misleading. We used HAND and slope for HRU classification: areas with HAND value less than 5m were classified as lowlands; areas and with a HAND value greater than 5 meters and a slope steeper than 5 degrees (8.75%) were classified as hillslopes; all other areas were classified as uplands (Gharari et al., 2011). Each HRU operates in parallel in the model, ensuring a detailed depiction of runoff generation mechanisms without spatial bias in parameterization.

- 1) **Lowland (Wetland):** Characterized by saturation excess overland flow (SOF) due to its proximity to the groundwater table and significant flow accumulation, with HAND and slope below the threshold of 5 meters and 5 degrees (8.75%) (Gharari et al., 2011).
- 2) **Hillslope:** Defined by shallow subsurface flow (SSF) due to higher vegetation density, shallow soils, and decreasing permeability with depth, with HAND >5 m and slope above 5 degrees.
- 3) **Upland (Plateau):** Identified by deep percolation (DP) towards groundwater and secondary Hortonian overland flow (HOF), with limited preferential subsurface flow, having HAND above 5m and slope below 5 degrees.

We utilized the wflow framework (<https://wflow.readthedocs.io/en/latest/>) FLEX-Topo with a spatially distributed configuration that uses gridded meteorological input and routing. This distributed configuration is primarily designed to leverage distributed meteorological inputs to capture the spatially heterogeneous hydrologic states across watersheds while employing lumped HRU-scale parameterization to maintain theoretical robustness.

To improve model accuracy and reduce parameter uncertainty, we eliminated the use of FLEX-Topo's routines for interception, snow/ice processes, and evapotranspiration. Instead, used meteorological fluxes from the Noah-MP model simulation and processed them to fit the FLEX-Topo model using the one-way coupling method described in Chapter 2 (Kim et al., 2021). FLEX-Topo now receives surface fluxes pre-calculated by National Water Model v2.2 Long Range configuration (McCreight et al., 2020) which utilizes the North American Land Data Assimilation System (NLDAS; Mitchell et al., 2004) as forcing data.

The “effective precipitation” flux, representing the potential water that can enter the soil matrix at a given timestep, is aggregated from precipitation and changes in canopy water storage and snow/ice storage computed in NWM. Similarly, actual evapotranspiration (AET) is directly adopted from NWM model output. This approach bypass the simpler storage-based interception and evapotranspiration module in FLEX-Topo, which requires calibrating multiple parameters. Using pre-calculated fluxes from NWM instead can reduce both parameter dimensionality and uncertainties (D.-H. Kim et al., 2021).

The overall structure of the urban-adjusted FLEX-Topo model used in this study is summarized in Figure 4-3. Rainfall on Effective Impervious Areas (EIA) is immediately partitioned as impervious runoff (Q_{eia}), which is the primary urban adjustment introduced to the model. The relationship between storage and runoff is governed by the maximum

unsaturated zone storage capacity ($Sumax$) and a corresponding storage-runoff β function. The Hillslope and Upland HRUs share the same structural framework, but variations in parameters such as $Sumax$, β , D (fraction of preferential recharge), and the percolation coefficient distinguish their runoff behaviors. Upland HRU considers infiltration excess overland flow (HOF), but its impact is minimal by design, and the default parameter value has been used in the study. FLEX-Topo differentiates Lowland HRU not only by varying parameter values but also by simulating capillary rise (cap) from deep groundwater to the unsaturated zone instead of percolation ($perc$). Urban adjustment on subsurface processes does not alter the original structure but enforces parameter scaling (Figure 4-3).

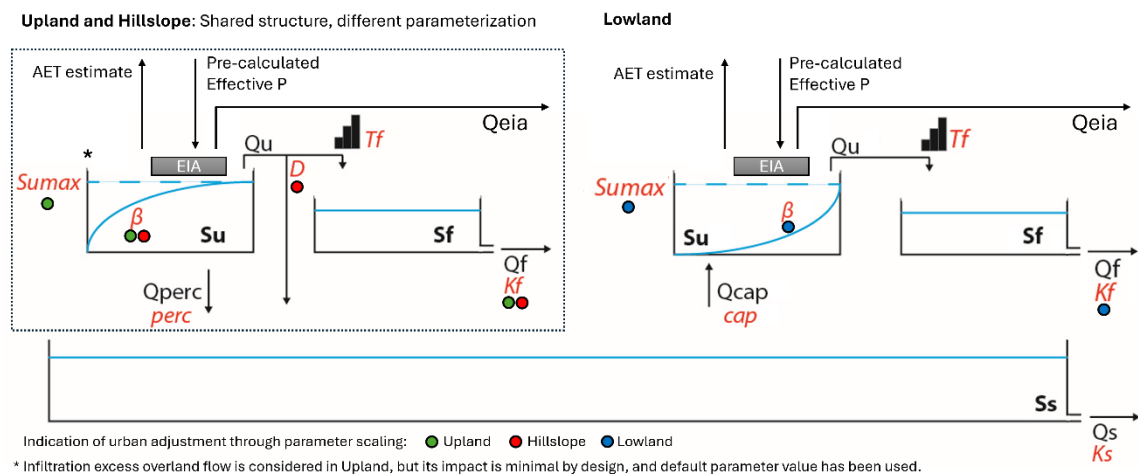


Figure 4-3. FLEX-Topo model structure schematics including EIA and meteorological input modifications made in the study. Modified from Euser et al. (2015).

Runoff from every unsaturated reservoir (Su) and HOF is processed with lag-function (Tf , a convolution operator; Fenicia et al., 2011) before entering the fast runoff reservoir (Sf). The response time of runoff exiting Sf (Qf) is controlled by the recession coefficient (Kf). Deep groundwater storage (Ss) is lumped and shared across all HRUs, with the recession rate of groundwater runoff (Qs) governed by the coefficient Ks . Finally, $Qeia$, Qf , and Qs are routed

spatially using a travel-time-based routing approach, similar to a fully-distributed unit hydrograph method.

4.3.2. Conceptualizing the urban impact

This section discusses how we adjusted the model to represent changes in hydrologic connectivity and runoff mechanisms using EIA. Three key aspects were considered: i) runoff from hydrologically connected EIA and impervious surfaces, ii) run-on from disconnected impervious to pervious surfaces, and iii) urban impacts on subsurface pathways.

Given the semi-distributed nature of the FLEX-Topo model (with a fully distributed state representation but lumped parameterization at the HRU level), we adopted a hybrid approach to incorporate these urban impacts. Surface processes related to runoff generation were adjusted uniformly across the watershed by directly applying the EIA concept. However, the lumped HRU parameterization necessitated a more refined methodology for subsurface processes. Here, we introduced a spatially variable parameter scaling approach that uses imperviousness data and established urban hydrology concepts/theories/statistics to capture the variability in subsurface processes.

- 1) Simple Impervious (Sim): This scenario only considers the partitioning of rainfall based on EIA, with adjustments limited to surface runoff processes.
- 2) Full Adjustment (FA): In addition to rainfall partitioning, this scenario integrates spatially variable parameter scaling for subsurface processes that are tailored to each HRU and their runoff mechanism. This allows the model to better reflect the spatial variability in subsurface storage, flow paths, and interactions influenced by urbanization.

Table 4-2 provides a detail in urban adjustments for two different scenarios. It highlights the general adjustments (surface), and specific adjustments (subsurface) made for each HRU type (Lowland, Hillslope, and Upland). In the Sim, adjustments are limited to surface processes such as rainfall partitioning and routing. Meanwhile, FA incorporates more comprehensive and tailored adjustments to subsurface processes. For further details on of parameters and their application, refer back to Figure 4-3.

Table 4-2. Summary of urban adjustment by HRU-type

	Lowland (SOF)	Hillslope (SSF)	Upland (HOF + DP)
Rainfall on EIA	Separately partitioned (without lag-function)		
Spatial Routing	Scaled with EIA only for overland flow		
Topography	Flat	Sloped	Flat
Depth to the groundwater table	Shallow	Deep	Deep
Run-on interaction in pervious surfaces	- Virtual increase in effective rainfall depth, with reduced $Sumax_l$ - Quicker response from SOF with recession coefficient adjustment (Kf_l)	- Quick lateral redistribution of soil water cancels the virtual increase of effective rainfall	- Virtual increase in effective rainfall depth, with reduced $Sumax_u$ - Quicker response from HOF with recession coefficient adjustment (Kfa_u)
Subsurface preferential pathways in unsaturated zone	- Conceptually insignificant	- Accelerate preferential flow with lateral bias (β_h, D_h) - Quicker response from preferential SSF with recession coefficient adjustment (Kf_h)	- Accelerated preferential flow with no directional bias (β_u) - Quicker response from preferential SSF with recession coefficient adjustment (Kf_u)

Runoff from impervious surfaces

Impervious surfaces facilitate rapid overland runoff with minimal delay. Smooth surfaces and stormwater infrastructure, such as drains and roadside ditches, accelerate sheet flow and channel it efficiently. Following the "full connectivity" assumption (Tague and Pohl-Costello, 2008), precipitation on EIA is directly partitioned as runoff (Q_{eia}) and conveyed to the nearest

stream channel, bypassing hillslope processes. To reflect this, the Kf value for EIA runoff was set to 1, ensuring immediate response.

For SOF in Lowland and HOF in Upland, Kf values were adjusted to account for disconnected impervious surfaces. This adjustment (Eq.4-1) was based on Manning's coefficient, where non-impervious NLCD land cover classes typically have 4 to 5 times higher value than impervious surfaces (Mattocks & Forbes, 2008). This also aligns with the typical differences in surface roughness across various channel types (Te Chow, 1959).

$$Kf_{scaled\ OVF} = Kf_{OVF} * \{ (1 - TIA) + 4.5 * (TIA - EIA) \} \quad (\text{Eq.4-1})$$

We also applied such scaling to travel-time-based gridded routing, which resembles the unit hydrograph approach, using Manning's coefficient to scale flow velocity in each cell (Eq.4-2):

$$Velocity_{scaled; i,j} = Velocity_{i,j} * \{ (1 - EIA) + 4.5 * EIA \} \quad (\text{Eq.4-2})$$

Drainage density was not considered, as it loses significance as an urban runoff predictor when it exceeds $0.9\ km/km^2$ (Ogden et al., 2011), a threshold often surpassed in urban areas (May et al., 1999; Ress et al., 2020).

Run-on from disconnected impervious surfaces to pervious surfaces

The EIA estimation technique used in this study incorporates soil infiltration potential, addressing how soil permeability near impervious surfaces influences run-on interactions (Sytsma et al., 2020); low permeability areas respond primarily to rainfall and soil moisture, while high permeability areas are influenced by the spatial connectivity between impervious and pervious surfaces. Saadi et al. (2020) emphasized soil moisture's role in predicting urban runoff behavior, with Schwartz and Smith (2014) noting that soil moisture conditions greatly affect the fate of runoff from disconnected impervious surfaces, or run-on. These conditions

also influence water distribution and flux exchange between soil and vegetation (Shields and Tague, 2015).

The conceptualization linking run-on interactions with EIA is based on the following premises: 1) Disconnected impervious area is represented as (TIA-EIA), and we assume that runoff enters the pervious surface within the model grid cell. 2) Hydrological characteristics of each HRU-type affect the infiltration potential of “run-on” water and lateral soil water redistribution. 3) The fate of run-on depends on the temporal variability of soil moisture in adjacent pervious areas.

In **Lowland** (dominated by SOF) and **Upland** (dominated by Deep percolation + HOF), flat topography indicates a low potential for lateral redistribution of soil water in unsaturated soil. This can be visualized as a "virtual increase" in rainfall depth at pervious areas to account for run-on from disconnected impervious surfaces and indirectly adjust soil moisture conditions, which appeared to play an important role in urban hydrologic modeling (Shields and Tague, 2015). This is achieved by reducing the unsaturated zone storage capacity parameter (Sumax, depth in mm) using Eq.4-3.

$$SUmax_{adapted} = SUmax * \frac{(Area_{pervious})}{(Area_{pervious} + TIA - EIA)} \quad (Eq.4-3)$$

In Hillslope (dominated by SSF), imperviousness level is generally not high, and this means the run-on from disconnected impervious surfaces is likely less impactful. More importantly, the topographical gradient and hydraulic characteristics in this landscape enhance lateral water redistribution through the soil matrix, even beneath impervious areas. This slope-driven redistribution reduces the necessity for a “virtual increase” in rainfall depth. Given these conditions, we did not adjust Sumax for Hillslope areas for simplicity, assuming run-on impact to be negligible in given structure of Hillslope HRU.

Urban impact on subsurface preferential pathways

Urban catchments exhibit generally shorter water residence times (Smith et al., 2023) with varied subsurface flow paths even though “older” water contribution can be significant under wet soil conditions (Wallace et al., 2021). Human-introduced macropore spaces mainly along underground pipes or utility trenches, referred to as "urban karsts", lead to quicker streamflow recession, increased seasonality, and reduced residence time (Bonneau et al., 2017, 2018). The urban adjustment aims to represent these changes and diversification of subsurface water residence time associated with preferential pathways.

Urban karsts influence both the rate and direction of subsurface water movement (Bonneau et al., 2017), and even a small fraction of disconnected macropores can significantly reduce the flow resistance in various conditions (Nieber & Sidle, 2010). Despite the significance of urban karst effect, we only implemented it in **Hillslope** and **Upland** landscape units. Lowland assumes active capillary rise from deep groundwater and “spill-and-fill” saturation overland flow as the dominant runoff mechanism. The average 2 meter depth of underground structures (US EPA, 2000) often lies below the hypothetical water table depth in the Lowland, making implementation of urban karst effect unnecessary in FLEX-Topo model structure.

The density of urban underground space (UUS), an indicator of any subsurface development (including utility infrastructures), typically ranges from 0.01 to $0.05m^3/m^2$ in urban environments (Bobylev, 2016). We hypothesize that surface total imperviousness (TIA) correlates with UUS, allowing us to estimate the extent of subsurface urban impact using a power-law relationship. UUS density is calculated within the typical range based on TIA and multiplied by TIA to estimate the potential extent of underground structures where urban karst

effect can occur. Given that the average depth of underground structures is approximately 2 meters (US EPA, 2000), we defined the unitless Urban Karst Effect Index (UKEI) to indicate the potential impact of urban development on subsurface hydrologic processes. The UKEI, calculated using Eq. 4-4, considers TIA twice — first to represent UUS density increasing with urbanization, and then to apply this density to estimate the fraction of the area with UUS beneath the surface.

$$\text{Urban Karst Effect Index (UKEI)} = (0.01 + 0.04 * TIA^{\frac{1}{e}}) / 2 * TIA \quad (\text{Eq.4-4})$$

In Hillslope and Upland areas, urban karst effects enhance preferential subsurface runoff, making it less dependent on the storage state. The mobilized preferential flow (Q_{u_pref} , unitless fraction; ranging 0~1) within unsaturated storage is calculated in FLEX-Topo as follows:

$$Q_{u_pref} = 1 - (1 - SU/SU_{max})^{\beta} \quad (\text{Eq.4-5})$$

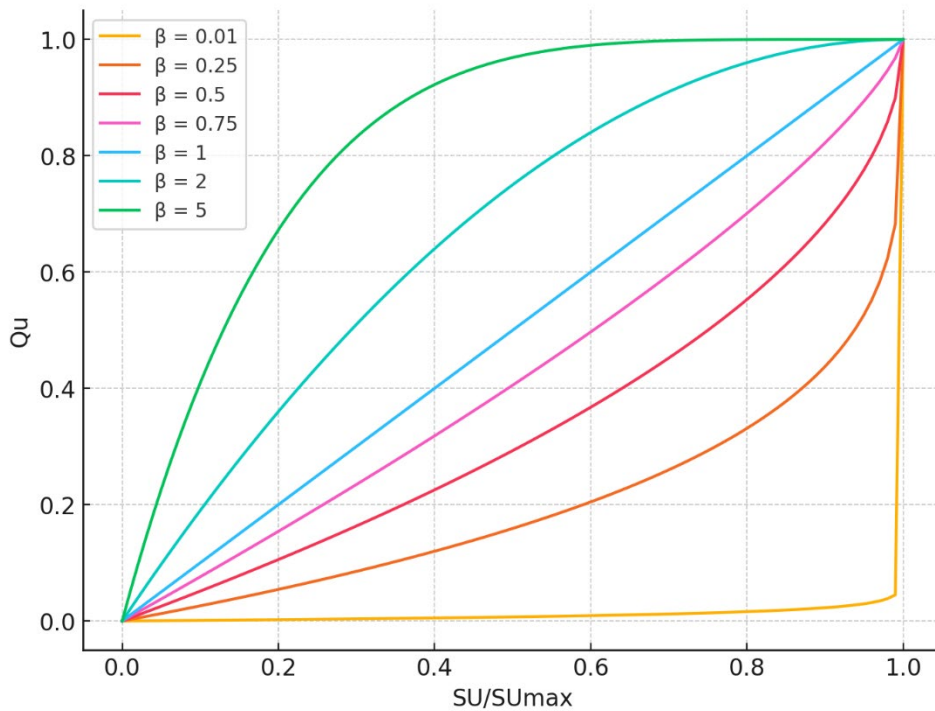


Figure 4-4. Relationship between Q_{u_pref} , SU/SU_{max} , and β

Qu_{pref} multiplies to the flux that enters the unsaturated zone storage for the timestep to determine how much preferential flow exits the unsaturated zone; very small β value result in fill-and-spill type of response, and higher β value result in substantially accelerated rate of preferential runoff happening from unsaturated zone (Figure 4-4).

Macropores or soil pipes in the soil matrix can increase the variance in Darcy flux by up to 20 times, even when the daily mean flux remains relatively unchanged (Nieber & Sidle, 2010). To reflect this on model behavior, we adjusted β (in reflected power-function; Moore, 1985) to emulate the quicker mobilization of preferential flow that bypasses storage.

The adjustment is achieved through the following empirical regression (Eq. 4-6), which is optimized to scale β , allowing an increase in preferential runoff from HRUs (Qu in Eq. 4-5) while limiting the maximum increase to 20 times across the entire range of UKEI, β (original parameter value before scaling), and unsaturated storage conditions (with UKEI ranging from 0 to 0.05, base β ranging from 0 to 5, and $Su/Sumax$ ranging from 0 to 1):

$$\beta_{scaled} = \beta * (1 + 15 * \frac{1^{0.5}}{\beta} * UKEI^{0.8}) \quad (Eq.4-6)$$

To prevent β from becoming unreasonably large, a cap is applied:

$$If \beta_{scaled} \geq 5, then \beta_{scaled} = 5$$

Eq.4-6 empirically scales the β parameter to simulate increased preferential flow due to urban karst effects while keeping runoff (Qu) within reasonable limits. This adjustment is tested and finalized with pre-experiment model runs that represented the whole watershed as a single reservoir, and optimized to ensure variability in subsurface flow without unrealistic amplification.

Urban Karst in Hillslope areas generally promote the lateral movement of preferential subsurface flow, driven not only by the topographical gradient but also by utility trenches that

divert vertical recharge into lateral flow (D’Aniello et al., 2021; Sharp Jr. et al., 2003). To account for this, we adjust the D parameter, which controls the balance between lateral subsurface flow (SSF) and vertical recharge to deep groundwater, to favor lateral SSF.

Our goal is to keep the products of Qu (preferential flow) and D constant because this product represents the proportion of flow contributing to deep groundwater recharge. This ensures that the preferential flow remains consistent with the physical expectation of increased lateral flow in Hillslope areas, without a significant increase in preferential recharge. The scaled D parameter is calculated as follows:

$$D_{scaled} * \{1 - (1 - Su/Sumax)^{\beta_{scaled}}\} = D * \{1 - (1 - SU/SUmax)^{\beta}\} \quad (\text{Eq.4-7})$$

By linearizing the term (1-Su/Sumax) around Su/Sumax = 0 using a first-order Taylor expansion, we simplify the general trend of Eq.4-7 to:

$$D_{scaled} \approx D * (\beta / \beta_{scaled}) \quad (\text{Eq.4-8})$$

This adjustment ensures that the model favors lateral flow due to urban karst effects in Hillslope while maintaining a realistic balance between lateral flow and vertical recharge.

In **Hillslope** and **Upland** HRUs, we modify Kf (coefficient for the recession of subsurface runoff) to represent the accelerated lateral movement of preferential subsurface flow caused by human-induced macropores. The celerity of water in a dual-porosity soil matrix can exceed that in a single-porosity matrix by 100 to 1000 times (Worthington, 2019), and hydraulic conductivity along macropores can be 29 to 550 times higher (Menichino et al., 2014). Since Kf specifically relates to the lateral travel of subsurface runoff, we scale it using the average of the lower-end values from Menichino et al. (2014) and Worthington (2019), resulting in Eq.4-9. The scaling factor for Kf can range from 1.0 to 3.225, representing the possible minimum and maximum adjustments based on the level of local imperviousness.

$$Kf_{scaled} = Kf * \{(1 - TIA) + UKEI * 64.5\} \quad (\text{Eq.4-9})$$

Human Water Uses: Imported Water and Pumping

Urban water usage, water diversions, storage, or groundwater pumping can significantly impact regional hydrological cycles (Hasenmueller et al., 2017), increases low season flow (White & Greer, 2006), and alter dry-season streamflow contribution (Fillo et al., 2021). Although there is a well-established link between increased dry-season baseflow and urbanization especially in drier climates (Townsend-Small et al., 2013), this study does not incorporate adjustments for human water use.

The exclusion of human water use from the model is primarily due to the high uncertainty associated with implementing these aspects which would require directly modifying internal model fluxes without robust evidence. Neither municipal water pumping and usage data (see “4.2. Study Area”) nor the catchment water balance analysis (see “4.4.1. Pre-Analysis of Water Balance in Study Watersheds”) indicated a significant imbalance in water budget. Furthermore, our aim is to develop a widely applicable model that does not rely on detailed municipal water management data, which is often difficult to obtain due to data ownership and limited access (Eggimann et al., 2017). To address human impacts adequately, comprehensive data from historical flow analyses that account for land use changes and climate variability, along with isotopic tracing, would be necessary to provide a more accurate representation of these processes.

In this context, we use a “black-box” approach with parameterization via Quasi-Monte Carlo method to replicate observed streamflow behaviors, including low flows, without explicitly accounting for human water use. Human impacts in urban areas are complex, with factors such as locally pumped groundwater contributing back to runoff via leaky pipes and

shallow groundwater (Burns et al., 2005). However, Burns et al. (2005) also noted that these processes often have a limited impact on groundwater recharge, discharge properties, or catchment residence time, which adds to their uncertainty. Given this complexity and uncertainty, our approach is designed for general applicability rather than detailed, location-specific analysis. We acknowledge the limitations of this “black-box” method, as it does not explicitly model specific human influences on water fluxes.

4.3.3. Calculation of Effective Impervious Area (EIA)

Urban influences on hydrological processes vary widely, and the hydrologic response can significantly differ based on impervious surface connectivity (Tague & Pohl-Costello, 2008). Therefore, this study focuses on the hydrological connectivity of impervious surfaces and how this could also affect underlying natural hydrological processes. While estimates of directly connected impervious areas (DCIA) require intensive field investigation and are often affected by the level of spatial detail (Lee & Heaney, 2003), statistically estimated EIA provides satisfactory results without extensive labor (Ebrahimian et al., 2016). Given the generally low spatial resolution (90m resolution to fully lumped watershed representation) of FLEX-Topo, adopting the statistically estimated EIA is reasonable as details in spatial information lose value if the model structure cannot fully utilize it (D.-H. Kim et al., 2024).

Recent studies highlight that impervious surface connectivity is influenced by rainfall depth, soil types, and antecedent soil moisture conditions (Sytsma et al., 2020). Such connectivity is more affected by rainfall rate and soil moisture conditions when the soil has low permeability, while the spatial pattern of disconnecting pervious areas becomes more influential when the soil is highly permeable. Ebrahimian et al., (2018) proposed an EIA estimation technique using the Asymptotic Curve Number (CN_{∞}), which represents the

maximum runoff potential under fully saturated conditions. The method considers factors such as soil type, land use, and moisture level to estimate a refined relationship between event runoff and the size of the event. This method requires fractional impervious area and hydrologic soil group data, making it appealing for its simplicity and reliance on readily available inputs.

While the technique developed by Ebrahimian et al., (2018) is designed to estimate EIA at a watershed scale, we tested its application at the model grid cell scale using the National Land Cover Database 2016 (NLCD 2016) imperviousness data and an area-weighted surface saturated hydraulic conductivity (Ksat) dataset (Buchanan et al., 2018), primarily sourced from SSURGO with missing values filled from STATSGO. However, during initial inspections, it was observed that EIA estimates showing unjustifiable extreme variance between neighboring cells even when Ksat is identical and the difference between TIA is minimal.

The relationship between EIA and asymptotic CN in the original CN- EIA equation is non-linear, with a relatively flat progression at lower CN_{∞} values, followed by an extremely sharp increase as CN_{∞} reaches 90. For instance, in our watersheds, EIA remains around 0.2 across a wide range of TIA values (0.2 to 0.8), but then EIA nearly doubles as TIA reaches 0.9. This abrupt transition resulted in a lack of spatial continuity in EIA estimation is inconsistent with Tobler's First Law of Geography (Tobler, 1970) which emphasizes that similar and nearby areas should exhibit similar characteristics. Therefore, we decided that the original CN-EIA method may not be well-suited for calculating EIA in the distributed model grid cells of our study watersheds, where a more gradual and proportional response would be expected.

The relationship between CN and EIA, represented in fractions (f_{EIA}), is based on a series of regressions, and logical connection between them necessitated preserving their equations' general forms. Our attention was focused on the linear regression model for α (Eq.4-10), which represents the relationship between the asymptotic CN in EIA ($CN_{EIA\infty} \approx 98$) and the remaining area ($CN_{r\infty}$). This component from Ebrahimian et al., (2018) is most directly pertinent to adjusting the CN-EIA relationship and can be summarized as follows:

$$\alpha = CN_{r\infty}/98 = 0.0116 CN_{\infty} - 0.1601 \quad (\text{Eq.4-10})$$

$$CN_{\infty} = CN_{EIA\infty}f_{EIA} + CN_{r\infty}(1 - f_{EIA}) = 98f_{EIA} + 98\alpha(1 - f_{EIA}) \quad (\text{Eq.4-11})$$

$$f_{EIA} = \frac{16 - 0.14 CN_{\infty}}{114 - 1.14 CN_{\infty}} \quad (\text{Eq.4-12})$$

Reducing the slope value in the α regression (Eq.4-10) can mitigate the abrupt transition observed in the CN-EIA relationship of Eq.4-12. We hypothesized that this slope could be less than 0.0116, to ultimately reduce sharp transition in Eq.4-12 and allow a more gradual response in spatially distributed EIA estimation. Utilizing Bayesian linear regression with data from Ebrahimian et al. (2018), we found that the slope converged to 0.01092. To further refine the model, we stabilized the intercept at 0.1176 through optimization using the DEoptim R package (Mullen et al., 2011), aiming to better fit our Bayesian linear regression to the data used in Ebrahimian et al. (2018) deriving the original linear regression for α . This modification results in an adjusted CN-EIA relationship, as represented in Eq.4-13, and this ultimately resulted in more gradual relationship between CN-EIA relationship (Figure 4-5).

$$f_{EIA} = \frac{11.52 - 0.07 CN_{\infty}}{109.52 - 1.07 CN_{\infty}} \quad (\text{Eq.4-13})$$

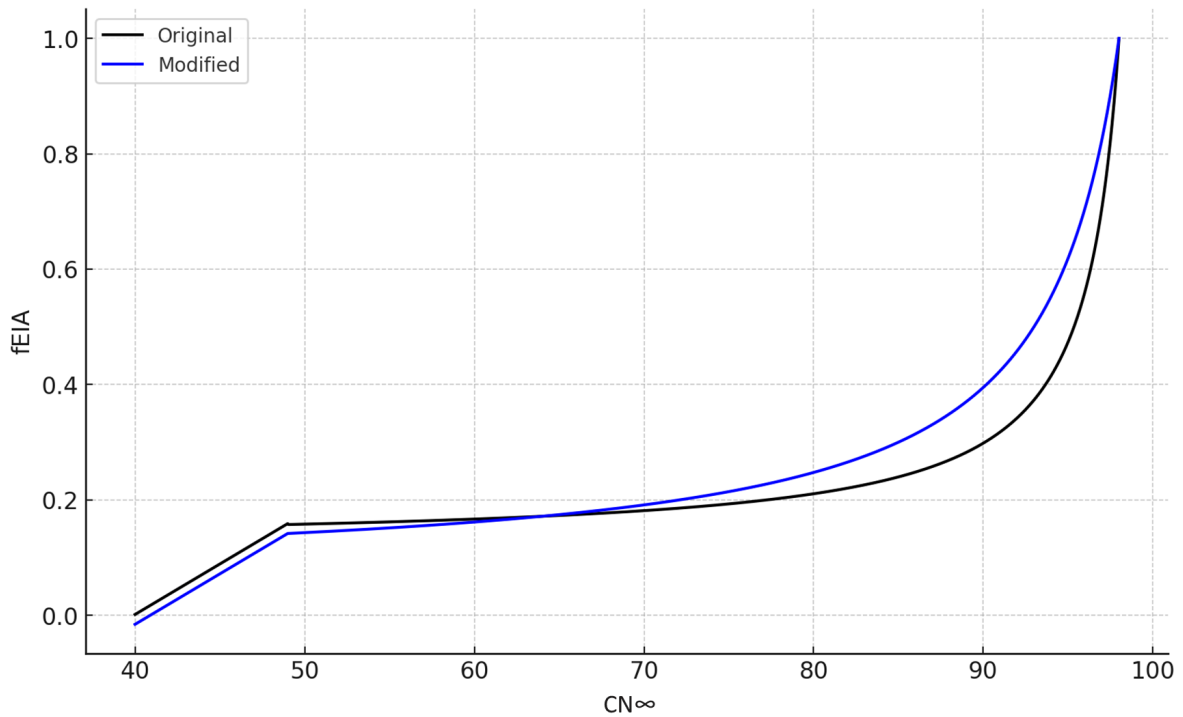


Figure 4-5. Comparison for fractional EIA calculated from the original Ebrahimian et al. (2018) and the modified version for the study watersheds.

Given that this method was originally designed for watershed-scale EIA estimation, rather than finer-scale applications, a soft validation was necessary. To ensure that our approach captures spatial variability while remaining comparable with conventional estimations, we aggregated the CN-EIA estimates from the grid-cell level to the watershed scale. These aggregated estimates were then validated against empirical watershed-scale EIA estimations compiled from previous studies (Alley & Veenhuis, 1983; Sultana et al., 2020; Sutherland, 1995; Wenger et al., 2008). Since empirical watershed-scale EIA estimations can exhibit high variability across different urbanization level and watershed environments, we filtered out outliers that were more than 1.96 standard deviations from the mean. The average of the remaining values was then compared with our aggregated CN-EIA estimate to assess the validity of our approach.

4.3.4. Model Experiment Design: Urban Adjustment Level and Spatial Resolution

The model experiment aims to evaluate the impact of model adjustment strategies for urban settings on the relationship between feasible parameter ranges and prediction efficiency. This approach employs statistical scores and hydrologic signatures commonly used for model performance evaluation to assess changes in streamflow and simulated watershed response. Instead of just calibrating the model for optimal streamflow prediction, the aim is to compare changes in parameter sensitivity and performance across different spatial resolutions of the model and varying level of urban impact representation on different hydrological processes.

The experiment compares the original FLEX-Topo model and two urban-adjusted models (“Simple Impervious” and “Full Adjustment”). This comparison provides insight on how the level of detail in urban adjustment influences model behavior, and how it interacts with the different model spatial scales (comprehensive details are presented in Table 4-2 & Table 4-4).

- 1) None (original FLEX-Topo)
- 2) Simple Impervious (Sim): Urban adjustment only for surface
- 3) Full Adjustment (FA): Urban adjustment for both surface and subsurface

A quasi-Monte Carlo approach was taken to calibrate and evaluate the model, but with strategies to overcome high dimensionality. We applied Sobol sequence sampling to efficiently explore the high-dimensional parameter space but focused on major parameter groups: Sumax, β , Kf, and D identified with their suggested range by Euser et al. (2015), Gao et al. (2014), and Gharari et al. (2014). Relational parameter constraints among different HRUs were established following guidelines from Euser et al. (2015) and Gharari et al. (2014) for major parameter groups, as it can significantly reduce the available parameter space (Table 4-3). This keeps the effective dimensionality far below 11 dimensions, allowing us to

effectively explore parameter spaces with 1024 (2^{10}) parameter sets sampled. Parameters that are not included in the major groups (e.g., capillary rise, percolation) were freely sampled using a uniform distribution. However, the Ks (Coefficient for recession of slow runoff reservoir; deep groundwater) was manually derived based on the slope of the low flow segment in the Master Recession Curve, which was fitted to the USGS observed streamflow data.

Preliminary analysis indicated that Nash-Sutcliffe Efficiency over 0.7 could be achieved by sampling parameters from a certain narrow range. However, we used the full parameter range to explore the width of model behavior, because the purpose of the study does not lie in showcasing the best achievable performance scores.

Table 4-3. Relational parameter constraints for major parameter groups, and their sampling range for the study watersheds

Parameter group	Description	Relational constraints	Sample range
Sumax	Max unsaturated zone storage capacity (mm)	Lowland < Hillslope = Upland	[35, 1000]
B	Beta function for reflected power function (Moore, 1985)	Hillslope < Upland < Lowland	[0.01, 5]
Kf	Coefficient for the recession of fast runoff reservoir	Upland < Hillslope < Lowland	[0.002, 1]
D	Fraction of preferential recharge from unsaturated zone to deep groundwater	Hillslope < Upland (No deep percolation in Lowland)	[0.05, 1]

To evaluate the effects of spatial resolution on urban adjustments in the model, two different resolutions were used:

- 1) Coarser 1km model: Resampled from the finer spatial data, representing areal portions of different HRU types and aggregating overall EIA values within each 1km grid cell.

Significant loss of fine-scale spatial arrangements and relationships observed in the finer resolution counterpart model (Figure 4-6).

- 2) High-resolution 90m model: Each grid cell is uniquely assigned a specific HRU type (Lowland, Hillslope, and Upland) along with corresponding EIA values and parameter scaling, maintaining detailed spatial relationships at the cost of higher computational demand.

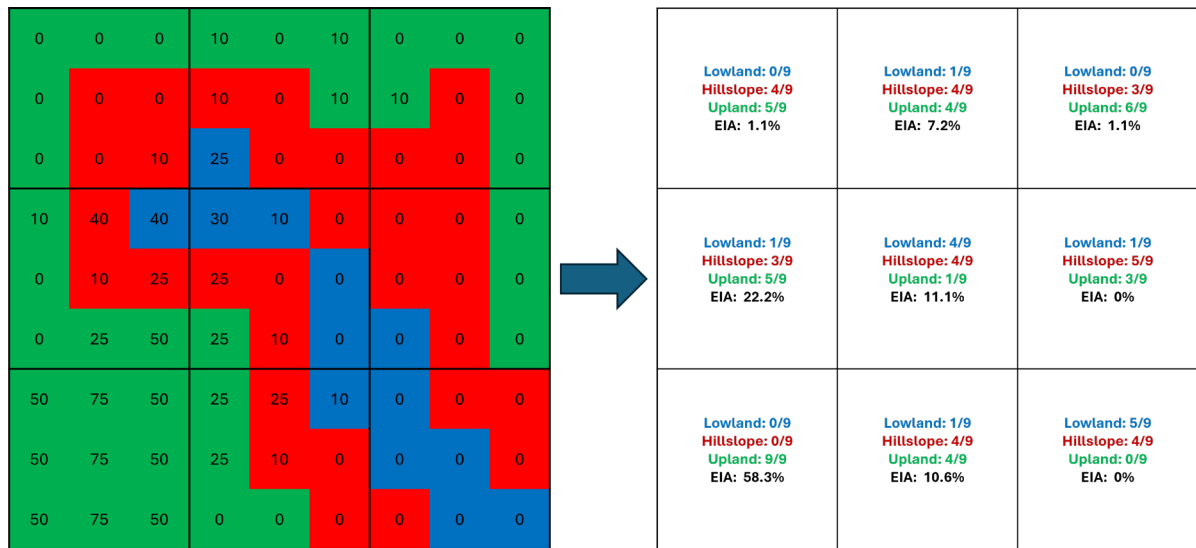


Figure 4-6. Example of resampling a finer model grid into coarser model grid

This research examined how different levels of urban adjustment and spatial resolution affect model performance in the two study watersheds. We first analyzed the top 10% performing models to compare the effects of urban representation (Sim vs FA) and spatial resolution (1 km vs 90 m) on performance metrics and hydrologic signatures. This comparative analysis provided a general overview of the impacts. To further assess the performance differences between the Sim and FA models under identical parameter inputs, we created scatter plots comparing NSE values, supplemented with the mean and standard deviation of the performance differences.

Table 4-4. Comparison plan for model configurations with different urban adjustment levels and affected model components in each of them. For comprehensive details, refer back to Table 4-2.

Spatial Resolution	Urban Adjustment Level	Affected Model Components
1km	None	<ul style="list-style-type: none"> No modification to the original process/structure
1km & 90m	Simple Impervious (Sim): EIA rainfall partitioning	<ul style="list-style-type: none"> Rainfall Partitioning from EIA Adjusted routing for impervious runoff
	Full Adjustment (FA): EIA rainfall partitioning + Parameter scaling to emulate subsurface urban impact	<ul style="list-style-type: none"> Rainfall Partitioning from EIA Adjusted routing for impervious runoff Parameter scaling based on EIA & TIA: Lowland ($Sumax_l$), Hillslope (β_h, Kf_h, D_h), and Upland ($Sumax_u, Kf_u$)

Models were simulated over five water years (October 2013 to September 2018), and the following metrics were employed to assess different aspects of model performance against USGS observation:

- 1) General evaluation: Nash-Sutcliffe efficiency (NSE). Examines overall fit with emphasis on high flow. Used for evaluating the models' parameter sensitivity.
- 2) Low flow conditions: Log transformed Nash-Sutcliffe efficiency. Focuses on the model's accuracy during low-flow periods.
- 3) Percent Bias for identifying systematic over- or under-prediction.
- 4) Richard-Baker flashiness index (Baker et al., 2004) for comparison of overall flashiness of watershed response (Eq.4-14).

$$RB\ Flashiness\ Index = \frac{\sum_{i=1}^n |Q_i - Q_{i-1}|}{\sum_{i=1}^n Q_i} \quad (Eq.4-14)$$

Q_i : flow at timestep i

Q_{i-1} : flow at timestep $i - 1$

n : total number of timesteps in the period of interest

- 5) Baseflow index (BFI). Assesses the model's ability to simulate the proportion of baseflow (the portion of streamflow that comes from groundwater or delayed sources such as Upland) versus quickflow (the portion of streamflow that responds rapidly to precipitation events). Calculated with “Hydrostats” R package (Bond, 2022) based on Ladson et al. (2013).

To further understand how urban adjustment affected model behaviors, we conducted a visual parameter sensitivity analysis using scatter plots. This compared the 1 km resolution original FLEX-Topo, Sim, and FA models across all 1,024 parameter sets. Additionally, we applied a Random Forest (Breiman, 2001; RF) model to estimate parameter importance, comparing both 1 km vs. 90 m resolutions and Sim vs. FA models. The Random Forest used FLEX-Topo parameter values as predictors, and feature importance was calculated based on the average decrease in variance each parameter contributed to the NSE prediction accuracy across all decision trees in the forest. While RF it is not widely adopted to evaluate parameter importance in deterministic hydrologic models, Spear et al. (2020) demonstrated that RF-derived feature importance can align with outcomes from the Regional Sensitivity Analysis method. Due to the relative constraints in our grouped parameter sampling, conventional sensitivity analysis methods were ineffective at producing meaningful information, leading us to opt for this machine learning approach. The RF model was trained using the Random Forest (Cutler & Wiener, 2022) and Caret R (Kuhn, 2008) packages, with 10-fold cross-validation to ensure robustness.

Building on our understanding of how urban adjustment and spatial resolution influence model performance, we conducted a deeper analysis to explore their impact on the practical application range. We selected the top 1% performing models from the urban-adjusted

scenarios (1 km vs. 90 m and Sim vs. FA) and compared performance across metrics and hydrologic signatures. Focusing on a watershed with stable model performance, we further investigated the internal runoff contributions, and decomposed hydrographs to visualize the runoff timing and contribution from EIA and natural mechanisms.

4.4. Results

4.4.1. Pre-Analysis of Water Balance in study watersheds

Water balance errors in the data driving the hydrologic model can significantly impact model performance and parameter sensitivity evaluation (Renard et al., 2010). Therefore, a pre-analysis of water balance was conducted using NLDAS precipitation (P), Noah-MP calculated actual evapotranspiration (AET), and USGS observed streamflow (Q).

This pre-analysis identified significant water balance errors in both study watersheds (Table 4-5). The San Diego watershed exhibited an error range of +13%, which is not severe given the highly variable annual precipitation driven by a series of short “atmospheric river” events and pronounced seasonality in streamflow, with prolonged low flow conditions potentially causing higher uncertainty in flow measurements (McMillan et al., 2012).

In contrast, the Fulton watershed showed significant errors far exceeding the typical range of data uncertainties in precipitation (combined 10-20%) and streamflow (2-19%) measurements (McMillan et al., 2012), with a combined error of +32%. This is despite analyzing over 10 water years and considering the minimal annual climatic variance and weak streamflow seasonality in the watershed.

Table 4-5. Average of annual water year water balance during the study period (WY 2014 - 2018)

Metric	San Diego (CA)	Fulton (GA)
P-AET-Q	+49mm	+428mm
(P-AET-Q)/P	+13%	+32%
Annual covariance: (P-AET-Q)/P	1.1	0.18
Annual covariance: Runoff Ratio	0.21	0.19

Further analysis revealed that the AET from Noah-MP in the Fulton watershed (368 mm) was significantly lower than regional historical estimates (600~700mm; Sanford & Selnick, 2013). Although urban areas in wetter climates may experience up to a 36% reduction in AET (Mazrooei et al., 2021), Fulton’s TIA (26%) was insufficient to cause such a large reduction in ET. We hypothesize that the Noah-MP parameter values for urban land use in the NWM configuration led to an underestimation of AET in any area classified as urban, regardless of the actual proportion of impervious surfaces. To address this issue, we made the following adjustment to obtain a more realistic AET value:

$$AET_{adj,urban,ij} = \lambda * AET_{non-urban\ mean} * (1 - TIA_{ij}) + AET_{urban,ij} * TIA_{ij} \quad (Eq.4-15)$$

Here, λ represents the empirical ratio between regional urban and non-urban ET, introduced to limit the adjusted AET maximum below the typical regional urban ET relationship. This adjustment reduced the water balance error in the Fulton watershed from +36% to +14% ($\lambda = 0.7$), reflecting an improvement in test model runs. The range was based on a regional approximation from Mazrooei et al. (2021), which also matched the aridity index estimate from Heidari et al. (2020). In contrast, the San Diego watershed showed only a 2% improvement in water balance error (+13% to +11%) following the AET adjustment, and this improvement was lost in FLEX-Topo test model runs, regardless of the value. The water-

limited nature of SD watershed was reproduced within the FLEX-Topo model, and water availability in the model limited the AET below AET forcing input.

Other potential factors—such as losing streams, local groundwater pumping, underprediction of low flow due to channel retention/obstruction/overgrowth, and rainwater harvesting—were considered but lacked supporting data. Rainfall uncertainties are often a major source of error in rainfall-runoff modeling, especially in smaller watersheds (Moulin et al., 2009). Therefore, we employed a simplified inverse modeling approach to adjust precipitation input, reducing overall model error (Bárdossy et al., 2022). Scaling NLDAS precipitation by a factor of 0.9 based on the water balance error reduced catchment water imbalance to 4% and 7% in Fulton and San Diego, respectively. More importantly, this rainfall adjustment improved model performance scores (NSE and log-NSE) in test runs, enabling more stable simulations.

4.4.2. EIA estimation and its spatial relationship with classified HRU

Figure 4-7 visualizes the relationship between TIA, Ksat, and EIA estimates from CN-EIA method. The spatial pattern of EIA was strongly influenced by TIA, but in the San Diego watershed, Ksat plays a significant role in differentiating the EIA outcomes. This suggests that consideration of soil hydraulic conductivity (Ksat) leads to more varied spatial patterns. In contrast, the Fulton watershed showed a strong negative correlation between TIA and Ksat, indicating that as impervious surfaces increase, soil hydraulic conductivity decreases. For instance, area with higher TIA (e.g., road network) showed very low Ksat. This relationship suggests that the CN-EIA method may need to be refined by incorporating the effects of urban development on local soil hydraulic conductivity which may be related to soil disturbance

near urban developments, potentially improving the accuracy of EIA estimates in areas where urbanization significantly alters soil properties.

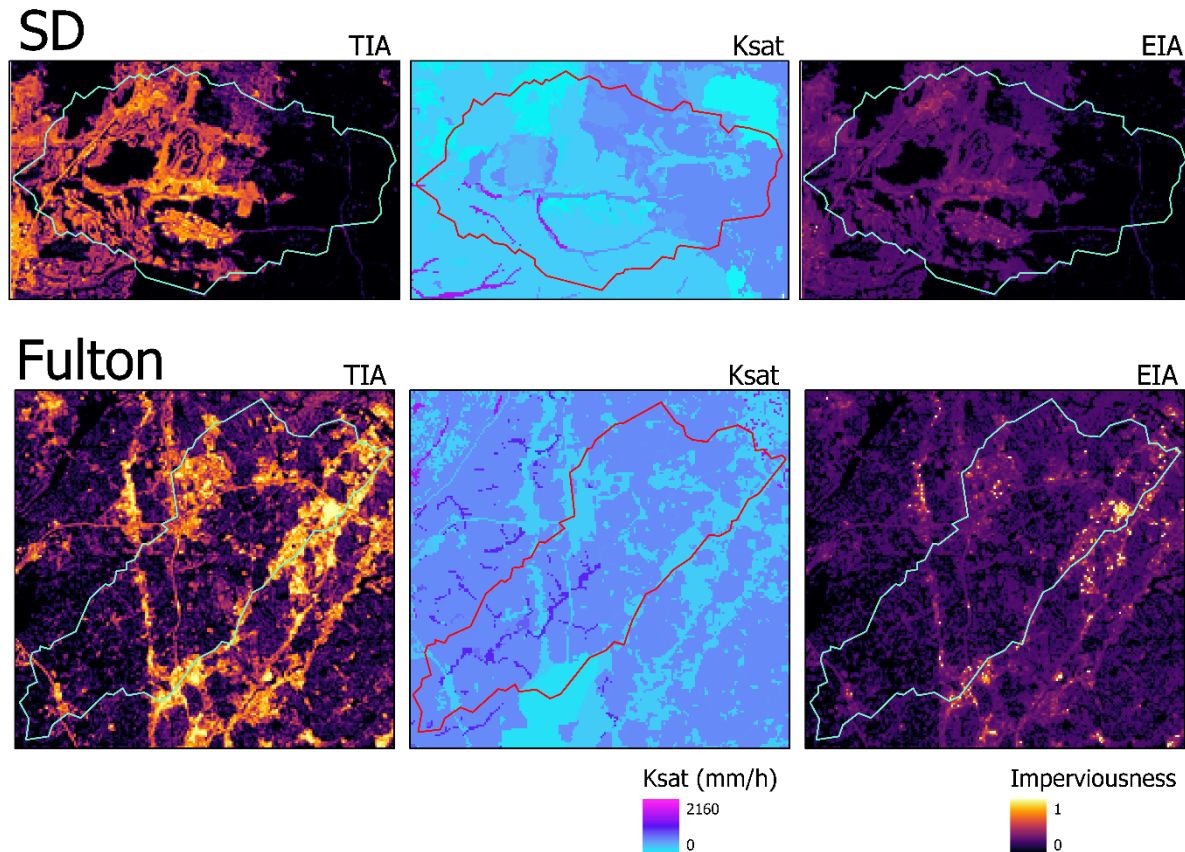


Figure 4-7. TIA, Ksat, and EIA in SD and Fulton watershed

The EIA estimation from the CN-EIA method, whether using the original Ebrahimian et al. (2018) approach or our modified method with Eq.4-13, was comparable to conventional simple empirical formulas when aggregated to the watershed scale, albeit with some positive biases. These empirical formulas are typically applicable only at the catchment scale and can produce widely varying estimates when TIA values fall outside the range for which they were developed. Therefore, while empirical formulas may be limited in scope, the CN-EIA method not only provides reliable local EIA estimates but also remains comparable at the watershed scale, making it a more versatile alternative.

Our modified CN-EIA method, incorporating Eq. 4-13, effectively addressed the spatial discontinuities observed in EIA estimation when using the original approach. Notably, in areas with medium to high imperviousness (TIA over 0.5) at the local grid cell scale, EIA estimates increased by up to 30% (equivalent to a 13-percentage point increase), depending on Ksat values. This adjustment smoothed out previously observed dips and spikes in spatial EIA. However, when these estimates were aggregated to the watershed scale, the impact was minimal, with both mean and median EIA showing less than a 1-percentage point difference (Table 4-6).

Table 4-6. Comparison of EIA estimation from empirical formulas' mean (compiled by Sultana et al., 2020), original and modified method of Ebrahimian et al. (2018).

Watershed	TIA	Empirical formulas (Sultana et al., 2020) Averaged	Original CN-EIA WS-Aggregated Mean; Median	Modified CN-EIA (Eq.4-13) WS-Aggregated Mean; Median
SD, CA	21.7%	8.1%	9.3%; 8.8%	9.9%; 8.8%
Fulton, GA	26.3%	11.7%	13%; 15.8%	13.7%; 14.9%

In the San Diego (SD) watershed, steep topography and large elevation changes result in hillslopes being the predominant HRU type. In contrast, upland is the most dominant HRU type in the Fulton watershed. Lowland areas make up only 8.9% of the SD watershed and 10.5% of the Fulton watershed (Table 4-7).

Table 4-7. HRU distribution in SD and Fulton study watersheds, and each proportion of TIA situated in each HRU to total watershed TIA

Watershed	Lowland (%); HRU-EIA; (HRU-TIA)	Hillslope (%); HRU-EIA; (HRU-TIA)	Upland (%); HRU-EIA; (HRU-TIA)
SD, CA	8.9%; 0.15; (0.35)	67.4%; 0.06; (0.11)	23.7%; 0.18; (0.46)
Fulton, GA	10.5%; 0.11; (0.21)	30.2%; 0.09; (0.13)	59.3%; 0.16; (0.33)

Distinct spatial arrangements between impervious land cover and HRU types were observed in each watershed. In both SD and Fulton, upland generally had the highest impervious area fraction. In the Fulton watershed, lower-density urban developments are more frequently situated in upland areas, with limited urban development in lowland regions. However, in SD, a significant amount of urban development, including high-density commercial land use, is situated in lowland areas and upland having generally having residential developments (Figure 4-8).

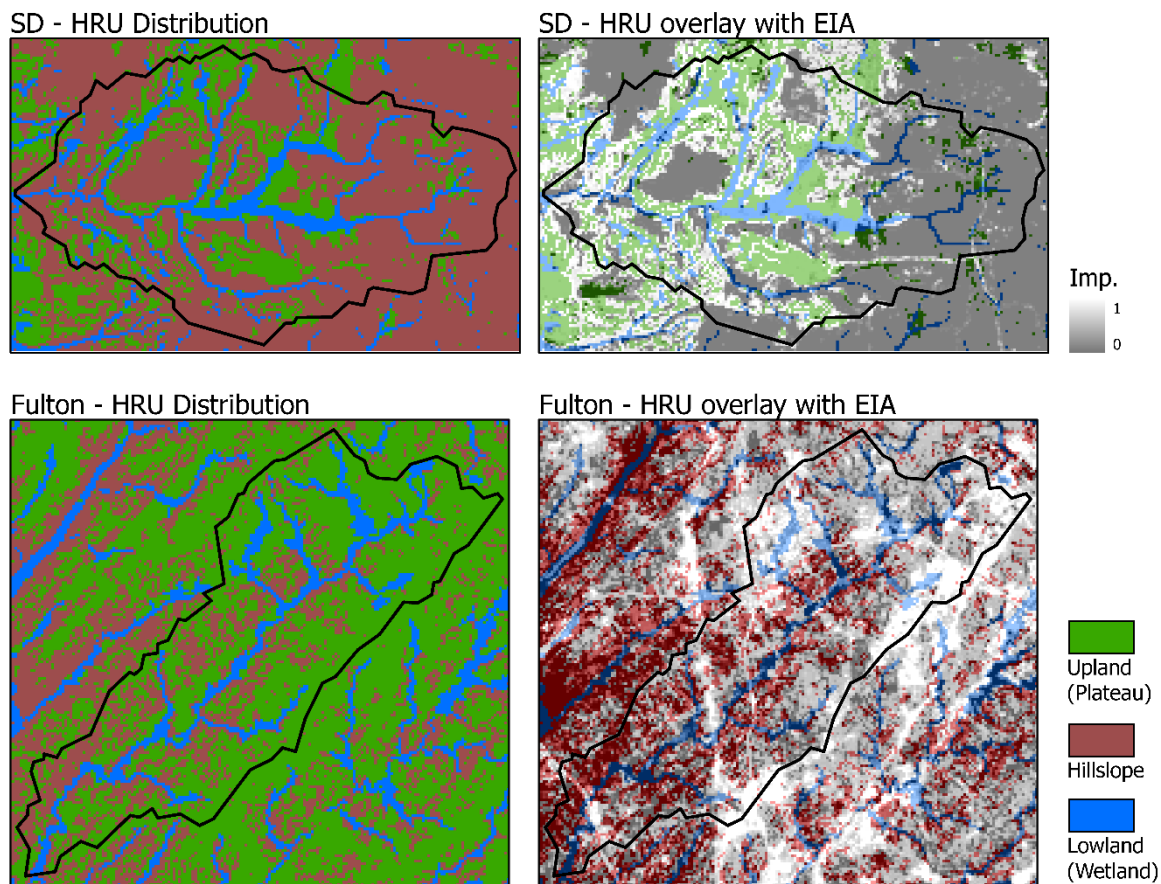


Figure 4-8. Lowland, Hillslope, and Upland HRU distribution and its overlay with EIA in 90m resolution. EIA is displayed with dynamical range adjustment for easy indication.

These differences in HRU-imperviousness arrangements are likely outcomes of climate, hydrology, landscape, and urbanscape co-evolution, and are expected to result in varying model behavior in two study watersheds. For example, the concentration of impervious surfaces in Lowland areas of SD is high. However, the majority is not connected, and this can lead to complex behavior in saturation-excess overland flow (SOF) that is sensitive to soil moisture conditions and quicker to contribute to runoff. In contrast, in Fulton, where impervious surfaces are more prevalent in Upland areas, the impact is simpler, splitting rainfall into immediate impervious runoff and deep percolation.

4.4.3. Comparative Analysis: General Insight

The comparative analysis of models demonstrated that both urban-adjusted versions (Simple Impervious and Full Adjustment) significantly outperform the original FLEX-Topo model across all metrics in both watersheds (Table 4-8). Hydrologic signatures also aligned more closely with observations. Improvements in NSE, RBI, and BFI were especially notable, with some improvement in PBIAS. However, while the Fulton watershed showed large increases in logNSE, the SD watershed did not, indicating difficulties in simulating low flow conditions. When comparing the 1 km Simple Impervious (Sim) and Full Adjustment (FA) models, there was weak evidence that additional urban adjustment improved overall model performance (Table 4-8). Although there was a minor improvement in logNSE, other metrics often showed a decline in accuracy.

When analyzing the impact of spatial resolution (1 km vs. 90 m) on model performance, the finer 90 m resolution generally resulted in a significant decline in performance across most metrics for both Sim and FA models, regardless of the watershed. The performance decline was particularly pronounced in the SD watershed, where logNSE, PBIAS, and RBI showed

significant degradation. This instability suggests that the model is currently unsuitable for fully representing hydrological processes in the SD watershed.

Table 4-8. Comparison of model performance metric and hydrologic signature average in top 10% performing (NSE) parameter sets for original FLEX-Topo, Sim, and FA model.

	Watershed	Resolution	NSE	logNSE	PBIAS	RBI	BFI
USGS observed	SD					0.216	0.287
	Fulton					0.143	0.375
Original FLEX-Topo	SD	1km	0.38	-1.89	62.08	0.06	0.57
	Fulton	1km	0.42	-0.4	69.77	0.06	0.64
Sim	SD	1km	0.51	-0.07	25.24	0.18	0.38
		90m	0.41	-1.62	187.68	0.08	0.41
	Fulton	1km	0.63	0.6	32.76	0.14	0.35
		90m	0.54	0.61	36.64	0.15	0.34
FA	SD	1km	0.52	0.03	21.7	0.2	0.34
		90m	0.41	-1.48	207.09	0.08	0.37
	Fulton	1km	0.63	0.69	27.08	0.14	0.34
		90m	0.53	0.65	37.38	0.13	0.32

The comparison between Sim and FA models at 90 m resolution showed a similar trend to the 1 km cases: a minor improvement in logNSE but overall degradation in other metrics, indicating no clear benefit from additional urban adjustment. Therefore, the individual effects of urban adjustment level and model resolution remained consistent when comparing the 1 km Sim and 90 m FA models.

Given the small differences between Sim and FA models, we selected the top-10% performing parameter sets (NSE) for both models and compared the NSE distribution under identical parameter inputs. As shown in Figure 4-9, the Sim model consistently produced higher NSE values than the FA model (positive mean value indicates NSE from Sim is higher).

While the standard deviation was smaller in the 90 m resolution model, this is likely due to its overall lower performance. Notably, NSE values from Sim and FA models began to converge as they approached the highest scores.

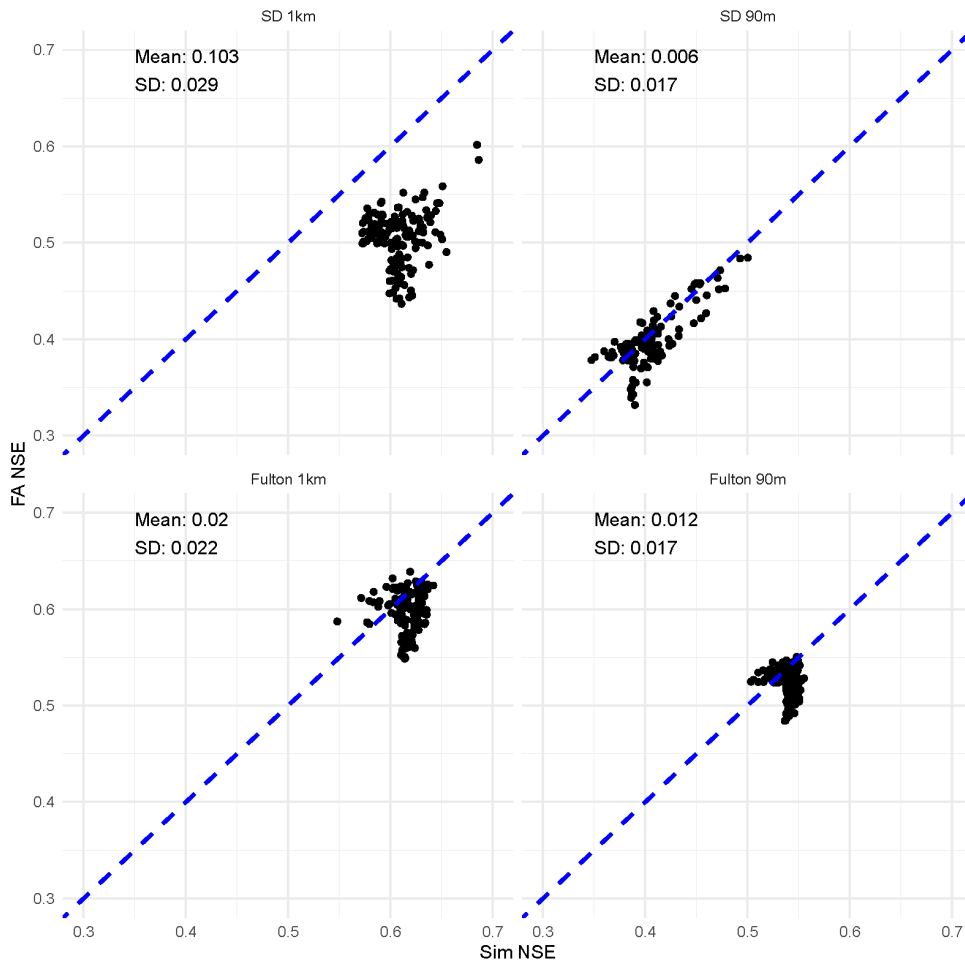


Figure 4-9. Comparison of NSE performance in Sim and FA under identical parameter set inputs.

4.4.4. Parameter Sensitivity

Urban adjustment improved model performance, but Sim and FA models showed increasingly similar NSE values for identical parameter inputs as they approached the highest performing region. This suggests that the additional urban adjustments introduced in the FA model have a limited impact on model behavior, especially for higher-performing parameter sets. To verify this, we visually inspected parameter sensitivity using scatter plots.

Figure 4-10 revealed two main findings: 1) Urban adjustment, by correcting hydrologic process representation in the study watersheds, β became the most influential parameter, while the model's sensitivity to Kf parameters decreased. 2) The Sim and FA models exhibited particularly similar sensitivity to parameters in the higher-performing ranges.

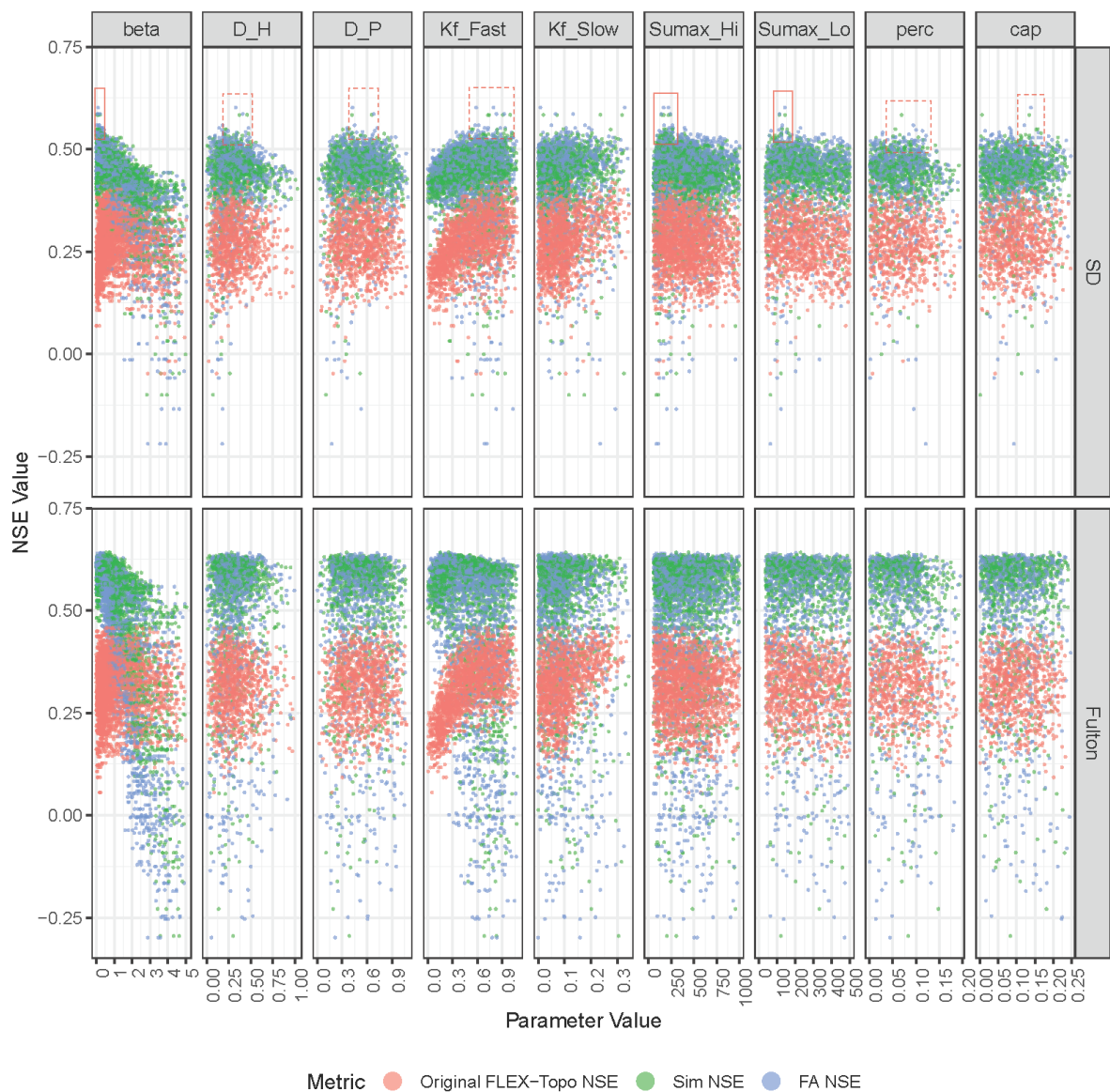


Figure 4-10. Relationship between parameter value and NSE performance in 1km models. Scatter points are stacked together in certain parameter groups for legibility. Kf_Fast (*Kf* for overland flows), Kf_Slow (*Kf* for subsurface flows), and Sumax_Hi (Hillslope and Upland).

Steep performance spikes observed in the SD watershed (Figure 4-10, red boxes) suggest a strong preference for a narrow range of parameter values. The SD watershed appears to require very specific parameter combinations to achieve reasonable performance across all metrics. This preference for very small Beta, relatively small Sumax indicates that SD watershed strongly favors “fill-and-spill” type of runoff response, which also closely associate with deep groundwater runoff. This may necessitate the calibration of Ks parameter rather than simply deriving it from observation data. It is possible that the sample size, parameter range, or parameter constraints were not optimal for capturing the full spectrum of favorable parameter combinations. However, it is also possible that FLEX-Topo structure lacks certain process representations that are critical for reproducing the runoff pattern in SD watershed, because such specific parameter requirements might indicate that the parameters are compensating for missing processes.

Figure 4-11 shows the parameter importance analyzed across different model configurations for the SD and Fulton watersheds, using the Random Forest algorithm on the top 10% performing parameter sets (based on NSE). While the major parameter groups consistently showed moderately high importance, Kf, D, and Sumax parameters varied significantly depending on the watershed, HRU, and model configuration. Surprisingly, Sumax often recorded very low importance, despite its critical role in the model structure.

β from Lowland HRUs was the only parameter that showed relatively high importance in both watersheds, exhibiting a similar response to changes in urban adjustment level and spatial resolution. Although not consistent, a slight pattern emerged: the importance of storage-related parameters (Sumax and β) generally decreased as spatial resolution became finer,

while the importance of parameters governing runoff from Hillslope HRU (Kf and D) increased.

Overall, the Random Forest analysis did not reveal strong patterns in parameter importance. Despite attempts to link these differences to the results of the urban scape analysis in the SD and Fulton watersheds, the effort was largely unsuccessful.

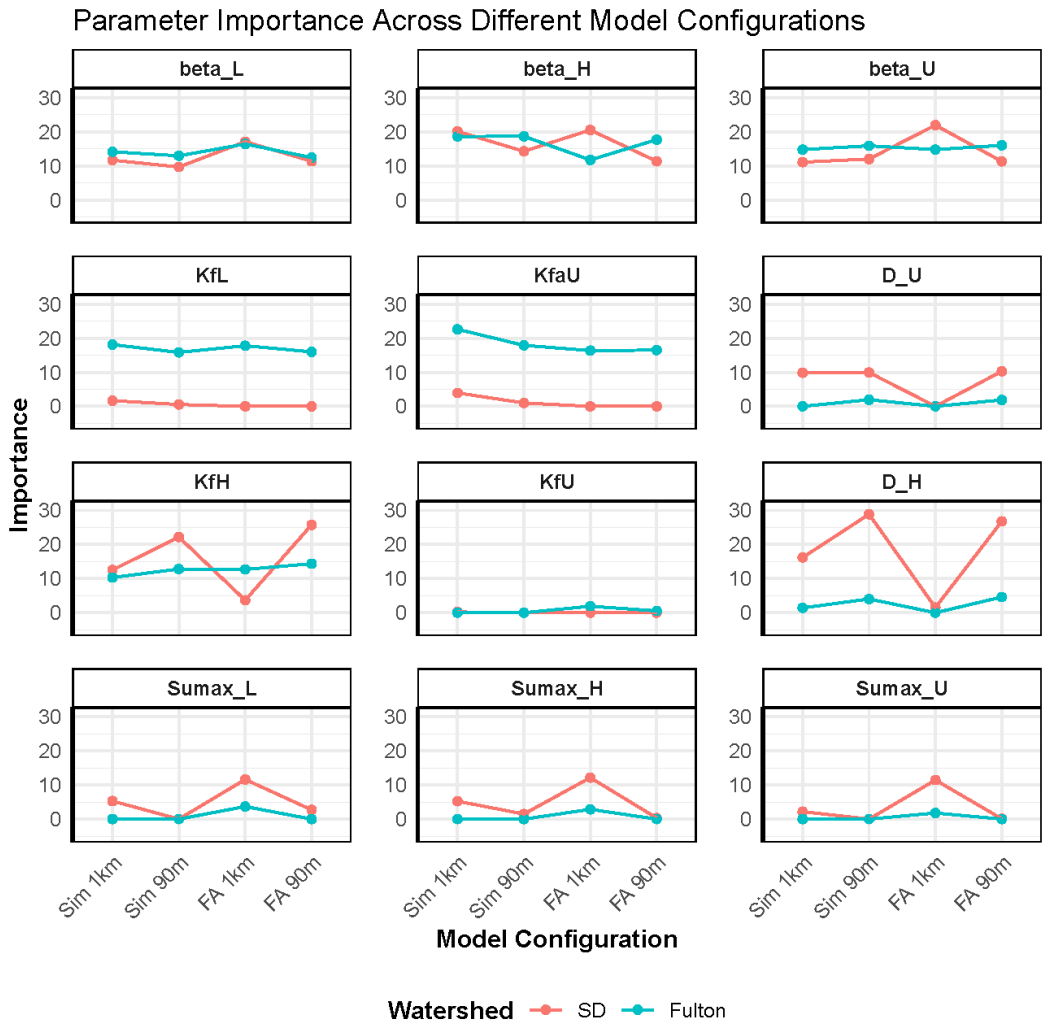


Figure 4-11. Parameter importance estimated by Random Forest algorithm (top 10% performing models)

4.4.5. Extended Comparative Analysis

The initial comparative analysis examined top 10% parameter sets to assess the impact of urban adjustment levels and spatial resolution on model outcomes. However, our calibration approach was not comprehensive enough that this subset still included poorly performing sets, which can potentially skew the "average" performance. To address this, we now focus on the top 1% of best-performing models, allowing us to concentrate on the most relevant portion of the parameter space, where differences between urban adjustment methods are more likely to be pronounced and have practical significance.

When comparing the top 1% models, the same general trends observed in the top 10% subsets persisted (Figure 4-12). The 1 km models consistently outperformed the 90 m models, and the Sim generally outperformed the FA configuration. However, the performance gap between different urban adjustment levels became nearly negligible as previously observed in Figure 4-7, and the degradation from finer spatial resolutions was less pronounced within the top-performing parameter sets.

While the performance gap became less significant, distinct differences emerged between the SD and Fulton watersheds. In the SD watershed, the finer 90 m resolution models exhibited performance declines across most of metrics and signature (except logNSE), further aggravating the existing errors. In contrast, the Fulton watershed demonstrated more stable performance across both resolutions, with higher urban adjustment levels often improving model performance, particularly in logNSE and Bias. Interestingly, the decline in performance from a finer resolution was more moderate in Fulton, with the difference in absolute error for RBI and BFI being less than 0.05 and 0.08, respectively. The high-performing FA model in

Fulton consistently outperformed the Sim model in logNSE and even in NSE within the 1 km resolution.

In summary, the analysis of the top 1% performing models underscores the complexity of interactions between urban adjustment levels, spatial resolution, and watershed characteristics. While the overall trends are consistent with the broader analysis, it revealed that the effects of urban adjustment and spatial resolution are highly dependent on specific watershed conditions.

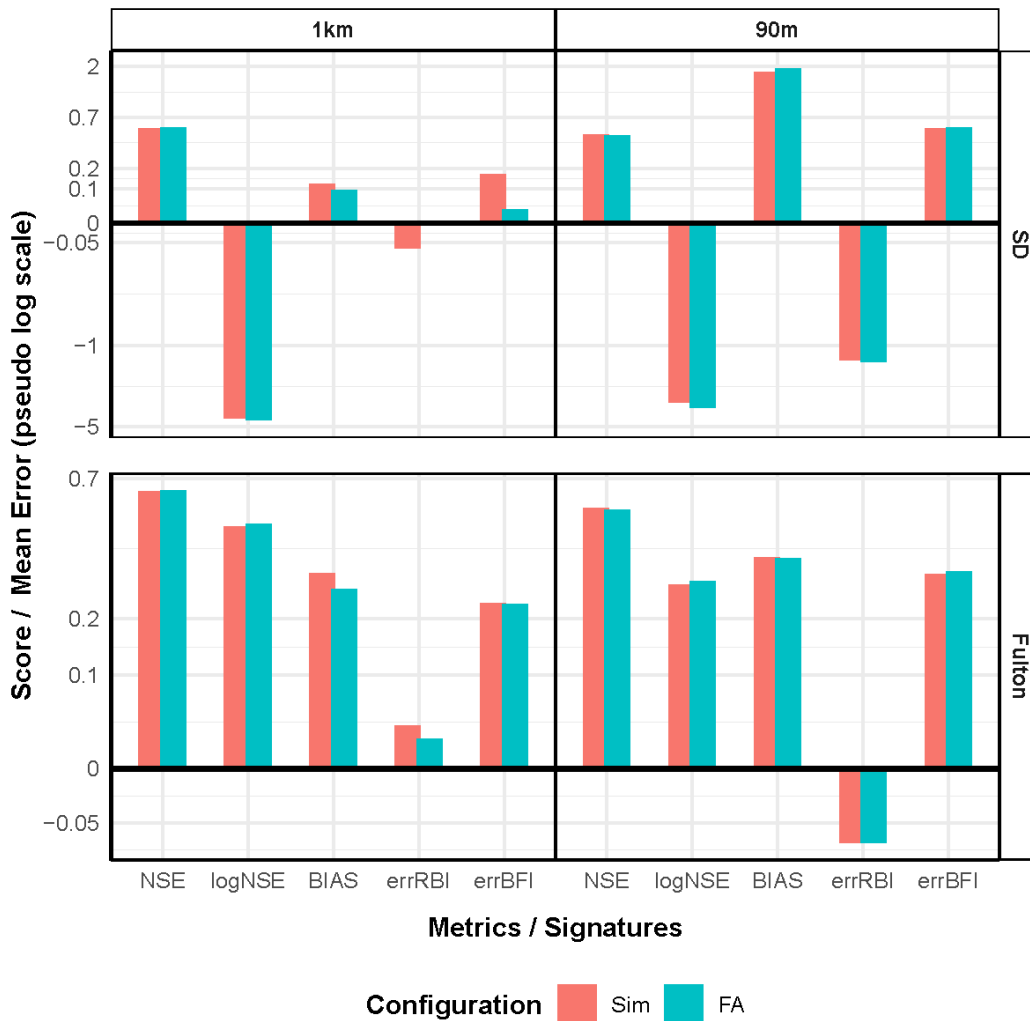


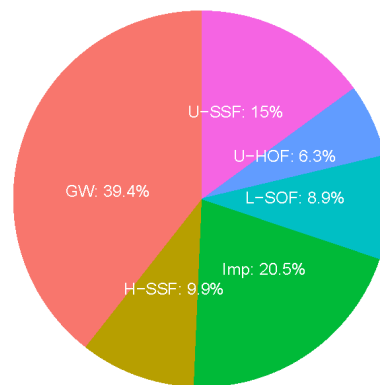
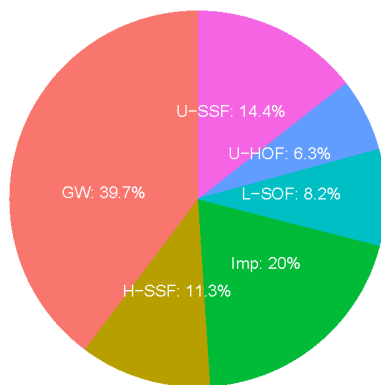
Figure 4-12. Average performance metric scores and hydrologic signature values from top 1% performing Sim and FA models

Due to instability in SD watershed’s performance, we proceeded only with Fulton watershed to analyze runoff contributions and hydrograph. Figure 4-13 showed that, despite differences in model configurations, runoff contributions from various HRUs across the ensemble generally displayed only minor changes in Fulton watershed. The FA model indicates increased contributions from groundwater and Hillslope SSF, while runoff from Upland, particularly SSF and HOF, has decreased.

Runoff contribution

Sim 1km

Sim 90m



FA 1km

FA 90m

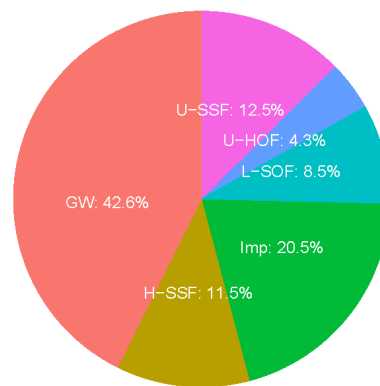
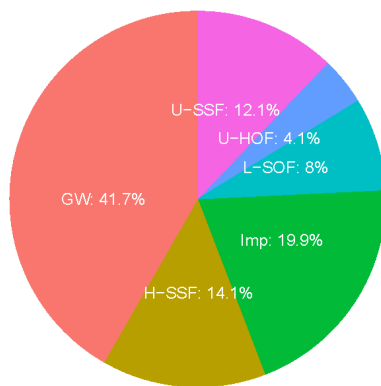


Figure 4-13. Runoff contribution from HRUs. GW: deep groundwater runoff, U-SSF & U-HOF: Upland preferential subsurface flow and Hortonian overland flow, L-SOF: Lowland Saturation excess overland flow, H-SSF: Hillslope preferential subsurface flow, Imp: Direct runoff from EIA.

Given that Upland comprises 59.3% of the watershed area, it is clear further urban adjustment can result in altered runoff contribution dynamics inside the model. The change in spatial resolution primarily impacted SSF from the Hillslope, which typically exhibits the lowest imperviousness. It can be suspected that spatial aggregation to a 1km resolution inaccurately elevated the EIA assigned to the Hillslope, leading to potential misrepresentation of the hydrologic response.

Hydrograph: Total, EIA, and Natural (Dec 29, 2016 - Jan 08, 2017)

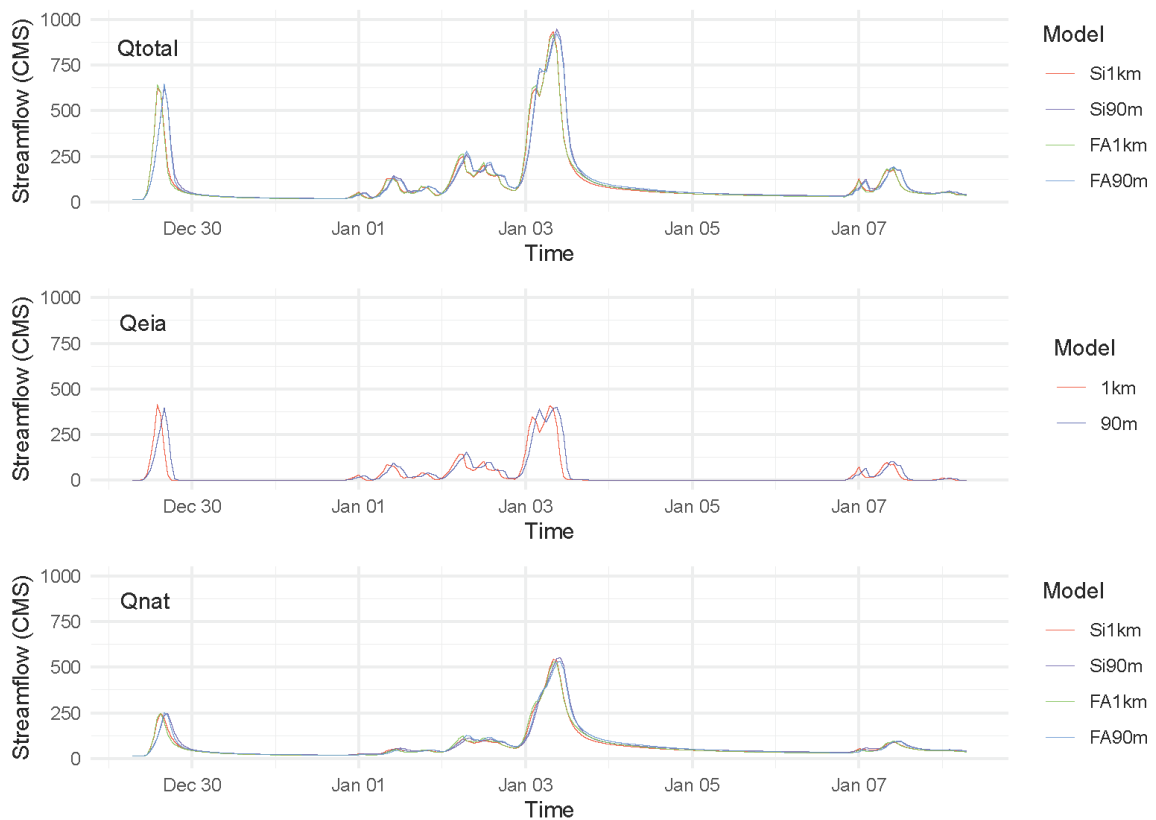


Figure 4-14. Decomposed Hydrograph from best performing 1% Sim and FA model ensemble in Fulton.

The hydrograph (Figure 4-14) demonstrates that the model resolution significantly impacts the timing of runoff events, with higher resolution models showing delayed response compared to 1km resolution models. This difference in timing is generally constant, but a bit more pronounced for the initial peak, and such an effect mostly comes from runoff from EIA.

The 1km resolution models also resulted in quicker peaks in non-impervious runoff, indicating that some parameters related to delay or routing is likely not scale independent. In contrast, the variation in urban adjustment levels appears to have almost zero effect on peak timing, but shows a small impact on runoff volume, rising and recession limbs in the natural runoff components.

4.5. Discussion

The incorporation of urban adjustment scenarios in our FLEX-Topo model yielded several unexpected outcomes, both aligning with and challenging conventional assumptions in urban hydrologic modeling. These findings provide insights into the complexities of representing urban impacts in watershed models and highlight the need for careful consideration when increasing model complexity.

4.5.1. EIA, Urban Adjustment, and Model Performance/Behavior

The inclusion of urban adjustment scenarios, which account for rainfall partitioning from effective impervious areas (EIA), significantly outperformed the original FLEX-Topo configuration. Our method to derive spatially distributed EIA, based on Ebrahimian et al. (2018), utilizes both impervious land cover and saturated hydraulic conductivity data. Although the original method was not designed for grid-cell-scale application, our findings demonstrated its ability to provide robust foundation directly relevant to rainfall partitioning in urban hydrologic modeling. These scenarios achieved statistical scores that were unattainable through parameter calibration alone within the original model.

This improvement is expected, as accounting for imperviousness is fundamental in modeling urban hydrology (Ebrahimian et al., 2016), which was not considered in the original

FLEX-Topo design. Incorporating impervious runoff improved peak flow timing and magnitude during regular events, which was reflected in better NSE scores. Models in Fulton showed stable performance, while those in the SD watershed underperformed and appeared to require very specific range of parameter ranges to achieve higher performance, indicating the need for extensive calibration depending on watershed characteristics. Although the performance differences among varying levels of urban adjustment were relatively small, they offer important insights.

Interestingly, the Full Adjustment (FA) model does not consistently outperform the Simple Impervious (Sim) configuration. In fact, Sim could outperformed FA in some cases, despite FA configuration being explicitly designed to represent diverse subsurface hydrologic impacts from imperviousness and urbanization. The smaller gap between model performance between FA and Sim among parameter sets that produce good outcomes, along with FA's superior performance in the top 1%, suggests that while our FA approach may have altered the models' sensitivity to parameters, it did not diminish their overall influence. This is likely because, although impervious surfaces are well-distributed across the watershed, areas with high impervious levels are limited. As a result, the watershed-scale base parameter values have a greater influence than the changes introduced by the FA model to the local parameterization of subsurface processes based on the spatial variability of urbanization levels. However, incorporating subsurface urban adjustment (FA) appeared to alter runoff contributions from certain HRUs, even when models used nearly identical parameter sets. While hydrographs were generally almost indistinguishable, minor differences in rising limb and flow recession were observed during some of prolonged storm events, where slower natural runoff contributions are expected to be more significant.

While urban adjustment was designed to improve realism by incorporating subsurface complexity and spatial heterogeneity, its advantage was limited. Increasing model complexity can lead to prediction uncertainty, but physically constraining the model structure can limit prediction uncertainty even with more parameters (Schoups et al., 2008). Similarly, knowledge-based model constraints can mitigate model complexity and improve outcomes (Hrachowitz et al., 2014). However, while the study viewed the FA configuration as a hypothetically sound constraint for FLEX-Topo, it ultimately lacked the robustness needed to deliver practical benefits.

These results indicate that theoretically formulating physical characteristics of urban impacts and implementing them into existing models requires extra caution, even when the method simply scales the corresponding parameters without altering the model structure. This aligns with findings that theoretically interchangeable components may not be numerically compatible when they are affecting other model structures and internal states (D.-H. Kim et al., 2021).

In summary, our results highlight the significant performance improvements achieved through urban adjustment scenarios when utilizing Effective Impervious Area (EIA) for rainfall partitioning. However, the limited benefits of full adjustment scenarios underscore the challenges of applying concept-based approaches to consider spatially variable urban hydrologic processes (Salvadore et al., 2015). These insights emphasize the importance of using only the most reliable and directly relevant descriptors to inform and adjust models for urban applications.

4.5.2. Spatial resolution and Model Performance/Behavior

The 1 km model consistently outperformed the 90 m model in general accuracy, even though the 90 m model is designed to capture interactions and variability at a finer scale. While it is known that finer spatial resolution does not necessarily guarantee better performance (Aerts et al., 2022), the extent of advantage in the coarser model was unexpected. The loss of spatial information about the arrangement between HRUs and impervious surfaces adds another layer of data uncertainty in the 1km model. FLEX-Topo employs a fully distributed model state with lumped HRU parameterization at the watershed. This semi-distributed structure, combined with additional spatial uncertainty, can intensify the challenge of identifying optimal parameters (de Lavenne et al., 2016).

Despite the significant decline in streamflow prediction performance at the 90m resolution, the models with different resolution models showed only minor differences in runoff volume and runoff contribution from each HRU, with the major differences observed in runoff timing. This supports findings that resolution is more relevant for distribution function, such as routing, but may not be as critical as long as a land cover fraction, which governs the aggregation of vertical hydrologic fluxes, is well-represented (Bormann et al., 2009). Although the FA approach introduces additional input uncertainty due to misalignments between HRU types and imperviousness data, which affect subsurface parameter scaling, both models showed similar responses to changes in resolution. This suggests that the loss of detailed spatial information, such as the arrangement of different spatial inputs, may have a limited impact on hydrological simulations. This finding is consistent with the results in Chapter 3, which demonstrated that accurately representing the area of each land cover class in a watershed is more important than retaining spatial patterns in distributed physically-based

models WRF-Hydro (D.-H. Kim et al., 2024). While similar outcomes were observed across distributed models with varying structures, it is still important to consider that different representations of urban areas and parameterizations may exhibit different sensitivities to changes in resolution.

The performance difference was primarily caused by a consistent gap in runoff timing between the two resolutions, suggesting that some parameters related to runoff timing may not be scale independent. This finding is comparable to S. Kim et al. (2021), who demonstrated that using finer resolution for land surface model (aggregation function) in WRF-Hydro showed marginal improvement, but using finer routing grid with parameters calibrated for coarser resolution models resulted in significantly worse error. While resolution differences affected some parameter importance, it did not have a significant impact on the outcomes of better performing models. This indicates that parameters associated with the aggregation of vertical fluxes may be transferable across different resolution models (Samaniego et al., 2010) in our study, whereas parameter related to routing functions are not.

These findings suggest that the challenges associated with spatial input, resolution, parameterization, and performance are still not fully understood in hydrological modeling. Analyzing the intrinsic spatial scale and resolution of model processes (Saksena et al., 2021) could be a valuable and efficient strategy, even for urban implementation of semi-distributed process-based conceptual models and their calibration.

4.5.3. Limitations

This study has several limitations that should be acknowledged. First, the selected study watersheds may represent cases where urban development did not significantly alter underlying subsurface processes. This potential lack of pronounced urban impact might limit

the applicability of the findings to more heavily urbanized watersheds. However, even limited urban impact showed improvements in model performance, indicating the effectiveness of the urban adjustment scenarios.

Second, both study watersheds exhibited imbalances in NLDAS precipitation, Noah-MP calculated actual evapotranspiration (AET) and observed streamflow. These discrepancies required adjustments to precipitation and AET, just to achieve stable model simulations, which may have introduced additional uncertainties.

Third, the parameter-scaling equations developed to represent urban impacts on subsurface processes (see “4.3.4. Conceptualizing the Urban Impact”) were initially optimized in a fully lumped model setup and designed to keep hydrological alterations within a reasonable range based on empirical statistics. However, when applied in distributed models at 1km and 90m resolutions, the influence of these equations diminished significantly, indicating a smoothing effect across spatial scales. This raises concerns that these equations may be overly conservative, potentially limiting their effectiveness in distributed applications.

Lastly, our analysis assumed limited impact from dynamic human water use and imports on streamflow conditions and used “black-box” approach, based on municipal water usage datasets (Dieter et al., 2018; Luukkonen et al., 2023) and water balance analysis. Therefore, it was anticipated that the exploration of parameter spaces could manage these factors without significant uncertainty. However, poor logNSE in the SD watershed may indicate that our approach to identifying the hydrological influence of human water use was too simplistic. Although these challenges may limit the generalizability of the findings and applicability of the models, the study still provides valuable insights into implementing urban aspects in existing hydrologic models.

4.6. Conclusions

This study explored the implementation of urbanization impacts on natural runoff mechanisms within an existing landscape-oriented hydrologic model. The novelty lies in the attempt to incorporate anthropogenic impacts on hydrologic processes that vary across hydrologic landscapes and their influence on watershed-scale model behavior.

By combining publicly available land data with established theories, the study aimed to enhance purpose-specific modeling without significant increases in model uncertainty or dimensionality. The urban adjustment significantly improved model performance, achieving statistical scores unattainable through parameter calibration alone in the original model. This underscores the importance of considering imperviousness in urban hydrology modeling.

Two unexpected outcomes emerged:

- 1) **Urban Adjustment Level:** The EIA rainfall partitioning proved far more crucial than implementing other spatially variable urban impacts. The Sim (EIA-only) configuration often outperformed full adjustment scenarios, suggesting that benefits from additional complexity or constraints without physically relevant evidence can be easily offset with increased unnecessary uncertainties.
- 2) **Spatial Resolution:** Coarser lumped spatial resolution (1km) generally outperformed finer resolution (90m), even at the cost of losing information about spatial arrangements between hydrologic landscapes (HRU) and impervious surfaces. This indicates that accurately capturing the most relevant spatial aspect for hydrological flux calculation is often more critical than retaining full detailed information at a finer scale, even in urban hydrologic modeling.

Despite some limitations, this approach demonstrates significant potential for practical management purposes in a wetter Fulton watershed, and highlights the potential of using a combination of models in urban hydrological studies. While the urban adjustment of the FLEX-Topo cannot fully replace specialized models, it offers a complementary perspective by illustrating how different landscape units within a watershed respond to urbanization. This coexistence of models allows for a more robust analysis, where urban adjusted FLEX-Topo provides insights into causal relationships and broader landscape impacts, while specialized models focus on detailed, site-specific planning. Together, they can enable a more comprehensive evaluation of the potential impacts of urbanization and land-use and land-cover (LULC) changes across various spatial scales in urban areas.

The unexpected outcomes highlight the need for further research to bridge the gap between local-scale urban hydrological processes and watershed-scale behaviors in modeling. It emphasizes the importance of balancing model complexity with practical applicability in water resource management and urban planning. As urban areas continue to expand and climate patterns shift, developing robust, adaptable models becomes increasingly crucial.

4.7. References

- Aerts, J. P. M., Hut, R. W., van de Giesen, N. C., Drost, N., van Verseveld, W. J., Weerts, A. H., & Hazenberg, P. (2022). Large-sample assessment of varying spatial resolution on the streamflow estimates of the wflow_sbm hydrological model. *Hydrology and Earth System Sciences*, 26(16), 4407–4430. <https://doi.org/10.5194/hess-26-4407-2022>
- Baker, D. B., Richards, R. P., Loftus, T. T., & Kramer, J. W. (2004). A New Flashiness Index: Characteristics and Applications to Midwestern Rivers and Streams I. *JAWRA Journal of the American Water Resources Association*, 40(2), 503–522. <https://doi.org/10.1111/j.1752-1688.2004.tb01046.x>
- Bárdossy, A., Kilsby, C., Birkinshaw, S., Wang, N., & Anwar, F. (2022). Is Precipitation Responsible for the Most Hydrological Model Uncertainty? *Frontiers in Water*, 4. <https://doi.org/10.3389/frwa.2022.836554>

- Becker, A., & Braun, P. (1999). Disaggregation, aggregation and spatial scaling in hydrological modelling. *Journal of Hydrology*, 217(3), 239–252. [https://doi.org/10.1016/S0022-1694\(98\)00291-1](https://doi.org/10.1016/S0022-1694(98)00291-1)
- Bond, N. (2022, June 1). hydrostats: Hydrologic Indices for Daily Time Series Data (Version 0.2.9). Retrieved from <https://cran.r-project.org/web/packages/hydrostats/index.html>
- Bormann, H., Breuer, L., Gräff, T., Huisman, J. A., & Croke, B. (2009). Assessing the impact of land use change on hydrology by ensemble modelling (LUCHEM) IV: Model sensitivity to data aggregation and spatial (re-)distribution. *Advances in Water Resources*, 32(2), 171–192. <https://doi.org/10.1016/j.advwatres.2008.01.002>
- Boyd, M. J., Bufill, M. C., & Knee, R. M. (1993). Pervious and impervious runoff in urban catchments. *Hydrological Sciences Journal*, 38(6), 463–478. <https://doi.org/10.1080/02626669309492699>
- Breiman, L. (2001). Random Forests. *Machine Learning*, 45(1), 5–32. <https://doi.org/10.1023/A:1010933404324>
- Cutler, F. original by L. B. and A., & Wiener, R. port by A. L. and M. (2022, May 23). randomForest: Breiman and Cutler’s Random Forests for Classification and Regression (Version 4.7-1.1). Retrieved from <https://cran.r-project.org/web/packages/randomForest/index.html>
- Dieter, C. A., Maupin, M. A., Caldwell, R. R., Harris, M. A., Ivahnenko, T. I., Lovelace, J. K., et al. (2018). Estimated use of water in the United States in 2015 (No. 1441). Circular. U.S. Geological Survey. <https://doi.org/10.3133/cir1441>
- Dunne, T., & Leopold, L. B. (Luna B. (1978). Water in environmental planning, 818.
- Ebrahimian, A., Wilson, B. N., & Gulliver, J. S. (2016). Improved methods to estimate the effective impervious area in urban catchments using rainfall-runoff data. *Journal of Hydrology*, 536, 109–118. <https://doi.org/10.1016/J.JHYDROL.2016.02.023>
- Ebrahimian, A., Gulliver, J. S., & Wilson, B. N. (2018). Estimating effective impervious area in urban watersheds using land cover, soil character and asymptotic curve number. *Hydrological Sciences Journal*, 63(4), 513–526. <https://doi.org/10.1080/02626667.2018.1440562>
- Eggimann, S., Mutzner, L., Wani, O., Schneider, M. Y., Spuhler, D., Moy de Vitry, M., et al. (2017). The Potential of Knowing More: A Review of Data-Driven Urban Water Management. *Environmental Science & Technology*, 51(5), 2538–2553. <https://doi.org/10.1021/acs.est.6b04267>
- Ekka, A., Keshav, S., Pande, S., van der Zaag, P., & Jiang, Y. (2022). Dam-induced hydrological alterations in the upper Cauvery river basin, India. *Journal of Hydrology: Regional Studies*, 44, 101231. <https://doi.org/10.1016/j.ejrh.2022.101231>
- Epps, T. H., & Hathaway, J. M. (2019). Using spatially-identified effective impervious area to target green infrastructure retrofits: A modeling study in Knoxville, TN. *Journal of Hydrology*, 575, 442–453. <https://doi.org/10.1016/J.JHYDROL.2019.05.062>
- Euser, T., Hrachowitz, M., Winsemius, H. C., & Savenije, H. H. G. (2015). The effect of forcing and landscape distribution on performance and consistency of model structures. *Hydrological Processes*, 29(17), 3727–3743. <https://doi.org/10.1002/hyp.10445>

- Fletcher, T. D., Andrieu, H., & Hamel, P. (2013). Understanding, management and modelling of urban hydrology and its consequences for receiving waters: A state of the art. *Advances in Water Resources*, 51, 261–279. <https://doi.org/10.1016/j.advwatres.2012.09.001>
- Gao, H., Hrachowitz, M., Fenicia, F., Gharari, S., & Savenije, H. H. G. (2014). Testing the realism of a topography-driven model (FLEX-Topo) in the nested catchments of the Upper Heihe, China. *Hydrol. Earth Syst. Sci*, 18, 1895–1915. <https://doi.org/10.5194/hess-18-1895-2014>
- Gharari, S., Hrachowitz, M., Fenicia, F., Gao, H., & Savenije, H. H. G. (2014). Using expert knowledge to increase realism in environmental system models can dramatically reduce the need for calibration. *Hydrology and Earth System Sciences*, 18(12), 4839–4859. <https://doi.org/10.5194/hess-18-4839-2014>
- Heidari, H., Arabi, M., Warziniack, T., & Kao, S.-C. (2020). Assessing Shifts in Regional Hydroclimatic Conditions of U.S. River Basins in Response to Climate Change over the 21st Century. *Earth's Future*, 8(10), e2020EF001657. <https://doi.org/10.1029/2020EF001657>
- Hrachowitz, M., Fovet, O., Ruiz, L., Euser, T., Gharari, S., Nijzink, R., et al. (2014). Process consistency in models: The importance of system signatures, expert knowledge, and process complexity. *Water Resources Research*, 50(9), 7445–7469. <https://doi.org/10.1002/2014WR015484>
- Johnson, S. L., & Sayre, D. M. (1973). Effects of Urbanization on Floods in the Houston, Texas Metropolitan Area. <https://doi.org/10.3133/wri733>
- Kaushal, S., McDowell, W., Wollheim, W., Johnson, T., Mayer, P., Belt, K., & Pennino, M. (2015). Urban Evolution: The Role of Water. *Water*, 7(12), 4063–4087. <https://doi.org/10.3390/w7084063>
- Kim, D.-H., Naliaka, A., Zhu, Z., Ogden, F. L., & McMillan, H. K. (2021). Experimental Coupling of TOPMODEL with the National Water Model: Effects of Coupling Interface Complexity on Model Performance. *Journal of the American Water Resources Association*. <https://doi.org/10.1111/1752-1688.12953>
- Kim, D.-H., Johnson, J. M., Clarke, K. C., & McMillan, H. K. (2024). Untangling the impacts of land cover representation and resampling in distributed hydrological model predictions. *Environmental Modelling & Software*, 172, 105893. <https://doi.org/10.1016/j.envsoft.2023.105893>
- Kim, S., Shen, H., Noh, S., Seo, D. J., Welles, E., Pelgrim, E., et al. (2021). High-resolution modeling and prediction of urban floods using WRF-Hydro and data assimilation. *Journal of Hydrology*, 598, 126236. <https://doi.org/10.1016/J.JHYDROL.2021.126236>
- Kuhn, M. (2008). Building Predictive Models in R Using the caret Package. *Journal of Statistical Software*, 28, 1–26. <https://doi.org/10.18637/jss.v028.i05>
- Ladson, A. R., Brown, R., Neal, B., & Nathan, R. (2013). A Standard Approach to Baseflow Separation Using The Lyne and Hollick Filter. *Australasian Journal of Water Resources*, 17(1), 25–34. <https://doi.org/10.7158/13241583.2013.11465417>
- de Lavenne, A., Thirel, G., Andréassian, V., Perrin, C., & Ramos, M.-H. (2016). Spatial variability of the parameters of a semi-distributed hydrological model. In *Proceedings of IAHS (Vol. 373, pp. 87–94)*. Copernicus GmbH. <https://doi.org/10.5194/piahs-373-87-2016>

- Lee, J. G., & Heaney, J. P. (2003). Estimation of Urban Imperviousness and its Impacts on Storm Water Systems. *Journal of Water Resources Planning and Management*, 129(5), 419–426. [https://doi.org/10.1061/\(asce\)0733-9496\(2003\)129:5\(419\)](https://doi.org/10.1061/(asce)0733-9496(2003)129:5(419))
- Leopold, L. B. (1968). *Hydrology for Urban land Planning-A Guidebook on the Hydrologic Effects of Urban Land Use*. Circular. <https://doi.org/10.3133/CIR554>
- Lim, T. C. (2016). Predictors of urban variable source area: a cross-sectional analysis of urbanized catchments in the United States. *Hydrological Processes*, 30(25), 4799–4814. <https://doi.org/10.1002/HYP.10943>
- Luukkonen, C. L., Alzraiee, A. H., Larsen, J. D., Martin, D., Herbert, D. M., Buchwald, C. A., et al. (2023). Public supply water use reanalysis for the 2000-2020 period by HUC12, month, and year for the conterminous United States [Data set]. U.S. Geological Survey. <https://doi.org/10.5066/P9FUL880>
- Mazrooei, A., Reitz, M., Wang, D., & Sankarasubramanian, A. (2021). Urbanization Impacts on Evapotranspiration Across Various Spatio-Temporal Scales. *Earth's Future*, 9(8), e2021EF002045. <https://doi.org/10.1029/2021EF002045>
- McCreight, J., Mills, T. J., FitzGerald, K., Fersch, B., donaldwj, Cabell, R., et al. (2020, February 21). NCAR/wrf_hydro_nwm_public: WRF-Hydro® v5.1.2. <https://doi.org/10.5281/ZENODO.3678643>
- McMillan, H., Krueger, T., & Freer, J. (2012). Benchmarking observational uncertainties for hydrology: rainfall, river discharge and water quality. *Hydrological Processes*, 26(26), 4078–4111. <https://doi.org/10.1002/hyp.9384>
- Miles, B., & Band, L. E. (2015). Green infrastructure stormwater management at the watershed scale: Urban variable source area and watershed capacitance. *Hydrological Processes*, 29(9), 2268–2274. <https://doi.org/10.1002/hyp.10448>
- Mitchell, K. E., Lohmann, D., Houser, P. R., Wood, E. F., Schaake, J. C., Robock, A., et al. (2004). The multi-institution North American Land Data Assimilation System (NLDAS): Utilizing multiple GCIP products and partners in a continental distributed hydrological modeling system. *Journal of Geophysical Research: Atmospheres*, 109(D7). <https://doi.org/10.1029/2003JD003823>
- Moore, R. J. (1985). The probability-distributed principle and runoff production at point and basin scales. *Hydrological Sciences Journal*, 30(2), 273–297. <https://doi.org/10.1080/02626668509490989>
- Moulin, L., Gaume, E., & Obled, C. (2009). Uncertainties on mean areal precipitation: assessment and impact on streamflow simulations. *Hydrology and Earth System Sciences*, 13(2), 99–114. <https://doi.org/10.5194/hess-13-99-2009>
- Mullen, K. M., Ardia, D., Gil, D. L., Windover, D., & Cline, J. (2011). DEoptim: An R Package for Global Optimization by Differential Evolution. *Journal of Statistical Software*, 40, 1–26. <https://doi.org/10.18637/jss.v040.i06>
- Ogden, F. L., Raj Pradhan, N., Downer, C. W., & Zahner, J. A. (2011). Relative importance of impervious area, drainage density, width function, and subsurface storm drainage on flood runoff from an urbanized catchment. *Water Resources Research*. <https://doi.org/10.1029/2011WR010550>
- Putnam, A. L. (1972). Effect of urban development on floods in the Piedmont Province of North Carolina (No. 72–304). Open-File Report. U.S. Geological Survey. <https://doi.org/10.3133/ofr72304>

- Renard, B., Kavetski, D., Kuczera, G., Thyer, M., & Franks, S. W. (2010). Understanding predictive uncertainty in hydrologic modeling: The challenge of identifying input and structural errors. *Water Resources Research*, 46(5), 5521. <https://doi.org/10.1029/2009WR008328>
- Saadi, M., Oudin, L., & Ribstein, P. (2020). Beyond imperviousness: the role of antecedent wetness in runoff generation in urbanized catchments. *Water Resources Research*. <https://doi.org/10.1029/2020WR028060>
- Saksena, S., Merwade, V., & Singhofen, P. J. (2021). An Alternative Approach for Improving Prediction of Integrated Hydrologic-Hydraulic Models by Assessing the Impact of Intrinsic Spatial Scales. *Water Resources Research*, 57(10), e2020WR027702. <https://doi.org/10.1029/2020WR027702>
- Salvadore, E., Bronders, J., & Batelaan, O. (2015). Hydrological modelling of urbanized catchments: A review and future directions. *Journal of Hydrology*, 529(P1), 62–81. <https://doi.org/10.1016/j.jhydrol.2015.06.028>
- Samaniego, L., Kumar, R., & Attinger, S. (2010). Multiscale parameter regionalization of a grid-based hydrologic model at the mesoscale. *Water Resources Research*, 46(5). <https://doi.org/10.1029/2008WR007327>
- Sanford, W. E., & Selnick, D. L. (2013). Estimation of Evapotranspiration Across the Conterminous United States Using a Regression With Climate and Land-Cover Data1. *JAWRA Journal of the American Water Resources Association*, 49(1), 217–230. <https://doi.org/10.1111/jawr.12010>
- Schoups, G., Giesen, N. C. van de, & Savenije, H. H. G. (2008). Model complexity control for hydrologic prediction. *Water Resources Research*, 44(12). <https://doi.org/10.1029/2008WR006836>
- Schwartz, S. S., & Smith, B. (2014). Slowflow fingerprints of urban hydrology. *Journal of Hydrology*, 515, 116–128. <https://doi.org/10.1016/j.jhydrol.2014.04.019>
- Shields, Catherine, and Christina Tague. “Ecohydrology in Semiarid Urban Ecosystems: Modeling the Relationship between Connected Impervious Area and Ecosystem Productivity.” *Water Resources Research* 51, no. 1 (2015): 302–19. <https://doi.org/10.1002/2014WR016108>.
- Shuster, W. D., Bonta, J., Thurston, H., Warnemuende, E., & Smith, D. R. (2005). Impacts of impervious surface on watershed hydrology: A review. *Urban Water Journal*, 2(4), 263–275. <https://doi.org/10.1080/15730620500386529>
- Smith, J. A., Baeck, M. L., Morrison, J. E., Sturdevant-Rees, P., Turner-Gillespie, D. F., & Bates, P. D. (2002). The regional hydrology of extreme floods in an urbanizing drainage basin. *Journal of Hydrometeorology*, 3(3), 267–282. [https://doi.org/10.1175/1525-7541\(2002\)003<0267:TRHOEF>2.0.CO;2](https://doi.org/10.1175/1525-7541(2002)003<0267:TRHOEF>2.0.CO;2)
- Smith, A., Tetzlaff, D., Marx, C., & Soulsby, C. (2023). Enhancing urban runoff modelling using water stable isotopes and ages in complex catchments. *Hydrological Processes*, 37(2), e14814. <https://doi.org/10.1002/hyp.14814>
- Spear, R. C., Cheng, Q., & Wu, S. L. (2020). An Example of Augmenting Regional Sensitivity Analysis Using Machine Learning Software. *Water Resources Research*, 56(4), e2019WR026379. <https://doi.org/10.1029/2019WR026379>
- Tague, C., & Pohl-Costello, M. (2008). The potential utility of physically based hydrologic modeling in ungauged urban streams. *Annals of the Association of*

- American Geographers, 98(4), 818–833.
<https://doi.org/10.1080/00045600802099055>
- Te Chow, V. (1959). Open channel hydraulics.
- Tobler, W. R. (1970). A Computer Movie Simulating Urban Growth in the Detroit Region. *Economic Geography*, 46, 234–240. <https://doi.org/10.2307/143141>
- Townsend-Small, Amy, Diane E. Pataki, Hongxing Liu, Zhaofu Li, Qiusheng Wu, and Benjamin Thomas. “Increasing Summer River Discharge in Southern California, USA, Linked to Urbanization.” *Geophysical Research Letters* 40, no. 17 (2013): 4643–47. <https://doi.org/10.1002/grl.50921>.
- US EPA. (2000). Technology Fact Sheet (No. 832- F- 00–071).
- Van De Ven, F. H. M. (1990). Water balances of urban areas. *Hydrological Processes and Water Management in Urban Areas. Lectures and Papers, UNESCO/IHP Symposium, Duisburg, Lelystad, Amsterdam, and Rotterdam, 1988*, 21–32.
- Wagener, T., Sivapalan, M., Troch, P., & Woods, R. (2007). Catchment Classification and Hydrologic Similarity. *Geography Compass*, 1, 1–31.
<https://doi.org/10.1111/j.1749-8198.2007.00039.x>
- Wallace, S., Biggs, T., Lai, C.-T., & McMillan, H. (2021). Tracing sources of stormflow and groundwater recharge in an urban, semi-arid watershed using stable isotopes. *Journal of Hydrology: Regional Studies*, 34, 100806.
<https://doi.org/10.1016/j.ejrh.2021.100806>
- Wolman, M. G. (1967). A Cycle of Sedimentation and Erosion in Urban River Channels. *Geografiska Annaler: Series A, Physical Geography*, 49(2–4), 385–395.
<https://doi.org/10.1080/04353676.1967.11879766>

Chapter 5. Conclusion

This dissertation advances the understanding of hydrologic modeling through the integration of watershed data, process knowledge, and diverse models. By experimenting with different model configurations across various watershed environments, this research offers practical insights into improving predictive accuracy and process representation, enriching both academic knowledge and practical modeling strategies in hydrology.

The findings from Chapter 2 illustrate the value of coupling models with distinct spatial and process representations. One-way coupling TOPMODEL with Noah-MP, the land surface model of the NWM, improved streamflow predictions, suggesting that the complex subsurface representation in the current NWM can be simplified using this approach. Coupling options that preserved the internal states of both models performed best, surpassing the accuracy of regular TOPMODEL or NWM. This demonstrates the value of integrating distributed meteorological inputs and land-atmosphere flux consideration with a simplified runoff module.

The intention is not to promote TOPMODEL as the sole candidate for this type of coupling. Instead, it is to advocate the flexible integration of various simple hydrologic models that best aligns the unique watershed characteristics, runoff mechanisms, climate, and objectives of modeling. Additionally, the research emphasized the critical role of the coupling interface in model performance and parameter sensitivity. While the coupling expands our modeling capacity, detailed coupling method and interface should be considered as a potential source of uncertainty, requiring a cautious approach to ensure consistency and accuracy.

Chapter 3 studied the influence of land cover representation and resampling on hydrologic simulations using WRF-Hydro/NWM. The study revealed that the areal proportion of land

cover classes within a catchment model significantly affects modeled vertical hydrologic fluxes and simulated streamflow characteristics. In contrast, the spatial arrangement of land cover in the model had a marginal impact. These findings challenge the necessity of detailed spatial representations of land cover in large-scale hydrologic modeling, supporting the development of flexible spatial configurations within modular frameworks. The research encourages advancements in land surface modeling that effectively balance vertical and lateral process representation without introducing excessive complexity.

In Chapter 4, the study investigated the incorporation of urbanization impacts on a landscape-oriented hydrologic model that is suitable for top-down modeling strategies. The results revealed that incorporating effective imperviousness significantly enhances model performance. Conversely, a more complex configuration accounting for urban impacts on subsurface processes did not lead to better results. Additionally, models with coarser spatial resolution consistently outperformed those with finer resolution models despite the loss of detailed spatial information. These findings highlight the importance of capturing the most relevant spatial aspect for hydrological flux calculation from spatial input rather than simply aiming to retain full details. Introducing extra complexity without robust physical evidence may introduce unnecessary uncertainty. The research advocates for a balanced approach, even in urban hydrological modeling, emphasizing practical applicability and understanding the causal relationships between urbanization, landscape characteristics, and hydrological changes.

Currently, there is no definitive guideline for selecting inputs or spatial scales for specific contexts. However, our findings suggest that increasing model complexity does not always enhance its ability to fully utilize detailed spatial data. It is important to remain open to testing

these relationships and to considering simpler models or configurations that may be more effective in certain situations.

Overall, this dissertation underscores the challenges of developing a scalable hydrologic modeling approach. Scalability is crucial to building a modular framework that can test models, relate their suitability and behavior with a wide range of watershed environments, and digest such insight into information that can transfer between models and watersheds. The research showed that increased complexity and spatial detail do not necessarily enhance model performance. Instead, it confirms that the balanced approach, which considers both complexity and conceptual clarity, is more effective. These findings highlight the need for more robust, flexible, and transparent modeling practices, essential for expanding the hydrologic knowledge base to address future environmental changes and enhancing water resource management amidst evolving hydrologic demands.